UNIVERSITY OF CALIFORNIA SAN DIEGO

The trophic ecology of reef-building corals: the influence of resource availability on coral nutrition at multiple scales

A dissertation submitted in partial satisfaction of the
requirements for the degree Doctor of Philosophy

in

Marine Biology

by

Michael Douglas Fox

Committee in charge:

Professor Jennifer Smith, Chair
Professor Andreas Andersson
Professor Elsa Cleland
Professor Stuart Sandin
Professor Brice Semmens

2018

The Dissertation of Michael Douglas Fox is approved, and it is acceptable in quality and form for publication on microfilm and electronically:

_____

_____

_____

_____

_____
Chair

University of California San Diego

2018

DEDICATION

To my parents, Mary Kay and Douglas Fox, who always encouraged me to follow my dreams and instilled in me a passion for natural history at an early age. Thank you for always believing in me and for your never-ending support.

EPIGRAPH

"From our present vantage point in time, when every square meter of earth has been surveyed by satellite and can be 'goggled' at will, our challenge is no longer to discover what is there, but to understand how the many complex parts of the Earth's systems interact. The challenge is not to push outward but to connect together."

Charles F. Kennel, Director of Scripps Institution of Oceanography 1997-2006
From the Forward of the book, *Ocean: Reflections on a Century of Exploration*
by Wolf. H Berger

TABLE OF CONTENTS

LIST OF TABLES

Chapter 1

Chapter 2

Chapter 3

LIST OF FIGURES

Chapter 1

Chapter 2

Chapter 3

ACKNOWLEDGEMENTS

Thank you to my advisor, Jennifer Smith, for her guidance and support over the past five years. I am incredibly grateful for the opportunities you have provided me to study and learn from some of the most remote and spectacular reefs on the planet. Jen's love of natural history and passion for benthic ecology is contagious and has helped me remember to step back and appreciate the little things even while we're working like crazy in the field. Thank you for the countless opportunities and for introducing me to an exceptional group of colleagues. I will never forget the experiences I have had and the lessons I've learned during the numerous expeditions that I have been a part of while in your lab.

I would also like to thank my committee, who has provided insightful feedback and constant encouragement over the last few years. Stuart, thank you for always being willing to chat with me about ways to analyze and explore data, those conversations have been invaluable to my development as an ecologist. Andreas, thank you for your mentorship and support over the 18 months it took to get some positive reviews for my first manuscript. The scientific process can be daunting at times but your positive attitude and thoughtful words of encouragement really helped me keep my eye on the prize. Elsa, thank you for the opportunity to take my first scientific writing class and for always encouraging me to strive for clear, concise communication that can convey my research to broad audiences. Brice, thank you for helping me think through some of the challenges of analyzing complex patterns with multivariate data and your invaluable mixing models. Our conversations these past few months have really helped to strengthen understanding of modeling stable isotope data and challenged me to think more quantitatively about the pros and cons of different analytical techniques. I'm grateful to all of you for your guidance throughout this process and I sincerely thank you for the time and energy you've put into helping me become a better scientist.

I am fortunate to have an exceptional group of colleagues who have also contributed significantly to this dissertation and my growth as a scientist. Jen introduced me to Craig Nelson during one of our stopovers in Hawaii and he has become an important mentor and collaborator. Craig, thank you for inviting me to be a part of the CHAIN experiment in Hawaii, introducing my to the glory of peristaltic pumps, and for your mentorship over the past several years. Seth Newsome has been an unofficial advisor to me for many years and even played an important role in my master's research on giant kelp. Seth, above all, thank you for introducing me to stable isotopes, which have fundamentally changed the way I think about the world and will forever shape my research. I am also extremely grateful for the opportunity to join your lab last year to learn isotopic analysis of amino acids. Gareth Williams has been a friend and invaluable mentor since my first day at Scripps. Thank you G, for always being down to talk science, speedy yet thorough revisions, bringing me into that first project on Palmyra, and for encouraging me to think big. Finally, I lucked out and had some spectacular undergraduate volunteers that helped me process mountains of samples. I am sincerely grateful to Jessica Glanz, Ellis Juhlin, Spencer Brenning-Aday, and Annika Vawter who made lab work a lot more fun!

I also want to thank Brian Zgliczynski, Christian McDonald, and Rich Walsh for the logistical support and diving operations that make all of the remote fieldwork we do possible. BZ, I'm extremely grateful for all of the incredible opportunities I've had because of your hard work and dedication to organizing expeditions. Thanks to Maggie, Clint, Amanda, and BZ for the good times in the field and help with sampling.

Thank you to my friends in the Smith and Sandin Labs and the larger Scripps community. You guys are awesome. I will always miss the evening surf sessions on north side and the jogs to Blacks with the Scripps surf crew. There's no better place to work and stay inspired than a

campus on the beach and when you can combine that with good surf, bocce, and great people it's an amazing thing.

Last but not least, I am tremendously grateful for the love and support of Maggie Johnson who has been my best friend and greatest advocate these past few years. You are the most inspiring and supportive person I've ever met and I wouldn't be where I am today without you. Thank you for always revising my drafts, reminding me to keep things in perspective, and for putting up with me always talking about isotopes!

Chapter 1, in full, has been accepted at *Current Biology* and is in press. Fox, Michael D.; Williams, Gareth J.; Johnson, Maggie D.; Radice, Veronica Z.; Zgliczynski, Brian J.; Kelly, Emily L.A.; Rohwer, Forest L.; Sandin, Stuart A.; Smith, Jennifer E. The dissertation author was the primary investigator and author of this material.

Chapter 2, in full, has been submitted to *Ecology Letters*. Fox, Michael D.; Elliott Smith, E.A.; Smith, Jennifer E.; Newsome, Seth D. The dissertation author was the primary investigator and author of this material.

Chapter 3, in part, is currently being prepared for submission for publication of the material. Fox, Michael D.; Nelson, Craig E.; Quinlan, Zach A.; Remple, Kristina.; Putnam, Hollie M.; Smith, Jennifer E.; Oliver, Thomas A. The dissertation author was the primary investigator and author of this material.

VITA

2008 B.S., University of San Diego

2013 M.S., Moss Landing Marine Labs, California State University Monterey Bay

2018 Doctor of Philosophy, University of California, San Diego

PUBLICATIONS

Fox, M.D., GJ Williams, MD Johnson, VZ Radice, BJ Zgliczynski, ELA Kelly, F Rohwer, SA Sandin, JE Smith (2018) Gradients in primary production predict the trophic strategies of mixotrophic corals at multiple spatial scales. *Current Biology,* in press.

Silbiger, NA, CA Nelson, K Remple, JK Sevilla, ZA Quinlan, HM Putnam, MD Fox, MJ Donahue (2018) Nutrient pollution disrupts key ecosystem functions on coral reefs. *Proc Soc B* 285: 20172718.

Williams, GJ, SA Sandin, BJ Zgliczynski, MD Fox, JM Gove, JS Rogers, KA Furby, A Hartman, ZR Caldwell, NN Price, JE Smith (2018) Biophysical drivers of coral trophic depth zonation. *Marine Biology* 165: 60.

Quinlan, ZA, K Remple, MD Fox, NJ Silbiger, JK Sevilla, TA Oliver, HM Putnam, L Wegley-Kelly, CA Carlson, MJ Donahue, CE Nelson (2018) Flourescent organic exudates of corals and algae on tropical reefs are compositionally distinct and increase with nutrient enrichment. *Limnology and Oceanography Letters* LOL210074.

Moritz, C, F Ducarme, MJ Sweet, MD, Fox, BJ Zgliczynksi, N Ibrahim, A Basheer, KA Furby, ZR Caldwell, C Pisapia, G Grimsditch, A Abdulla (2017) The "resort effect": can tourist islands act as a refuge for coral reef species? *Diversity and Distributions* 23: 1301-1312.

Fox, MD (2016) Biomass loss reduces growth and resource translocation in giant kelp, *Macrocystis pyrifera*. *Marine Ecology Progress Series* 562: 65-77.

Nakajima, R, N Nakatomi, H Kurihara, MD Fox, JE Smith, K Okaji (2016) Crown-of-thorns starfish larvae feed on organic matter released from corals. *Diversity* 8:4.

Enochs, IC, DP Manzello, E Donham, G Kolodziej, R Okano, L Johnston, C Young, J Iguel, CB Edwards, MD Fox, L Valentino, S Johnson, D Benavente, SJ Clark, R Carlton, T Burton, Y Eynaud, NN Price (2015) Shift from coral to macroalgal dominance on a volcanically acidified reef. *Nature Climate Change* 5: 1083-1088.

Foley, MM, RG Martone, MD Fox, CV Kappel, LA Mease, AL Erickson, BS Halpern, KA Selkoe, P Taylor, C Scarborough (2015) Using ecological thresholds to inform resource management: current options and future possibilities. *Frontiers in Marine Science* 2:95.

Adey, W, J Halfar, A Humphreys, M Suskiewicz, D Belanger, P Gagnon, MD Fox (2015) Subarctic rhodolith beds promote longevity of crustose coralline algal buildups and their climate archiving potential. *Palaios* 30: 281-293.

Fox, MD (2013) Resource translocation drives $\delta^{13}C$ fractionation during recovery from disturbance in giant kelp, *Macrocystis pyrifera*. *Journal of Phycology* 49: 811-15.

Dikou, A, C Ackerman, C Banks, A Dempsey, MD Fox, M Gins, P Hester, A Parnes, S Roach, J Rohde, C Spital, M Tapleshay, L Thomas (2009) Ecological assessment to detect imminent change, Admiral Cockburn Land and Sea National Park, Turks and Caicos Islands. *Marine Ecology* 30: 425-436.

ABSTRACT OF THE DISSERTATION

The trophic ecology of reef-building corals: the influence of resource availability on coral nutrition at multiple scales

by

Michael Douglas Fox

Doctor of Philosophy in Marine Biology

University of California San Diego, 2018

Professor Jennifer E. Smith, Chair

Understanding the natural processes that drive resource distribution and the associated response of organisms is a principal goal in ecology. Mixotrophic organisms are particularly interesting in this regard because their fitness is linked to the resources essential for both primary producers (e.g., light and nutrients) and consumers (e.g., food). Reef-building corals are among the most widely distributed mixotrophs and form the foundation of one of the most productive and diverse marine ecosystems, coral reefs. To date, a disproportionate amount of research has focused on the role of endosymbiotic microalgae in defining coral nutrition and we have a limited understanding of how corals respond to variation in food availability through time and space. This dissertation examines how mixotrophic corals can modify their nutritional modes in accordance with resource availability at multiple spatial scales. The Southern Line Islands of Kiribati in the central Pacific Ocean span a known upwelling gradient and have distinct

differences in nearshore primary production. Combining remotely sensed estimates of surface chl-*a* as a proxy for food availability and stable isotope analysis of a common coral species, I found that corals are more heterotrophic at more productive islands. I then extended this relationship globally by synthesizing published isotopic data on corals and found that large-scale patterns of chl-*a* can predict how heterotrophic corals are likely to be. I then developed a more precise method to studying coral trophic ecology at finer spatial scales. Using $\delta^{13}C$ analysis of amino acids, I found extreme trophic plasticity (0-100% contribution of heterotrophic nutrition) among conspecific corals at the scale of meters to kilometers around Palmyra Atoll. Finally, I conducted a nutrient enrichment experiment to examine the physiological responses of corals to changes in autotrophic nutrition in the absence of heterotrophic nutrition. I found that elevated nutrient concentrations have species-specific effects on coral calcification likely due to modifications in resource sharing between corals and their endosymbionts. Collectively, the results of my dissertation address a critical knowledge gap in coral biology and provide a framework to resolve the importance of heterotrophic nutrition in the persistence of coral reef ecosystems in an era of global change.

INTRODUCTION

Resource availability is a fundamental driver in ecosystem structure and functioning. It can regulate patterns of species diversity and competition (Tilman 1982; Wilson & Tilman 1993), constrain food web structure (Rosenzweig & MacArthur 1963; Oksanen *et al.* 1981), and alter trait variation among individuals (Ellison & Gotelli 2002). While patterns of resource availability have long been studied in terrestrial systems, our understanding of resource variation and its influence on marine ecosystem structure is more limited (Micheli 1999). This is likely due to the challenges of quantifying patterns of primary production and the biomass of primary producers across the spatiotemporal scales at which they occur.

Spatial and temporal variation in phytoplankton biomass directly influences the trophic structure and productivity of marine ecosystems. The importance of these microscopic primary producers is readily observed in highly productive ecosystems that support some of the world's most valuable fisheries (Pauly & Christensen 1995). In the clear, seemingly oligotrophic waters of the tropics, however, the ecological and trophic importance of phytoplankton is less conspicuous. Indeed, Charles Darwin first marveled at how coral reef ecosystems in the tropics could be so productive in such a resource-limited environment (Darwin 1842). We now know that a key feature to sustaining elevated rates of ecosystem production on coral reefs is the efficient recycling of nutrients between reef-building corals and their symbiotic microalgae (Muscatine & Porter 1977; Muscatine & D'Elia 1978). The coral-algal symbiosis evolved 160 million years ago and was essential for the global proliferation of reef-building corals and their survival of several mass extinction events (LaJeunesse *et al.* 2018). As such, many studies on coral biology and coral reef ecology have focused primarily on the role of the endosymbiotic microalgae within corals in defining the structure and functioning of these pantropical

ecosystems. Reef-building corals, however, are also voracious predators (Yonge 1930) and the ecological benefits of heterotrophic nutrition to corals have largely been overlooked (Ferrier-Pagès *et al.* 2011).

Mixotrophic corals rely on two modes of nutrition, autotrophy via their endosymbiotic microalgae (endosymbionts) and heterotrophy via predation and particle capture. In shallow water, corals obtain most of their daily metabolic requirements from their endosymbionts, which are often considered their most important source of nutrition (Falkowski et al. 1984, Muscatine et al. 1984). However, near-constant feeding has been observed in many coral taxa (Lewis & Price 1975, Sebens et al. 1996), and chemosensory abilities allow corals to accurately detect prey (Lehman & Porter 1973) and track patterns of food availability (Palardy et al. 2006). This allows corals to consume a substantial amount of the zooplankton biomass on reefs (Glynn 1973, Yahel et al. 2005), which suggests that predation is important for coral metabolism and has direct implications for coral reef ecosystem functioning (Houlbrèque & Ferrier-Pagès 2009).

Globally, the health of coral reef ecosystems is declining due to local anthropogenic impacts and global climate change (Pandolfi *et al.* 2003; Bellwood *et al.* 2004; Hughes *et al.* 2017). As such, there is a need to re-evaluate some of the core knowledge gaps that have developed during our study of coral reef ecosystems over the past several decades. Among these, the role of heterotrophic nutrition in coral persistence and recovery in a changing ocean must be examined at larger spatiotemporal scales. Notably, numerous lab experiments have highlighted that heterotrophic nutrition can enhance coral fecundity, accelerate recovery following acute disturbance, and improve survival during bleaching events (Ferrier-Pagès *et al.* 2011). Therefore patterns of resource availability (i.e., particulate food resources) may be a critical element determining coral persistence in the future.

Recent advances in remote-sensing technologies and stable isotope analyses present an opportunity to address the influence of resource availability on the trophic ecology of reef-building corals at scales beyond those previously feasible. Many coral reef islands across the Pacific exist in much more productive and resource-rich (i.e., inorganic nutrients and particulate food) waters than previously considered (Gove *et al.* 2016). Further, corals and planktivorous fishes exhibit positive relationships with nearshore primary production (Williams *et al.* 2015a; Williams *et al.* 2015b), implying a biological response to increased resource availability around coral reef islands. This dissertation seeks to leverage these new technologies to gain insight into how reef-building corals respond to patterns of food availability at different scales. Specifically, the goals of this dissertation are to establish if the trophic ecology of reef-building corals is variable across space and to develop a framework for more rigorously investigating the importance of heterotrophic nutrition and resource availability to the persistence of coral populations.

In Chapter 1, I explored variation in coral trophic strategies at regional and global scales. I used a natural gradient of oceanic primary production in the central equatorial Pacific to study how a common coral species altered its use of heterotrophic nutrition across five islands in the Southern Line Islands of Kiribati. I then expanded the scope of this study by quantifying nearshore primary production at an additional 11 locations around the globe for which estimates of coral nutrition via stable isotope analysis existed in the literature. This resulted in a global dataset that encompassed 15 species of coral from 16 locations around the world. The results from this chapter highlighted two important aspects of coral biology. First, the same coral species can increase its reliance on heterotrophic nutrition in accordance with elevated nearshore primary production (as a proxy for food availability) at small spatial scales within a single

archipelago. Second, this chapter showed that global patterns of nearshore primary production can predict estimates of coral heterotrophy inferred from bulk tissue stable isotope analysis. Collectively, these results revealed that coral nutrition is more tightly coupled with patterns of primary production across the tropics than previously considered.

The results of chapter 1 underscored the importance of accurately quantifying the contribution of heterotrophic nutrition to reef-building corals. In Chapter 2, I used $\delta^{13}C$ analysis of individual amino acids to develop a more accurate method for quantifying heterotrophic contributions to coral diets. This new approach revealed that some corals species could be extremely flexible in their trophic strategies. The amino acid isotope analysis provided the most precise quantification of *in situ* coral diets to date, which showed that conspecific colonies can vary their use of heterotrophic nutrition from 0-100% at the scale of meters to kilometers.

In Chapter 3, I shifted focus away from the heterotrophic nutrition of corals to study how patterns of inorganic nutrient availability (a limiting resource for a coral's endosymboitic algae) can influence autotrophic nutrition in corals. Natural patterns of particulate resource availability for corals are often coupled with elevated concentrations of inorganic nutrients. As such, it is important to disentangle the relative influence of each of these resources on coral nutrition in order to more accurately predict organismal responses *in situ*. This chapter focused on two species of Hawaiian corals that were exposed to five different levels of elevated nutrient concentrations (Nitrate and Phosphate) designed to span the natural range measured across multiple Pacific Islands. The results of this experiment revealed that the endosymbiotic algal communities of each coral species responded similarly to increased nutrient concentrations. In contrast, skeletal growth of each species was differentially affected by the increased primary

production of their endosymbionts. Notably, this chapter revealed that the dynamics of autotrophic nutrition within coral-algal symbioses might not be consistent across species.

The results of this dissertation contribute to our broader understanding of the relationship between oceanic primary production and the trophic ecology of shallow water mixotrophs. Most importantly, the results presented herein provide a much-needed framework for studying coral trophic ecology across species and over larger spatiotemporal scales, which will ultimately improve our capacity to model the trajectories of coral populations in a changing ocean.

References

Bellwood, D.R., Hughes, T.P., Folke, C. & Nystrom, M. (2004). Confronting the coral reef crisis. *Nature* 429, 827-833.

Darwin, C.R. (1842). *The structure and distribution of coral reefs. Being the first part of the geology of the voyage of the Beagle, under the command of Capt. Fitzroy, R.N. during the years 1832-1836*. Smith Elder and Co., London.

Ellison, A.M. & Gotelli, N.J. (2002). Nitrogen availability alters the expression of carnivory in the northern pitcher plant, *Sarracenia purpurea*. *Proc. Natl. Acad. Sci. USA.*, 99, 4409-4412.

Ferrier-Pagès, C., Hoogenboom, M. & Houlbrèque, F. (2011). The role of plankton in coral trophodynamics. In: *Coral Reefs: an ecosystem in transition* (eds. Dubinsky, Z & Stambler, N). Springer Netherlands, pp. 215-229.

Gove, J.M., McManus, M.A., Neuheimer, A.B., Polovina, J.J., Drazen, J.C., Smith, C.R., Merrifield, M.A., Friedlander, A.M., Ehses, J.S., Young, C.W., Dillon, A.K. & Williams, G.J. (2016). Near-island biological hotspots in barren ocean basins. *Nat Commun*, 7, 10581.

Hughes, T.P., Kerry, J.T., Álvarez-Noriega, M., Álvarez-Romero, J.G., Anderson, K.D., Baird, A.H., Babcock, R.C., Beger, M., Bellwood, D.R. & Berkelmans, R. (2017). Global warming and recurrent mass bleaching of corals. *Nature*, 543, 373-377.

LaJeunesse, T.C., Parkinson, J.E., Gabrielson, P.W., Jeong, H.J., Reimer, J.D., Voolstra, C.R. & Santos, S.R. (2018). Systematic Revision of Symbiodiniaceae Highlights the Antiquity and Diversity of Coral Endosymbionts. *Curr. Biol.*

Micheli, F. (1999). Eutrophication, Fisheries, and Consumer-Resource Dynamics in Marine Pelagic Ecosystems. *Science*, 285, 1396-1398.

Muscatine, L. & D'Elia, C.F. (1978). The uptake, retention, and release of ammonium by reef corals. *Limnol. Oceanogr*, 23, 725-734.

Muscatine, L. & Porter, J.W. (1977). Reef corals: mutualistic symbioses adapted to nutrient-poor environments. *Bioscience*, 27, 454-460.

Oksanen, L., Fretwell, S.D., Arruda, J. & Niemela, P. (1981). Exploitation ecosystems in gradients of primary productivity. *The American Naturalist*, 118, 240-261.

Pandolfi, J.M., Bradbury, R.H., Sala, E., Hughes, T.P., Bjorndal, K.A., Cooke, R.G., McArdle, D., McClenachan, L., Newman, M.J., Paredes, G., Warner, R.R. & Jackson, J.B. (2003). Global trajectories of the long-term decline of coral reef ecosystems. *Science*, 301, 955-958.

Pauly, D. & Christensen, V. (1995). Primary production required to sustain global fisheries. *Nature*, 374, 255-257.

Rosenzweig, M.L. & MacArthur, R.H. (1963). Graphical Representation and Stability Conditions of Predator-Prey Interactions. *The American Naturalist*, 97, 209-223.

Tilman, D. (1982). *Resource competition and community structure*. Princeton university press.

Williams, G.J., Gove, J.M., Eynaud, Y., Zgliczynski, B.J. & Sandin, S.A. (2015a). Local human impacts decouple natural biophysical relationships on Pacific coral reefs. *Ecography*, 38, 751-761.

Williams, I.D., Baum, J.K., Heenan, A., Hanson, K.M., Nadon, M.O. & Brainard, R.E. (2015b). Human, Oceanographic and Habitat Drivers of Central and Western Pacific Coral Reef Fish Assemblages. *PLoS ONE*, 10, e0120516.

Wilson, S.D. & Tilman, D. (1993). Plant competition and resource availability in response to disturbance and fertilization. *Ecology*, 74, 599-611.

Yonge, C.M. (1930). Studies on the physiology of corals. I. Feeding mechanisms and food. *Scient. Re. Gr. Barrier Reef Exped.* , 1, 13-57.

CHAPTER 1

Gradients in primary production predict trophic strategies of mixotrophic corals across spatial scales

Michael D. Fox, Gareth J. Williams, Maggie D. Johnson, Veronica Z. Radice,
Brian J. Zgliczynski, Emily L.A. Kelly, Forest L. Rohwer, Stuart A. Sandin, Jennifer E. Smith

ABSTRACT

Mixotrophy is among the most successful nutritional strategies in terrestrial and marine ecosystems. The ability of organisms to supplement primary nutritional modes along continua of autotrophy and heterotrophy fosters trophic flexibility that can sustain metabolic demands under variable or stressful conditions. Symbiotic, reef-building corals are among the most broadly distributed and ecologically important mixotrophs, yet we lack a basic understanding of how they modify their use of autotrophy and heterotrophy across gradients of food availability. Here we evaluate how one coral species, *Pocillopora meandrina*, supplements autotrophic nutrition through heterotrophy within an archipelago, and test if this pattern holds across species globally. Using stable isotope analysis ($\delta^{13}C$) and satellite-derived estimates of nearshore primary production (chlorophyll-*a*, as a proxy for food availability), we show that *P. meandrina* incorporates a greater proportion of carbon via heterotrophy when more food is available across five central Pacific islands. We then show that this pattern is consistent globally using data from 15 coral species across 16 locations spanning the Caribbean, Indian, and Pacific Oceans. Globally, surface chlorophyll-*a* explains 77% of the variation in coral heterotrophic nutrition, 86% for one genus across 10 islands, and 94% when controlling for coral taxonomy within archipelagos. These results demonstrate, for the first time, that satellite-derived estimates of nearshore primary production provide a globally relevant proxy for resource availability that can explain variation in coral trophic ecology. Thus, our model provides a pivotal step towards resolving the biophysical couplings between mixotrophic organisms and spatial patterns of resource availability in the coastal oceans.

INTRODUCTION

Mixotrophic organisms can balance their reliance on different nutritional modes (i.e., autotrophy and heterotrophy) in accordance with spatiotemporal fluctuations in resource availability. This trophic flexibility allows mixotrophs to adapt to a wide range of terrestrial and aquatic biomes, making mixotrophy one of the most ubiquitous nutritional strategies on earth (Selosse *et al.* 2016). Most mixotrophs subsist along a continuum of autotrophy and heterotrophy, such as vascular plants that can supplement autotrophic nutrition along gradients of limiting resources through carnivory or mycoheterotrophy (Ellison & Gotelli 2002; Matsuda *et al.* 2012). Dynamic marine environments favor mixotrophic organisms, which are broadly distributed and provide crucial linkages for energy flow between trophic levels (Stoecker *et al.* 2017). Many cnidarians and sponges have evolved a tight symbiosis with microalgae to sustain high rates of primary production in oligotrophic regions (Muscatine & Porter 1977; Venn *et al.* 2008). Of these animals, mixotrophic reef-building corals form the foundation of one of the most biodiverse and productive marine ecosystems, yet our understanding of how corals adjust nutritional modes in response to natural gradients in resource availability (e.g., inorganic nutrients and particulate resources) remains limited (Ferrier-Pagès *et al.* 2011). Given their pantropical distribution, mixotrophic corals represent an opportunity to examine the biophysical coupling between resource availability and the trophic ecology of mixotrophic organisms across spatial scales.

Reef-building corals obtain energy from both autotrophy, via their endosymbiotic microalgae of the genus *Symbiodinium*, and heterotrophy via the capture of allochthonous particles (Furla *et al.* 2005). While the physiological benefits of this trophic plasticity were acknowledged by early studies of coral biology (Muscatine & Porter 1977), the ecological

success of scleractinian corals has long been attributed to their symbiotic nature (Veron 1995). Indeed, photosynthetically fixed carbon translocated from endosymbionts to the coral host can contribute more than 100% of the daily metabolic requirements of corals (Muscatine *et al.* 1981; Davies 1984; Grottoli *et al.* 2006); however much of the fixed carbon is respired or released as mucus rather than incorporated into host biomass (Falkowski *et al.* 1984; Tremblay *et al.* 2015). Heterotrophy on the other hand, provides corals with carbon and essential nutrients (e.g., nitrogen and phosphorus) that directly support growth and reproduction (Ferrier-Pagès *et al.* 2003; Cox 2007). The physiological importance of heterotrophy for corals is widely accepted, yet a disproportionate amount of research to date has focused on the role of endosymbionts in defining coral nutrition (Ferrier-Pagès *et al.* 2011).

Heterotrophic nutrition can mitigate the negative effects of environmental stressors on coral physiology. For example, heterotrophy can increase coral recovery rates following acute stress, decrease overall mortality, and help reestablish the coral-algal symbiosis following thermally-induced bleaching (Grottoli *et al.* 2006; Rodrigues & Grottoli 2006; Palardy *et al.* 2008; Tremblay *et al.* 2016). Heterotrophic nutrition can increase coral fecundity (Cox 2007) and also facilitate calcification under low pH conditions, which is critical for coral growth and therefore the structural development and persistence of reefs through time (Edmunds 2011; Drenkard *et al.* 2013). *In situ,* increased rates of heterotrophy by corals are often considered a response to the contrasting gradients of light and resource availability (Anthony & Fabricius 2000) and are thought to increase with depth (Muscatine *et al.* 1989). However, some corals may feed continuously across depth in areas where heterotrophic resources are more abundant (Alamaru *et al.* 2009; Williams *et al.* 2018). Food availability for corals is linked with nearshore primary production (PP_n) (Gove *et al.* 2016). Thus future reductions in PP_n, caused by increased

ocean stratification (Behrenfeld *et al.* 2006) and moderate to strong El Niño events (Brainard *et al.* 2018) likely represent an unanticipated stressor on the persistence of coral populations in a warming ocean. Understanding the relationship between PP_n and coral trophic ecology will improve our capacity to accurately predict the implications of global change on coral populations over space and time.

To date, our understanding of heterotrophic nutrition in corals is largely laboratory-based (Ferrier-Pagès *et al.* 2003; Houlbrèque *et al.* 2003; Ferrier-Pagès *et al.* 2011; Hoogenboom *et al.* 2015; Tremblay *et al.* 2015; Tremblay *et al.* 2016), thus limiting our ability to assess coral feeding at broader, more ecologically relevant scales. New techniques are required to propel our understanding of coral nutrition beyond individual colonies and to scale these patterns up to entire reef ecosystems. An essential first step is to link regional variation in environmental conditions with the biological responses of corals. Remotely sensed estimates of surface chlorophyll-*a* (chl-*a*) (Gove *et al.* 2013) have revealed significant increases in phytoplankton biomass in the nearshore regions of oceanic islands across the Pacific (Gove *et al.* 2016). Notably, these satellite-derived chl-*a* estimates are correlated strongly with PP_n throughout the photic zone as well as the relative abundance of zooplankton, a primary food resource for corals (Croll *et al.* 2005; Hazen & Johnston 2010). Remotely sensed surface chl-*a* may therefore provide a globally relevant proxy for estimating PP_n and heterotrophic resource availability on coral reefs. Similarly, stable isotope analyses ($\delta^{13}C$ and $\delta^{15}N$) of coral hosts and their endosymbionts can assess the relative contributions of heterotrophic and autotrophic nutrition across multiple coral species and spatial scales (Muscatine *et al.* 1989; Rodrigues & Grottoli 2006; Williams *et al.* 2018).

To test for a link between heterotrophic resource availability and the trophic response of mixotrophic corals, we compared the $\delta^{13}C$ and $\delta^{15}N$ values of corals to satellite-derived estimates of PP_n (using chl-*a* as a proxy for plankton biomass). At an archipelago scale, we measured the degree of heterotrophy in a common reef-building coral (*Pocillopora meandrina*) collected across depths (5-30 m) at five uninhabited islands in the Southern Line Islands of Kiribati (SLI) and modeled these against concurrent changes in PP_n. To determine if the same relationship held globally, we synthesized published $\delta^{13}C$ and $\delta^{15}N$ values for 15 coral species from 16 locations across the Red Sea, Caribbean, Indian and Pacific Oceans and modeled these against climatological estimates of PP_n for each location.

METHODS

Experimental Model and Subject Details

The Southern Line Islands, of the Republic of Kiribati consist of four low-lying limestone islands (Flint, Vostok, Starbuck, and Malden) and one atoll (Millennium) (Fig. 1.1A). These coral-dominated islands (Smith *et al.* 2016) represent reef ecosystems that have likely adapted to long-term differences in inorganic nutrient availability and primary production (PP) due to variation in regional oceanography in the absence of local human impacts. All research was conducted on the leeward (west) fore reef habitat of each island between October and November 2013. Sites were selected based on previously published data and were representative of island-scale averages for benthic community structure (Smith *et al.* 2016).

For the first part of this study, we sought to compare the trophic ecology of a common reef-building coral across a natural, long-term gradient in nearshore primary production. We chose to examine a species that is widely distributed coral throughout the Pacific and Indian oceans, *Pocillopora meandrina*. We recognize the challenges of accurately identifying

Pocillopora species visually in the field given the high level of morphological plasticity within this genus (Johnston *et al.* 2017). However, the relative abundance of *P. meandrina* throughout the Line Islands (Williams *et al.* 2010; Williams *et al.* 2013) supports our identification. We removed approximately 2-3 cm^2 branch tips from the top-center of five similarly sized colonies of *P. meandrina.* All sampled colonies were separated by at least 5m when abundant and collections were made strictly along the isobaths at each depth. Samples in the SLI were collected at 5, 10, 15, 20, 25, 30 m on each island and placed in individual UV protective sample bags. During transport to the research vessel, samples were stored in the dark and on ice and then frozen at -20° C until analysis.

We also examined the relationship between coral trophic ecology and nearshore primary production on a global scale using previously published coral isotope data from the literature. Coral host tissue and endosymbiont $d^{13}C$ and $d^{15}N$ values were acquired from published studies (Table 1.S4). Only data from studies that collected corals at 10 m depth and presented independent means of host and endosymbiont fractions were included. This depth was selected because it is among the most commonly surveyed depth on fore reef habitats (Smith *et al.* 2016) and therefore most relevant to previous studies of coral reef benthic communities. When isotopic means were not provided in a table, values were extracted from figures using Data Thief 3.0 (www.datathief.org). If multiple coral species were sampled at the same location, their isotopic values were averaged to create a site-specific mean in order to avoid pseudoreplication among each level of chl-*a* in our statistical analyses.

Oceanographic context of the Southern Line Islands

To quantify differences in ambient inorganic nutrient concentrations across the SLI, triplicate water samples (50mL) were collected at 5, 10, 15, 20, and 30 m at each site, filtered (0.7 µm GF/F filters, Whatman) and frozen at -20° C until analysis. Samples were analyzed for dissolved inorganic nitrogen (DIN = NO_3^- + NO_2^- + NH_4^+) and soluble reactive phosphorus (SRP) at the University of Hawaii Hilo EPSCoR analytical laboratory. Inter-island variation in nutrient concentrations were compared using a two-way fixed factor analysis of variance (ANOVA) to examine the effects of island and depth and their possible interaction. Assumptions of normality and homoscedasticity were verified by using the Anderson-Darling test and Levene's test, respectively. There was significant interaction between island and depth for DIN ($F_{16,40} = 5.083$, $p < 0.001$, Fig. 1.1C). This interaction, however, was driven by differences in nutrient concentrations at the same depths across islands. The only intra-island differences across depth occurred on Malden (Tukey HSD: 5 m < 15, 25, 30 m) and the difference was <0.5µmol. Phosphate concentrations did not vary with depth but differed among islands ($F_{4,40} = 70.66$, $p < 0.001$). As such, we considered inorganic nutrient concentrations to be homogenous throughout the upper 30 m and pooled the data to present an integrated mean for the water column. *In situ* photosynthetically active radiation (PAR) was recorded with a LI-COR 4π quantum sensor (LI-1400, LICOR USA) that was deployed at 10 m depth for 2-4 diel cycles at each island. The relative light environment at each island over longer time scales was assessed by determining the depth of light penetration at 490 nm (K490) from the MODIS data package, *sensu* (Gove *et al.* 2016).

To quantify patterns of island-scale PP we used the eight-day 0.0417° (~4-km) spatial resolution product of chl-*a* (mg m^{-3}) derived from the Moderate Resolution Imaging

Spectroradiometer (MODIS; https://modis.gsfc.nasa.gov/). Data were obtained for 2004-2015 (12 years) to provide climatological means of surface chl-*a* concentrations across the SLI, *sensu* [6]. Briefly, pixels that fell within 3.27 km of the 30 m isobath of each island were excluded to avoid data confounded by optically shallow water. Next, a full pixel width (4.4 km) buffer region was extended beyond the 3.27 km exclusion zone and used to select a single band of pixels around each island. These pixels were averaged to create island-scale climatological estimates of chl-*a* concentrations as a proxy for nearshore PP and heterotrophic resource availability.

The mean number of pixels used around the smallest oceanic islands in this study (Palmyra Atoll and all islands in the SLI) was 13. Therefore, climatological chl-*a* estimates were derived for other locations using the mean of the13 most proximate pixels along shore of the collection site. This standardized the spatial areas considered for the PP climatologies at each location and allowed for more ecologically relevant estimates along continental coastlines such as in the Red Sea or from large islands, such as Jamaica.

By using chl-*a* data from optically clear waters we avoid confounding data from nearshore waters that may be influenced by terrestrial runoff or other anthropogenic impacts (Gove *et al.* 2013). Consequently, our chl-*a* estimates are not made on the reef and may therefore underestimate the overall chl-*a* concentration and plankton abundance. However, this proxy to nearshore primary production is a powerful predictor of the biological responses of coral reef communities, most notably corals and planktivorous fish (Williams *et al.* 2015a; Williams *et al.* 2015b). Satellite-derived chl-*a* estimates from 29 Pacific islands also accurately reflect phytoplankton biomass throughout the euphotic zone (Gove *et al.* 2016).The mean chl-*a* concentration at each island during our cruise in October-November 2013 mirrored the long-term climatologies for the region and was strongly correlated with *in situ* DIN concentrations (r =

0.97). Thus, we believe that remotely sensed chl-*a* accurately reflect surface chl-*a* conditions near coral reef environments over longer time scales and that this metric provides a relevant estimate of food abundance for coastal mixotrophs in the tropics.

Stable isotope analysis of Pocillopora across islands and depths in the SLI

Coral host and endosymbiont fractions were isolated following established methods (Muscatine *et al.* 1989; Rodrigues & Grottoli 2006; Hughes *et al.* 2010; Williams *et al.* 2018). An airbrush was used to remove tissue from the skeleton using 10 mL of 0.07 µm filtered seawater (FSW). The resulting blastate was homogenized with an electric tissue homogenizer. The animal fraction was isolated through centrifugation at 2,000g for 5 min to pellet most of the endosymbionts. The supernatant (animal fraction) was decanted and the symbionts fraction was suspended in 2 mL of FSW, centrifuged again. The supernatant from this was added to the animal fraction, which was centrifuged a final time to pellet any residual endosymbionts and 2 mL were loaded onto a pre-combusted GF/F filter (Whatman). To minimize the contamination of the endosymbiont fraction by coral host tissue (and therefore optimize our ability to detect true heterotrophic signals), the endosymbiont fraction was then resuspended in 5 mL FSW, pressure filtered through 83 and 20 µm nitex mesh and pelleted at 2,000 g. This filtration was repeated once more before 1 mL of the endosymbiont fraction was loaded onto a pre-combusted GF/F. Each sample was briefly rinsed with 1mL 1N HCl to remove calcium carbonate from the coral sample and rinsed with 1 mL of DI water (Nahon *et al.* 2013). Acidified and non-acidified samples were tested against each other to ensure that rinsing with a weak acid did not affect nitrogen isotope values. We examined acidification effects on both tissue fractions (n=5) using paired t-tests and found no effect of this light acidification on $d^{15}N$ of either tissue type

(t_{host}=1.50, p=0.21; $t_{symbiont}$= -0.08, p=0.94). No differences were observed for $d^{13}C$ either; suggesting $CaCO_3$ contamination is minimal following this protocol with *P. meandrina* (t_{host}= -1.69, p=0.17; $t_{symbiont}$= -0.42, p=0.69). The mean offset between acidified and non-acidified samples were: $d^{13}C_{host}$ = -0.02 ±0.02 ‰, $d^{15}N_{host}$ = -0.01 ± 0.02‰, $d^{13}C_{symbiont}$ = -0.03 ± 0.15‰, $d^{15}N_{symbiont}$ = -0.03 ± 0.02‰. As such, we elected to briefly acidify each sample to minimize the risk of $CaCO_3$ contamination and $d^{13}C$ and $d^{15}N$ were determined from the same sample.

The isolated fractions were analyzed for $d^{13}C$, $d^{15}N$ and µg C:N with a Costech 4010 Elemental Combustion Analyzer interfaced with a Thermo Finnigan Delta Plus XP stable isotope mass spectrometer (San Jose, CA) at Scripps Institution of Oceanography. Isotopic values are expressed as $d^{13}C/^{15}N$, where $\delta = 1000 \times [(R_{sample} / R_{standard}) -1]$ and R_{sample} or $R_{standard}$ are the ratio of the heavy to light isotope in parts per thousand, or per mil (‰). The C^{13}/C^{12} and N^{15}/N^{14} ratios are expressed relative to the levels of ^{13}C in Vienna-Pee Dee Belemnite (V-PDB) and ^{15}N in atmospheric N_2. Repeated measurements (n=60) of internal working standards exhibited a precision of 0.01‰ for $\delta^{13}C$ and 0.2‰ for $\delta^{15}N$. The internal standards of calcium carbonate and ammonium sulfate were calibrated against NBS 18 and IAEA-1, respectively. Ten percent of all samples (n=18) were run in duplicate with a measurement error ± 0.12‰ for $\delta^{13}C$ and ± 0.31‰ for $\delta^{15}N$.

The amount of heterotrophic carbon incorporated by *Pocillopora* was inferred by calculating the difference between the $\delta^{13}C$ values of the coral host and endosymbiont fractions ($\Delta^{13}C = d^{13}C_{host} - d^{13}C_{endosymbiont}$) (Muscatine *et al.* 1989). This metric has been shown to accurately track intra-island variations in resource availability across sites and depth in this coral species within the Line Islands (Williams *et al.* 2018). To verify that the dominant coral food sources (e.g. zooplankton and particulate organic matter (POM)) had more negative $\delta^{13}C$ values

than the coral host and endosymbiont tissue (Muscatine *et al.* 1989; Grottoli & Wellington 1999) (to ensure accurate interpretation of the $\Delta^{13}C$ metric), we collected reef-associated POM (2 L seawater filtered onto 25 mm GF/F) and zooplankton (>133 μm, collected across full diel cycles using an autonomous plankton sampler, *sensu* (Williams *et al.* 2018)) from 10 m depth at 3 leeward sites per island. Both sample types were concentrated on pre-combusted GF/F filters and briefly acidified as above. For each zooplankton filter (n=3 per island), duplicate subsamples were averaged together to account for the heterogeneous distribution of plankton across the filter.

To extract chlorophyll-*a,* endosymbionts were pelleted from 2 mL of coral blastate from each coral at 10, 20, and 30 m. The animal fraction was decanted and the algal pellet was homogenized in 1 mL in *N,N*-dimethylformamide (DMF) and the pigments were extracted for 24 hrs at 4 °C following. The sample was then centrifuged for 5 min at 7,000 x g to remove all particulate debris and the supernatant was analyzed with a diode array spectrophotometer (Agilent, UV-vis 8453) following the equations of (Wellburn 1994) for a spectrophotometer with 1 nm resolution. Pigment concentrations were normalized to surface area of each coral fragment determined by wax dipping (Stimson & Kinzie 1991), initial blastate volume, and solvent volume. Endosymbiont density was quantified by 6 replicate counts on a Hausser hemocytometer and normalized to initial blastate volume and coral surface area.

Quantification and Statistical Analysis

To determine if coral host tissue was more similar to its dominant prey source (zooplankton) on more productive islands, we examined the difference between the coral host tissue with zooplankton $d^{13}C$ and $d^{15}N$ values at each island using only corals from 10 m (to be consistent with the depth of zooplankton collections). We used a one-way ANOVA to test for differences in zooplankton $d^{13}C$ among islands. Assumptions of normality and homoscedasticity

were verified by using the Anderson-Darling test and Levene's test, respectively. Zooplankton $d^{13}C$ did not vary among islands ($F_{(4,10)} = 1.59$, $p = 0.5$) so we used island-specific zooplankton $d^{13}C$ values to examine the relationship between coral host and zooplankton $d^{13}C$ ($\Delta^{13}C_{host\text{-}zooplankton}$). We used a standard linear model to assess the relationship between $\Delta^{13}C_{host\text{-}zooplankton}$ and $\Delta^{15}N_{host\text{-}zooplankton}$ as a function of surface chl-*a* at each island.

Spatial variability in $d^{13}C$, $d^{15}N$, and C:N and their relative differences between tissue fractions (Δ) across depths and islands was examined using an analysis of covariance (ANCOVA) on mean values (n=5 per depth except Flint 30 m, n=3) to account for non-independence among replicate samples within each level of depth. Assumptions of normality and homoscedasticity were verified by using the Anderson-Darling test and Levene's test, respectively. We included depth as a covariate to test for differences in the slope of the relationship between tissue chemistry and depth across the SLI (significant interaction term) and for differences in the magnitude of the heterotrophic signal (significant effect of island). Significant differences in the slopes of island-specific regressions of mean values *vs.* depth were determined individually in pairwise contrasts (Zar 2007).

Coral pigment content was log transformed to satisfy the assumptions of normality and homoscedasticity and compared across islands and depth with a two-way fixed factor ANOVA. The relationship between coral pigment content and endosymbiont density and their respective influence on coral $\Delta^{13}C$ was examined using Pearson's correlations for all coral samples from 10 m pooled across the SLI (n=25).

Global relationships between coral isotopic ratios and nearshore primary production

The physiology and trophic strategies of scleractinian corals vary considerably across taxa (Hoogenboom *et al.* 2015). We acknowledge that averaging the $\Delta^{13}C$ estimates of multiple species reduces our ability to examine species-specific patterns and intra-site variability, but this allowed us to test our observed relationship in the most statistically rigorous fashion. To account for the influence of coral taxonomy on our observed relationship between $\Delta^{13}C$ and surface chl-*a,* we refined the global dataset to only include data from coral families that were replicated in at least two separate locations (intra-archipelago replication excluded). The resulting dataset thus excluded samples from the Acroporidae and Meandrinidae (Jamaica) and Oculinidae (Maldives) families from the mean $\Delta^{13}C$ estimates at those locations. The resulting family-level dataset contained $\Delta^{13}C$ estimates from all 16 locations but only for corals from four families (Agariciidae, Astrocoeniidae, Faviidae, Pocilloporidae). Using this refined dataset, we tested the consistency of our observed linear relationship between $\Delta^{13}C$ and chl-*a* at both island and regional scales.

To examine the influence of spatial autocorrelation on heterotrophy estimates from geographically clustered islands, we fitted a linear mixed effects model (lme4 package for R (Bates *et al.* 2015)) with region included as a random effect (model 1) on the intercept as: mean $\Delta^{13}C \sim$ mean chl-*a* + (1|Region). Region explained zero percent of the model variance while surface chl-*a* was a significant predictor variable ($p < 0.01$, $r^2 = 0.78$). To further address this concern, we compared the performance of this model with a standard general linear model (model 2) (residuals of our data were normally distributed, were not auto-correlated, and showed no sign of heteroscedasticity) using Akaike Information Criterion (MuMIn package (Barton 2015)) corrected for small sample size AICc (Hurvich & Tsai 1989). Both models confirmed that

chl-*a* was a significant predictor variable and indicated that the effect of surface chl-*a* concentration on coral $\Delta^{13}C$ was consistent within and across regions, regardless of ocean basin ($p < 0.01$). The slope and y-intercept of both models were identical; therefore we selected the more parsimonious general linear model of island means as the model of best fit ($\Delta AICc = -5.19$ relative to model 1).

To test for a spatial bias driven by uneven sampling within individual regions (1-6 islands per archipelago), we collapsed the island-mean estimates of heterotrophy into regional means (i.e. data from each island of an archipelago were averaged, thereby reducing the influence of spatial autocorrelation within archipelagos). Our expectation was that significant regional bias would reduce performance of the regional general linear model (model 3). Notably, this approach had no significant effect on model performance (model 2: $F_{1,14} = 44.44$, $r^2 = 0.77$, $p < 0.001$; model 3: $F_{1,5} = 18.35$, $r^2 = 0.79$, $p = 0.01$). Therefore, we used the standard general linear model of island-specific $\Delta^{13}C$ estimates to most accurately capture the variation across all 16 locations.

To further assess the performance of our selected linear model we performed a sensitivity analysis to assess the influence of taxonomy and geography on model performance by reducing the model in a step-wise fashion (Table 1.S3). First, we tested for a significant relationship between surface chl-*a* and all coral $d^{13}C$ and $\Delta^{13}C$ data for 15 species. Next, we removed islands whose mean $\Delta^{13}C$ value was created from multiple species (i.e., Jamaica, Eilat) and for a species with uniquely deplete $d^{13}C$, *Madracis spp.* (Muscatine *et al.* 1989). Then, we further reduced the model to include only data from a single species at all locations (excluding Jamaica and using *Stylophora pistillata* from the Gulf Eilat due to its genetic relatedness to *Pocillopora*). Finally, we examined the most simplistic model, only $d^{13}C$ and $\Delta^{13}C$ data for *Pocillopora* from the Line

Islands and the Maldives. We calculated coefficients of variation for the slope and y-intercept terms across all models (excluding model with raw data) to assess overall variation. See Table 1.S3 for statistical summaries of each model, respectively.

Finally, to disentangle the influence of geography *vs.* oceanographic processes related to resource availability (i.e., PP and upwelling) on coral and endosymbiont $d^{13}C$ and $d^{15}N$ values we examined linear relationships between absolute latitude (as a proxy for light and temperature) and estimated thermocline depth (as a proxy for resource delivery potential, as internal wave delivery of subthermocline resources are more probable in regions with shallower thermoclines (Rebert *et al.* 1985)). Thermocline depth was estimated as the depth of the 22° isotherm computed using objectively analyzed mean SST averaged across all available decades from the World Ocean Atlas (https://www.nodc.noaa.gov/OC5/woa13/). Thermocline depth in the tropical Pacific is well estimated by the depth of the 20° isotherm (Rebert *et al.* 1985), however, we used the 22° isotherm in order to include the Gulf of Eilat in our analysis, which can be mixed to depths in excess of 600 m (Lindell & Post 1995) and did not go below 22° in the world ocean atlas database. Mean temperatures from the surface to 1000m were determined for each island in the global dataset using a horizontal average of a 1° x 1° box centered on each island (Williams *et al.* 2018). Depth of the 22° isotherm was estimated from linear fits of temperature vs. depth for a temperature of 14-28° ($r^2 > 0.95$ for all models), which provided independent estimates of thermocline depth for each location. To account for the geographic proximity of several atolls in the Maldives, the atolls from this region were consolidated into north, central, and south groups (isotope data averaged across two atolls per region). Thus, the degrees of freedom in this analysis differed slightly from the global model presented above (df = 11 *vs.* 13). We compared linear models (Table 1.S4) based on mean isotope values as described above. We also examined coral

and endosymbiont $d^{15}N$ and $\Delta^{15}N$ across the Pacific and Indian oceans and for only *Pocillopora* from the Line Islands and the Maldives to control for regional oceanographic differences and elucidate how oceanic ^{15}N baselines influence coral $d^{15}N$. All statistical analyses were completed using R (R Core Team 2013 and related packages).

RESULTS

Oceanographic context of the Southern Line Islands (SLI)

The oceanic primary production gradient across the SLI is conspicuous, with climatological surface chl-*a* concentrations (2004-2015) separating the islands into distinct regions (Fig. 1.1A, 1.1B). Surface chl-*a* (a proxy for PP_n) was similar at the three southern islands (Flint, Vostok, and Millennium) while considerably higher and with less inter-annual variation at the northern two (Starbuck and Malden) ($F_{4,55} = 27.48$, $p < 0.01$; Tukey HSD: FLI, VOS, MIL < STA, MAL). The mean depth of light penetration at 490 nm (a proxy for light attenuation) from 2004-2015 ranged from 29-35 m, which suggests the light environment on these islands does not differ markedly on decadal time scales. Inorganic nutrient concentrations were latitude-dependent and closely associated with the chl-*a* gradient (Fig. 1.1C). Mean dissolved inorganic nitrogen (DIN) concentrations increased nine-fold (0.51-4.69 μmol) from south to north with a concomitant increase in soluble reactive phosphorus (SRP) (0.15-0.44 μmol, $F_{4,40} = 70.66$, $p < 0.01$). Within islands, inorganic nutrient concentrations were homogenous in the upper 30 m and consistent with measurements from 2009 (Kelly *et al.* 2014). During our study, *in situ* irradiance was similar throughout the SLI and there was no pattern between islands (i.e., the more productive islands did not have reduced irradiance relative to the

more oligotrophic islands). On sunny days, mean daily irradiance ranged from 374-546 μE m^{-2} s^{-1} and total integrated daily irradiance ranged from 11.76-17.04 E m^{-2} d^{-1}.

Coral and endosymbiont $\delta^{15}N$ values were influenced most strongly by location due to a baseline shift in $\delta^{15}N$ of nitrate that occurs along the oceanic primary production gradient in the equatorial Pacific (lower $\delta^{15}N$ values closer to the equator) (Altabet 2001). As a result, coral and endosymbiont $\delta^{15}N$ decreased from Flint to Malden. The endosymbiont fraction became more deplete in ^{15}N with depth at all islands while coral host $\delta^{15}N$ only declined with depth on Starbuck (Tables 1.S1, 1.S2). C:N values were elevated in the coral host fraction on Starbuck and Malden, which indicates the nitrogen content of the coral and endosymbiont fractions did not increase along the nutrient gradient (Table 1.S1). However, the overall chl-*a* content of *P. meandrina* endosymbionts increased from Flint to Malden (Island: $F_{(4,60)} = 21.26$, $p < 0.01$, TukeyHSD: FLI < VOS, MIL,STA <MAL). Pigment content generally increased from 10-30 m but was highly variable (Depth: $F_{(2,60)} = 6.61$, $p < 0.01$, TUKEY HSD: 10m <30 m, Fig. 1.S1). Endosymbiont density was positively correlated with chl-*a* content at 10 m depth across all islands (Pearson's correlation: $t_{(1,25)} = 5.27$, $p < 0.01$, $r = 0.73$).

Isotopic evidence for coral heterotrophy across islands and depth

The $d^{13}C$ values of coral and endosymbiont tissues can be influenced by differences in photosynthetic rates (autotrophic nutrition) and by the incorporation of allochthonous food sources via particle capture (referred to herein as heterotrophic carbon). Decreased rates of photosynthetic fractionation cause coral host and endosymbiont $d^{13}C$ values to decrease with depth (Muscatine *et al.* 1989). Planktonic communities and POM are the primary heterotrophic resources for corals. On most coral reefs these resources are depleted in ^{13}C (more negative $d^{13}C$)

relative to *Symbiodinium* spp. by at least 4-6 ‰ (Alamaru *et al.* 2009). Thus, increased heterotrophic nutrition leads to a reduction in coral host $d^{13}C$ values. The relative difference between the coral host and endosymbiont $d^{13}C$ ($\Delta^{13}C = d^{13}C_{host} - d^{13}C_{endosymbiont}$) can therefore be used to disentangle the relative effects of photosynthetic fractionation and incorporation of heterotrophic carbon. While not a quantitative estimate of the heterotrophic contribution to a corals metabolic demands, this isotopic proxy ($\Delta^{13}C$) provides insight to deviations from a fully autotrophic diet and reliably tracks intra-island gradients in resource availability (Muscatine *et al.* 1989; Rodrigues & Grottoli 2006; Williams *et al.* 2018).

Coral host and endosymbiont $d^{13}C$ values declined linearly with depth and $d^{13}C$ for both fractions ranged from -14 to -18 ‰ across the SLI (Fig. 1.1A-E, Table 1.S1). Host $d^{13}C$ was consistently lower than the endosymbiont fraction and was greatest at Flint (southernmost island) and lowest at Malden (northernmost). In contrast, endosymbiont $d^{13}C$ did not vary among islands. As an additional proxy of coral heterotrophy we also examined the relative similarity of coral host $\delta^{13}C$ and the mean $\delta^{13}C$ of the reef associated zooplankton at each island ($\Delta^{13}C_{host\text{-}zooplankton} = \delta^{13}C_{host} - \delta^{13}C_{zooplankton}$). Coral host $d^{13}C$ values became more similar to zooplankton $\delta^{13}C$ (more depleted in ^{13}C, lower $\Delta^{13}C_{host\text{-}zooplankton}$) with increasing surface chl-*a*, indicating a greater incorporation of heterotrophic carbon at the more productive islands ($\Delta^{13}C_{host\text{-}zooplankton} - F_{(1,3)} = 44.89$, $p = <0.01$, $r^2 = 0.94$, Fig. 1.1D). There was no relationship between coral and zooplankton $d^{15}N$ ($\Delta^{15}N_{host\text{-}zooplankton} - F_{(1,3)} = 0.97$, $p = 0.65$).

In contrast to the individual $\delta^{13}C$ values of the corals and endosymbiont tissues, $\Delta^{13}C$ ($\delta^{13}C_{host} - \delta^{13}C_{endosymbiont}$) varied as a function of chl-*a* across the SLI (Fig. 1.2F-J, Table 1.S1). *P. meandrina* $\Delta^{13}C$ was most negative on islands with higher surface chl-*a*. On Flint and Vostok (most oligotrophic), *Pocillopora* exhibited increased reliance on heterotrophic carbon sources

(more negative $\Delta^{13}C$) as a function of depth (from 5 to 30 m depth: Flint: slope = -0.23, $p < 0.01$, $r^2 = 0.97$ Vostok: slope = -0.19, $p = 0.05$, $r^2 = 0.67$, Fig. 1.2I, 1.2J, Table 1.S1). There was no depth dependence of $\Delta^{13}C$ on Millennium, Starbuck, or Malden (Fig. 1.2F, 1.2G, 1.2H). Importantly, $\Delta^{13}C$ was not related to coral surface area normalized chl-*a* concentrations (Pearson's correlation: $t_{(1,25)} = -1.89$, $p = 0.2$, $r = 0.1$) or endosymbiont densities ($t_{(1,25)} = 1.65$, $p = 0.2$, $r = 0.25$).

Coral $\Delta^{15}N$ and $\Delta C:N$ values showed no consistent relationships with islands or depth (Table 1.S2). $\Delta^{15}N$ values on Millennium were similar with those of Flint and Vostok but did not increase with depth. On Starbuck and Malden, $\Delta^{15}N$ values were generally lower and did not vary with depth. Coral $\Delta C:N$ was highest on Starbuck and Malden indicating greater concentrations of lipids in the animal fraction on the more productive islands.

Global patterns of coral $d^{13}C$ and $d^{15}N$ in relation to nearshore primary production

Coral $d^{13}C$ and $d^{15}N$ values vary with large-scale physical processes but $\Delta^{13}C$ is most tightly coupled with surface chl-*a* across 16 locations spanning three ocean basins. Latitude was positively related to coral and endosymbiont $d^{13}C$, respectively, but this relationship did not explain a significant amount of variation due to the low $\delta^{13}C$ values of *Madracis auretenra* on Curaçao (Fig. 1.S2, Table 1.S4). Latitude was unrelated to $\Delta^{13}C$. Coral and endosymbiont $d^{15}N$ showed no coherent pattern when considered globally (Table 1.S4). However, considering only *Pocillopora*, host and endosymbiont $d^{15}N$ (but not $\Delta^{15}N$) were well explained by latitude, chl-*a*, and estimated thermocline depth (Table 1.S4). $\delta^{15}N$ values were lowest in regions with shallower thermoclines and higher chl-*a*.

Coral and endosymbiont $d^{13}C$ values were tightly constrained across species and geography and did not vary as a function of surface chl-*a* (Fig. 1.3A-C, Table 1.S2, 1.S3). In contrast, surface chl-*a* explained 77% of the variation in mean coral $\Delta^{13}C$ across 16 locations ($F_{(1,14)} = 46.24$, r2= 0.77, $p < 0.01$, Fig. 1.3D, Table 1.S3). Additionally, depth of the 22° isotherm (a proxy for thermocline depth) explained 51-69% of the variation in coral $\Delta^{13}C$ (Fig. 1.S2, Table 1.S4). Our findings indicate that mixotrophic corals incorporate a greater proportion of heterotrophic carbon (more negative $\Delta^{13}C$) in regions where resource abundance is enhanced by shallower thermoclines and higher surface chl-*a* concentrations.

The linear relationship between $\Delta^{13}C$ and surface chl-*a* is globally consistent, irrespective of taxonomic resolution or spatial scale. For all species, coral or endosymbiont $d^{13}C$ values showed no relationship to chl-*a* but $\Delta^{13}C$, while variable, declined significantly with increased chl-*a* (Tables 1.S2, 1.S3). This relationship was similar when constrained to an archipelago scale (islands within the same region averaged together) to account for potential geographic sampling biases ($F_{(1,5)} = 18.35$, $p = 0.01$, $r2 = 0.79$). Controlling for four coral families common to all islands, surface chl-*a* remained a significant predictor but explained less variation than the original model at an island-scale ($F_{(1,14)} = 19.04$, $p < 0.01$ r2= 0.58). When we controlled for coral taxonomy within archipelagos this model explained much more variation ($F_{(1,5)} = 74.31$, $p < 0.01$, r2= 0.94). Across seven additional linear models that varied by total species number and sampling location, the slope of our observed relationship varied by 6% and explained 70-86% of the overall variation in coral $\Delta^{13}C$ (Table 1.S3). Coral host $d^{13}C$ was only related to surface chl-*a* in the two most simplified models and endosymbiont $d^{13}C$ was not related to surface chl-*a* in any model. Notably, surface chl-*a* explained 86% of the variation in *Pocillopora spp.* $\Delta^{13}C$ alone

from the Maldives and central Pacific with a similar slope and intercept to the global model (Table 1.S3).

DISCUSSION

Mixotrophic corals benefit greatly from heterotrophic nutrition but the role of oceanographic processes in structuring food availability, and the associated responses of corals, have not been widely studied (Palardy *et al.* 2005; Leichter & Genovese 2006; Williams *et al.* 2018). Our results indicate the trophic ecology of some corals is spatially flexible, such that corals will increase their use of heterotrophic nutrition when resources are abundant. Specifically, we provide empirical evidence that spatial gradients in nearshore primary production (PP_n) around coral reef islands can directly influence the nutritional status of mixotrophic corals on shallow reefs. Most importantly, we demonstrate that heterotrophic carbon incorporation ($\Delta^{13}C = \delta^{13}C_{host} - \delta^{13}C_{endosymbiont}$) is related to surface chlorophyll-*a* (chl-*a*) at a global scale for multiple coral species across three oceans. We also illustrate that PP_n gradients can influence coral trophic ecology across islands and archipelagos. Our findings support the recent observation that seabird-vectored nutrients may stimulate PP_n and subsequently enhance the growth and biomass of coral reef fish populations (Graham *et al.* 2018). Notably, our study is the first to link patterns of PP_n with the nutrition of coral communities (Fig. 1.3), which provides further evidence that variation in PP_n has strong implications for coral reef ecosystem functioning at multiple scales and trophic levels.

Our results support a working model that many corals will increase heterotrophy as a function of food availability. This is not surprising, as feeding in some coral species is nearly constant (Lewis & Price 1975; Ferrier-Pagès *et al.* 2003) and heterotrophic nutrition is often a

function of prey encounter rather than a necessity driven by metabolic deficit (Maier *et al.* 2010). Consequently, patterns of PP_n likely have significant influence on the nutritional status and energetic budgets of coral populations. Based on the strong agreement of our statistical analyses with this process-based model, we conclude that the nutritional status of mixotrophic corals is tightly coupled with patterns of PP_n on a global scale. Specifically, using surface chl-*a* as a proxy for PP_n we were able to estimate the $\Delta^{13}C$ value of multiple coral species at 10 m depth. For example, $\Delta^{13}C$ values were highly variable among thirteen species of coral from Jamaica (Table S2) (Muscatine *et al.* 1989), but when considered together, the mean $\Delta^{13}C$ converged on the value predicted by our linear regression. In another example, this relationship captured large seasonal variations in $\Delta^{13}C$ reported for *Orbicella faveolata* in the northern Florida Keys at 8 m depth (Swart *et al.* 2005). Using the climatological mean chl-*a* for this region (0.21 mg chl-*a* m^{-3}), our model was able to approximate the inter-annual mean $\Delta^{13}C$ (-1.1 ‰) reported by (Swart *et al.* 2005) within the error bounds of the linear regression ($\Delta^{13}C$ = 0.6 to -1.1‰). We acknowledge that this relationship may not be relevant for all species, as corals demonstrate diverse nutritional strategies (Lewis & Price 1975; Porter 1976; Hoogenboom *et al.* 2015) and differential feeding responses under stressful conditions (Grottoli *et al.* 2006; Grottoli *et al.* 2014). Furthermore, the relationship described here cannot resolve all variation in coral $\Delta^{13}C$ driven by changes in metabolic demands associated with seasonality or environmental conditions (e.g., temperature, light, nutrients) (Anthony & Fabricius 2000). This implies that the capacity of our model to predict coral trophic strategies will likely improve with the inclusion of additional environmental parameters. For example, in regions of strong seasonal upwelling, large drops in temperature can lower coral metabolic rates and suppress feeding during times of increased food availability (Palardy *et al.* 2005). Most importantly, our results show that the relationship

between $\Delta^{13}C$ and surface chl-*a* is effectively constant, whether for a single species (*P. meandrina*) or a global composite of $\Delta^{13}C$ means derived from 15 species across 16 locations (Leichter *et al.* 1996; Williams *et al.* 2018).

Our findings also provide strong evidence that at smaller spatial scales (islands and archipelagos) PP_n can influence how a common coral species relies on heterotrophic nutrition across depths. In oligotrophic waters, corals primarily subsist on autotrophy in the particulate-deplete but well-illuminated shallows (more positive $\Delta^{13}C$) and supplement with heterotrophy as particulate resource availability increases with depth (Muscatine *et al.* 1989; Leichter *et al.* 1996; Palardy *et al.* 2005; Williams *et al.* 2018). Consistent with this expectation, heterotrophic nutrition in *P. meandrina* increased with depth (more negative $\Delta^{13}C$) on the least productive islands in the SLI (Flint and Vostok). In more productive regions, deep-water internal waves frequently deliver inorganic nutrients and planktonic biomass from below the thermocline (Leichter *et al.* 1996; Leichter *et al.* 2012), leading to increased surface chl-*a* and greater food availability at shallower depths(Hazen & Johnston 2010; Sevadjian *et al.* 2012; Gove *et al.* 2016). Our results indicate that *P. meandrina* consumed more heterotrophic carbon (more negative $\Delta^{13}C$) across all depths on Millennium, Starbuck and Malden. This reduction in $\Delta^{13}C$ was driven by greater incorporation of carbon from zooplankton by the coral host (lower $\Delta^{13}C_{coral\text{-}zooplankton}$). Coral C:N ratios also increased, consistent with greater lipid content from heterotrophy in the host tissue, which can play an important role in coral resistance to and recovery following bleaching (Baumann *et al.* 2014). In contrast, $\delta^{15}N$ values did not show consistent patterns across the SLI, suggesting that these changes in heterotrophy may be rather small in the context of the overall nutritional budget of the corals. Thus, $\delta^{13}C$ may be a more informative proxy for detecting subtle changes in coral nutrition.

Satellite-derived estimates of PP_n provide useful estimates of food availability for shallow water corals, however these estimates do not capture all of the processes that influence food abundance and distribution on a given reef. For example, the $\Delta^{13}C$ values on Millennium did not vary with depth as expected based on surface chl-*a* concentrations alone (chl-*a* concentrations similar to Flint and Vostok, Fig. 1A). As the only atoll in the SLI, Millennium possesses a lagoon that exchanges water with the reef and the flushing of productive lagoon waters can influence PP_n (Gove *et al.* 2016). Notably, spatially explicit downwelling of zooplankton-rich water from Palmyra Atoll's lagoon interacts with internal waves to homogenize food availability across depths, leading to static $\Delta^{13}C$ values in *P. meandrina* from 10-30 m (Williams *et al.* 2018) and we hypothesize this is what is occurring at Millennium. Thus, where *inter*- and *intra*-island physical processes increase heterotrophic resources or re-distribute them throughout the water column, corals may feed opportunistically regardless of depth (Palardy *et al.* 2008; Williams *et al.* 2018).

To date, the physiological benefits of heterotrophic nutrition in corals have largely been determined in laboratory experiments (reviewed in (Houlbrèque & Ferrier-Pagès 2009)), though several studies have linked *in situ* feeding with resistance to and recovery following bleaching (Grottoli *et al.* 2006; Palardy *et al.* 2008). As such, corals on reefs with elevated PP_n and greater access to heterotrophic resources may have a greater capacity to survive and recover from acute disturbances (Anthony *et al.* 2009; Levas *et al.* 2013). On some coastal reefs, anthropogenic nutrient pollution can increase chl-*a* concentrations (Wooldridge 2009) and, more importantly, disrupt nitrogen to phosphorus ratios (N:P) which can increase bleaching sensitivity in corals (Wiedenmann *et al.* 2012). Our study identified 16 locations that span a three-fold gradient of naturally elevated surface chl-*a* (0.09-0.29 mg chl-*a* m^{-3}) yet the highest values are 1.5-6 times

lower than concentrations associated with increased bleaching sensitivity (>0.45 mg chl-*a* m^{-3}) (Wooldridge 2016) and reduced species diversity in polluted locations (2 mg chl-*a* m^{-3}) (Duprey *et al.* 2016). Thus, although in some coastal or more heavily impacted regions coral resistance to bleaching may not be correlated with surface chl-*a*, for many reefs slightly elevated chl-*a* likely confers benefits (Williams *et al.* 2015a). Future work to disentangle the roles of heterotrophic nutrition and background nutrient levels to coral persistence at will be valuable for refining projected coral reef trajectories in a warming ocean.

In conclusion, our study provides the first empirical evidence that coral trophic strategies track nearshore primary production (PP_n) at multiple spatial scales. Our established relationship between coral nutrition ($\Delta^{13}C$) and surface chl-*a* has high explanatory power and is based on freely available data. Importantly, our model can be applied to coral trophic ecology throughout the tropics because this metric of PP_n is globally comprehensive. Previous investigations of upwelling and PP_n on coral reefs have focused on the role of cooler, upwelled water to moderate temperatures and thus promote coral resistance to bleaching (Karnauskas & Cohen 2012; Riegl *et al.* 2015; Wall *et al.* 2015; Karnauskas *et al.* 2016). Given the strong connection between coral nutrition and PP_n described here, the contribution of heterotrophy to coral recovery from bleaching has likely been underestimated in areas of naturally elevated PP_n. As such, our model provides a framework to evaluate the importance of heterotrophy to the resilience of coral populations across regions with different background PP_n. This information is essential for improving estimates of the response of corals, and other mixotrophic communities, to predicted variations in PP_n in an era of global change.

ACKNOWLEDGEMENTS

We are grateful to the Environment and Conservation Division of the Republic of Kiribati for allowing us to conduct research within the Southern Line Islands. The authors thank the owner, captain, and crew of the M/Y Hanse Explorer for logistical support and field assistance. We also thank Jessica Glanz, Ellis Juhlin, Spencer Breining-Aday, Annika Vawter, and Ellen Williams for assistance in the lab. We thank the Moore Family Foundation, the Scripps family and several anonymous donors for their generous financial support. Finally, we are grateful to three anonymous reviewers for their time and valuable comments that have helped to improve this manuscript. MDF was supported by a Nancy Foster Scholarship from the NOAA Office of National Marine Sanctuaries.

Chapter 1, in full, has been accepted at *Current Biology* and is in press. Fox, Michael D.; Williams, Gareth J.; Johnson, Maggie D.; Radice, Veronica, Z.; Zgliczynski, Brian J.; Kelly, Emily L.A.; Rohwer, Forest L.; Sandin, Stuart A.; Smith, Jennifer E. The dissertation author was the primary investigator and author of this material.

References

Alamaru, A., Loya, Y., Brokovich, E., Yam, R. & Shemesh, A. (2009). Carbon and nitrogen utilization in two species of Red Sea corals along a depth gradient: Insights from stable isotope analysis of total organic material and lipids. *Geochem. Cosmochim. Ac.*, 73, 5333-5342.

Altabet, M.A. (2001). Nitrogen isotopic evidence for micronutrient control of fractional NO_3^- utilization in the equatorial Pacific. *Limnol. Oceanogr*, 46, 368-380.

Anthony, K.R. & Fabricius, K. (2000). Shifting roles of heterotrophy and autotrophy in coral energetics under varying turbidity *J. Exp. Mar. Biol. Ecol.*, 252, 221-253.

Anthony, K.R.N., Hoogenboom, M.O., Maynard, J.A., Grottoli, A.G. & Middlebrook, R. (2009). Energetics approach to predicting mortality risk from environmental stress: a case study of coral bleaching. *Funct. Ecol.*, 23, 539-550.

Barton, K. (2015). MuLIn: Multi-Model Inference. *R Package version 1.13.4*.

Bates, D., Mächler, M., Bolker, B.M. & Walker, S. (2015). Fitting linear mixed-effects models using lme4. *J. Stat. Software*, 67, 1-48.

Baumann, J., Grottoli, A.G., Hughes, A.D. & Matsui, Y. (2014). Photoautotrophic and heterotrophic carbon in bleached and non-bleached coral lipid acquisition and storage. *J. Exp. Mar. Biol. Ecol.*, 461, 469-478.

Behrenfeld, M.J., O'Malley, R.T., Siegel, D.A., McClain, C.R., Sarmiento, J.L., Feldman, G.C., Milligan, A.J., Falkowski, P.G., Letelier, R.M. & Boss, E.S. (2006). Climate-driven trends in contemporary ocean productivity. *Nature*, 444, 752.

Brainard, R.E., Oliver, T., McPhaden, M.J., Cohen, A., Venegas, R., Heenan, A., Vargas-Ángel, B., Roţjan, R., Mangubhai, S. & Flint, E. (2018). Ecological Impacts of the 2015/16 El Niño in the Central Equatorial Pacific. *Bull. Amer. Meteor. Soc.*, 99, S21-S26.

Cox, E.F. (2007). Continuation of sexual reproduction in *Montipora capitata* following bleaching. *Coral Reefs*, 26, 721-724.

Croll, D.A., Marinovic, B., Benson, S., Chavez, F.P., Black, N., Ternullo, R. & Tershy, B.R. (2005). From wind to whales: trophic links in a coastal upwelling system. *Mar. Ecol. Prog. Ser.*, 289, 117-130.

Davies, P.S. (1984). The role of zooxanthellae in the nutritional energy requirements of *Pocillopora eydouxi*. *Coral Reefs*, 2, 181-186.

Drenkard, E.J., Cohen, A.L., McCorkle, D.C., de Putron, S.J., Starczak, V.R. & Zicht, A.E. (2013). Calcification by juvenile corals under heterotrophy and elevated CO_2. *Coral Reefs*, 32, 727-735.

Duprey, N.N., Yasuhara, M. & Baker, D.M. (2016). Reefs of tomorrow: Eutrophication reduces coral biodiversity in an urbanized seascape. *Global Change Biol.*, 22, 3550-3565.

Edmunds, P.J. (2011). Zooplanktivory ameliorates the effects of ocean acidification on the reef coral *Porites* spp. *Limnol. Oceanogr.*, 56, 2402-2410.

Ellison, A.M. & Gotelli, N.J. (2002). Nitrogen availability alters the expression of carnivory in the northern pitcher plant, *Sarracenia purpurea*. *Proc. Natl. Acad. Sci. USA.*, 99, 4409-4412.

Falkowski, P.G., Dubinsky, Z., Muscatine, L. & Porter, J.W. (1984). Light and the bioenergetics of a symbiotic coral. *Bioscience*, 34, 705-709.

Ferrier-Pagès, C., Hoogenboom, M. & Houlbrèque, F. (2011). The role of plankton in coral trophodynamics. In: *Coral Reefs: an ecosystem in transition* (eds. Dubinsky, Z & Stambler, N). Springer Netherlands, pp. 215-229.

Ferrier-Pagès, C., Witting, J., Tambutte, E. & Sebens, K.P. (2003). Effect of natural zooplankton feeding on the tissue and skeletal growth of the scleractinian coral *Stylophora pistillata*. *Coral Reefs*, 22, 229-240.

Furla, P., Allemand, D., Shick, J.M., Ferrier-Pagès, C., Richier, S., Plantivaux, A., Merle, P.-L. & Tambutté, S. (2005). The Symbiotic Anthozoan: A Physiological Chimera between Alga and Animal1. *Integrative and Comparative Biology*, 45, 595-604.

Gove, J.M., McManus, M.A., Neuheimer, A.B., Polovina, J.J., Drazen, J.C., Smith, C.R., Merrifield, M.A., Friedlander, A.M., Ehses, J.S., Young, C.W., Dillon, A.K. & Williams, G.J. (2016). Near-island biological hotspots in barren ocean basins. *Nat Commun*, 7, 10581.

Gove, J.M., Williams, G.J., McManus, M.A., Heron, S.F., Sandin, S.A., Vetter, O.J. & Foley, D.G. (2013). Quantifying climatological ranges and anomalies for Pacific coral reef ecosystems. *PLoS ONE*, 8, e61974.

Graham, N.A.J., Wilson, S.K., Carr, P., Hoey, A.S., Jennings, S. & MacNeil, M.A. (2018). Seabirds enhance coral reef productivity and functioning in the absence of invasive rats. *Nature*, 559, 250.

Grottoli, A.G., Rodrigues, L.J. & Palardy, J.E. (2006). Heterotrophic plasticity and resilience in bleached corals. *Nature*, 440, 1186-1189.

Grottoli, A.G., Warner, M.E., Levas, S.J., Aschaffenburg, M.D., Schoepf, V., McGinley, M., Baumann, J. & Matsui, Y. (2014). The cumulative impact of annual coral bleaching can turn some coral species winners into losers. *Global Change Biol.*, 20, 3823-3833.

Grottoli, A.G. & Wellington, G.M. (1999). Effect of light and zooplankton on skeletal $\delta^{13}C$ values in the eastern tropical Pacific corals *Pavona clavus* and *Pavona gigantea*. *Coral Reefs*, 18, 29-41.

Hazen, E.L. & Johnston, D.W. (2010). Meridional patterns in the deep scattering layers and top predator distribution in the central equatorial Pacific. *Fish. Oceanogr.*, 19, 427-433.

Hoogenboom, M., Rottier, C., Sikorski, S. & Ferrier-Pagès, C. (2015). Among-species variation in the energy budgets of reef-building corals: scaling from coral polyps to communities. *J. Exp. Biol.*, 218, 3866-3877.

Houlbrèque, F. & Ferrier-Pagès, C. (2009). Heterotrophy in tropical scleractinian corals. *Biol Rev Camb Philos Soc*, 84, 1-17.

Houlbrèque, F., Tambutté, E. & Ferrier-Pagès, C. (2003). Effect of zooplankton availability on the rates of photosynthesis, and tissue and skeletal growth in the scleractinian coral *Stylophora pistillata*. *J. Exp. Mar. Biol. Ecol.*, 296, 145-166.

Hughes, A.D., Grottoli, A.G., Pease, T.K. & Matsui, Y. (2010). Acquisition and assimilation of carbon in non-bleached and bleached corals. *Mar. Ecol. Prog. Ser.*, 420, 91-101.

Hurvich, C.M. & Tsai, C. (1989). Regression and time series model selection in small samples. *Biometrika*, 76, 297-307.

Johnston, E.C., Forsman, Z.H., Flot, J.-F., Schmidt-Roach, S., Pinzón, J.H., Knapp, I.S.S. & Toonen, R.J. (2017). A genomic glance through the fog of plasticity and diversification in Pocillopora. *Sci. Rep.*, 7, 5991.

Karnauskas, K.B. & Cohen, A.L. (2012). Equatorial refuge amid tropical warming. *Nat. Clim. Chang.*, 2, 530-534.

Karnauskas, K.B., Cohen, A.L. & Gove, J.M. (2016). Mitigation of Coral Reef warming across the Central Pacific by the equatorial undercurrent: a past and future divide. *Sci. Rep.*, 6.

Kelly, L.W., Williams, G.J., Barott, K.L., Carlson, C.A., Dinsdale, E.A., Edwards, R.A., Haas, A.F., Haynes, M., Lim, Y.W., McDole, T., Nelson, C.E., Sala, E., Sandin, S., Smith, J., E., Vermeij, M.J., Youle, M. & Rohwer, F. (2014). Local genomic adaptation of coral reef-associated microbiomes to gradients of natural variability and anthropogenic stressors. *Proceedings of the National Academy of Sciences of the United States of America*, 111, 10227-10232.

Leichter, J.J. & Genovese, S.J. (2006). Intermittent upwelling and subsidized growth of the scleractinian coral *Madracis mirabilis* on the deep fore-reef slope of Discovery Bay, Jamaica. *Mar. Ecol. Prog. Ser.*, 316, 95-103.

Leichter, J.J., Stokes, M.D., Hench, J.L., Witting, J. & Washburn, L. (2012). The island-scale internal wave climate of Moorea, French Polynesia. *J. Geophys. Res. Oceans*, 117.

Leichter, J.J., Wing, S.R., Miller, S.L. & Denny, M.W. (1996). Pulsed delivery of subthermocline water to Conch Reef (Florida Keys) by internal tidal bores. *Limnol. Oceanogr.*, 41, 1490-1501.

Levas, S.J., Grottoli, A.G., Hughes, A., Osburn, C.L. & Matsui, Y. (2013). Physiological and biogeochemical traits of bleaching and recovery in the mounding species of coral Porites lobata: implications for resilience in mounding corals. *PloS one*, 8, e63267.

Lewis, J.B. & Price, W.S. (1975). Feeding mechanisms and feeding strategies of Atlantic reef corals. *J. Zool.*, 176, 527-544.

Lindell, D. & Post, A.F. (1995). Ultraphytoplankton succession is triggered by deep winter mixing in the Gulf of Aqaba (Eilat), Red Sea. *Limnol. Oceanogr.*, 40, 1130-1141.

Maier, C., Weinbauer, M.G. & Pätzold, J. (2010). Stable isotopes reveal limitations in C and N assimilation in the Caribbean reef corals Madracis auretenra, M. carmabi and M. formosa. *Mar. Ecol. Prog. Ser.*, 412, 103-112.

Matsuda, Y., Shimizu, S., Mori, M., Ito, S.I. & Selosse, M.A. (2012). Seasonal and environmental changes of mycorrhizal associations and heterotrophy levels in mixotrophic *Pyrola japonica* (Ericaceae) growing under different light environments. *Am. J. Bot.*, 99, 1177-1188.

Muscatine, L., McCloskey, L.R. & Marian, R.E. (1981). Estimating the daily contribution of carbon from zooxanthellae to coral animal respiration. *Limnol. Oceanogr.*, 26, 601-611.

Muscatine, L. & Porter, J.W. (1977). Reef corals: mutualistic symbioses adapted to nutrient-poor environments. *Bioscience*, 27, 454-460.

Muscatine, L., Porter, J.W. & Kaplan, I.R. (1989). Resource partitioning by reef corals as determined from stable isotope composition. I $\delta^{13}C$ of zooxanthellae and animal tissue vs depth. *Mar. Biol.*, 100, 185-193.

Nahon, S., Richoux, N.B., Kolasinski, J., Desmalades, M., Pages, C.F., Lecellier, G., Planes, S. & Lecellier, V.B. (2013). Spatial and temporal variations in stable carbon ($\delta^{13}C$) and nitrogen ($\delta^{15}N$) isotopic composition of symbiotic scleractinian corals. *PloS One*, 8, e81247.

Palardy, J.E., Grottoli, A.G. & Matthews, K.A. (2005). Effects of upwelling, depth, morphology and polyp size on feeding in three species of Panamanian corals. *Mar. Ecol. Prog. Ser.*, 300, 79-89.

Palardy, J.E., Rodrigues, L.J. & Grottoli, A.G. (2008). The importance of zooplankton to the daily metabolic carbon requirements of healthy and bleached corals at two depths. *J. Exp. Mar. Biol. Ecol.*, 367, 180-188.

Porter, J.W. (1976). Autotrophy, heterotrophy, and resource partitioning in Caribbean reef-building corals. *Am. Nat.*, 110, 731-742.

Rebert, J.P., Donguy, J.R., Eldin, G. & Wyrtki, K. (1985). Relations between sea level, thermocline depth, heat content, and dynamic height in the tropical Pacific Ocean. *J. Geophys. Res. Oceans*, 90, 11719-11725.

Riegl, B., Glynn, P.W., Wieters, E., Purkis, S., d'Angelo, C. & Wiedenmann, J. (2015). Water column productivity and temperature predict coral reef regeneration across the Indo-Pacific. *Sci Rep*, 5, 8273.

Rodrigues, L.J. & Grottoli, A.G. (2006). Calcification rate and the stable carbon, oxygen, and nitrogen isotopes in the skeleton, host tissue, and zooxanthellae of bleached and recovering Hawaiian corals. *Geochem. Cosmochim. Ac.*, 70, 2781-2789.

Selosse, M.-A., Charpin, M. & Not, F. (2016). Mixotrophy everywhere on land and in water: the grand écart hypothesis. *Ecol. Lett.*, doi: 10.1111/ele.12714.

Sevadjian, J.C., McManus, M.A., Benoit-Bird, K.J. & Selph, K.E. (2012). Shoreward advection of phytoplankton and vertical re-distribution of zooplankton by episodic near-bottom water pulses on an insular shelf: Oahu, Hawaii. *Cont. Shelf. Res.*, 50, 1-15.

Smith, J.E., Brainard, R., Carter, A., Grillo, S., Edwards, C., Harris, J., Lewis, L., Obura, D., Rohwer, F. & Sala, E. (2016). Re-evaluating the health of coral reef communities: baselines and evidence for human impacts across the central Pacific. *Proc. R. Soc. B*, 283, 20151985.

Stimson, J. & Kinzie, R.A. (1991). The temporal pattern and rate of release of zooxanthellae from the reef coral *Pocillopora damicornis* (Linnaeus) under nitrogen-enrichment and control conditions *J. Exp. Mar. Biol. Ecol.*, 153, 63-74.

Stoecker, D.K., Hansen, P.J., Caron, D., A. & Mitra, A. (2017). Mixotrophy in the Marine Plankton. *Ann. Rev. Mar. Sci.*, 9, 311-335.

Swart, P.K., Saied, A. & Lamb, K. (2005). Temporal and spatial variation in the $\delta^{15}N$ and $\delta^{13}C$ of coral tissue and zooxanthellae in *Montastraea faveolata* collected from the Florida reef tract. *Limnol. Oceanogr.*, 50, 1049-1058.

Tremblay, P., Gori, A., Maguer, J.F., Hoogenboom, M. & Ferrier-Pagès, C. (2016). Heterotrophy promotes the re-establishment of photosynthate translocation in a symbiotic coral after heat stress. *Sci. Rep.*, 6, 38112.

Tremblay, P., Maguer, J.F., Grover, R. & Ferrier-Pagès, C. (2015). Trophic dynamics of scleractinian corals: stable isotope evidence. *J. Exp. Biol.*, 218, 1223-1234.

Venn, A.A., Loram, J.E. & Douglas, A.E. (2008). Photosynthetic symbioses in animals. *J. Exp. Bot.*, 59, 1069-1080.

Veron, J.E.N. (1995). *Corals in space and time: the biogeography and evolution of the Scleractinia*. Cornell University Press.

Wall, M., Putchim, L., Schmidt, G.M., Jantzen, C., Khokiattiwong, S. & Richter, C. (2015). Large-amplitude internal waves benefit corals during thermal stress. *Proc. R. Soc. B.*, 282, 20140650.

Wellburn, A.R. (1994). The spectral determination of chlorophylls a and b, as well as total carotenoids, using various solvents with spectrophotometers of different resolution. *J. Plant Physiol.*, 144, 307-313.

Wiedenmann, J., D'Angelo, C., Smith, E.G., Hunt, A.N., Legiret, F.-E., Postle, A.D. & Achterberg, E.P. (2012). Nutrient enrichment can increase the susceptibility of reef corals to bleaching. *Nat. Clim. Chang.*, 3, 160-164.

Williams, G.J., Gove, J.M., Eynaud, Y., Zgliczynski, B.J. & Sandin, S.A. (2015a). Local human impacts decouple natural biophysical relationships on Pacific coral reefs. *Ecography*, 38, 751-761.

Williams, G.J., Knapp, I.S., Maragos, J.E. & Davy, S.K. (2010). Modeling patterns of coral bleaching at a remote Central Pacific atoll. *Mar. Pollut. Bull.*, 60, 1467-1476.

Williams, G.J., Sandin, S.A., Zgliczynski, B., Fox, M.D., Furby, K., Gove, J.M., Rogers, J.S., Hartmann, A.C., Caldwell, Z.R., Price, N.N. & Smith, J., E. (2018). Biophysical drivers of coral trophic depth zonation. *Mar. Biol.*, 165, 60.

Williams, G.J., Smith, J.E., Conklin, E.J., Gove, J.M., Sala, E. & Sandin, S.A. (2013). Benthic communities at two remote Pacific coral reefs: effects of reef habitat, depth, and wave energy gradients on spatial patterns. *PeerJ*, 1, e81.

Williams, I.D., Baum, J.K., Heenan, A., Hanson, K.M., Nadon, M.O. & Brainard, R.E. (2015b). Human, Oceanographic and Habitat Drivers of Central and Western Pacific Coral Reef Fish Assemblages. *PLoS ONE*, 10, e0120516.

Wooldridge, S.A. (2009). Water quality and coral bleaching thresholds: Formalising the linkage for the inshore reefs of the Great Barrier Reef, Australia. *Mar. Pollut. Bull.*, 58, 745-751.

Wooldridge, S.A. (2016). Excess seawater nutrients, enlarged algal symbiont densities and bleaching sensitive reef locations: 1. Identifying thresholds of concern for the Great Barrier Reef, Australia. *Mar. Pollut. Bull.*

Zar, J.H. (2007). *Biostatistical Analysis*. Fifth edn. Prentice-Hall, Inc., New Jersey.

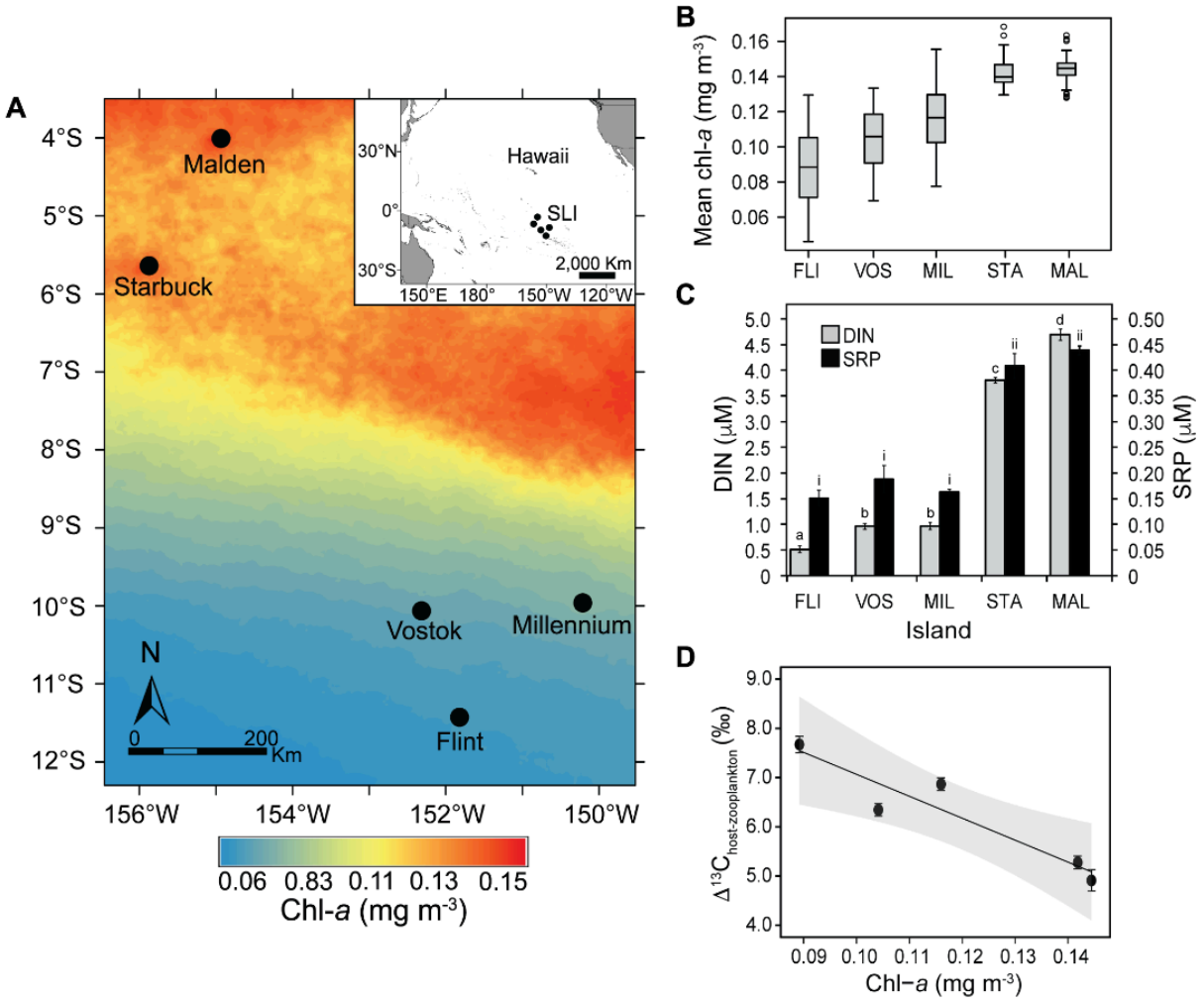

Figure 1.1. Oceanographic climate of the Southern Line Islands. A Satellite-derived climatological means of surface chlorophyll-*a* in the Southern Line Islands from 2004-2015. **B** Boxplot of annual mean chl-*a* concentrations calculated for each of the most proximate pixels to an island. The box represents lower and upper quartiles with the median value shown as a black line. Whiskers represent the minimum and maximum values that are not greater than 1.5 times the difference between the upper and lower quartiles. All data beyond this limit are displayed as points. **C** Mean inorganic nutrient concentrations across all depths (5, 10, 15, 25, 30 m; n=3 per depth). Error bars are ± 1SE. For dissolved inorganic nitrogen (DIN), letters denote significant differences at the $p < 0.05$ level and for soluble reactive phosphorus (SRP) differences are denoted with i or ii. **D** Mean differences between coral host and zooplankton $\delta^{13}C$ ($\Delta^{13}C_{coral\text{-}zooplankton}$) across the SLI as a function of mean surface chl-*a*. All data are from corals at 10 m (n=5) and the zooplankton values were calculated as the mean of duplicate samples from three different sites on the leeward coast (n=3) of each island. The line represents best-fit linear regression ($p < 0.01$, $r^2 = 0.94$) and the shaded region represents ± 1SE of the linear fit. See also Fig. S1.

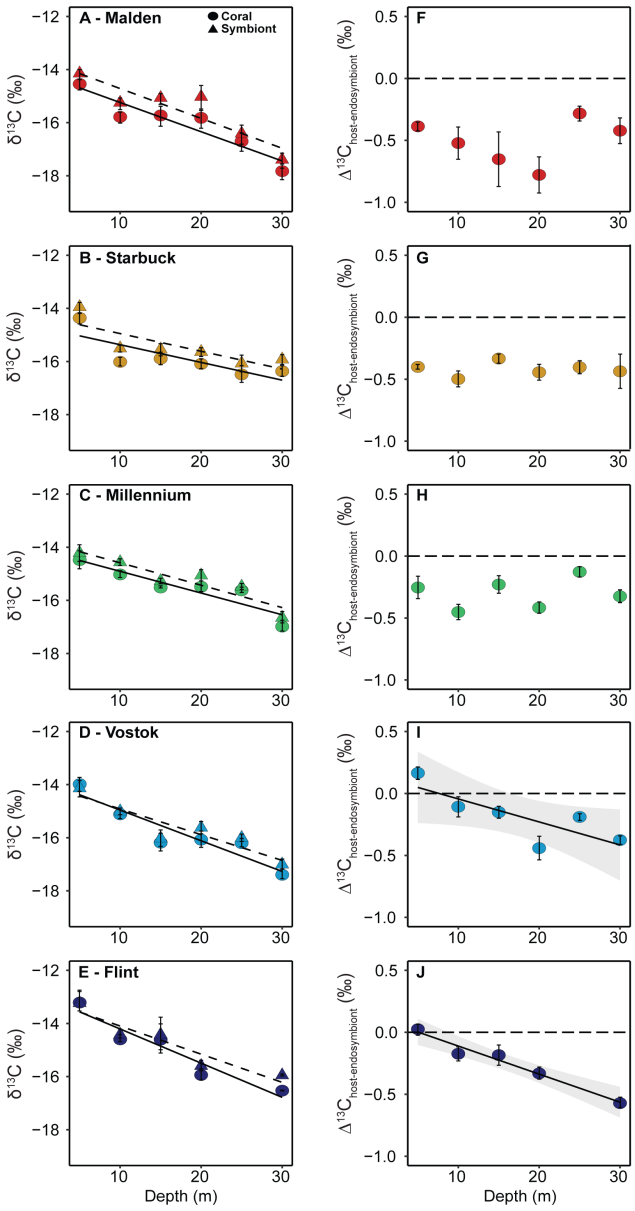

Figure 1.2. *Pocillopora meandrina* host and endosymbiont d^{13}C and Δ^{13}C across depth in the SLI. Islands are ordered top to bottom from north to south, in order of decreasing surface chl-*a*. Data are presented for depths 5-30 m in 5 m intervals (n-6 per island) In plots **A-E**, the lines are provided to help visualize the relationship between tissue d^{13}C and depth in the coral host (solid) and endosymbiont (dashed) fractions. In plots **F-J** the dashed line represents **Δ^{13}C** ($\delta^{13}C_{host}$ -$\delta^{13}C_{endosymbiont}$) = 0, or no difference in d^{13}C between coral host and endosymbiont tissues. All data points and error bars represent mean values ± 1SE (n = 5) except for Flint 30 m (n = 3). Lines of best fit are displayed for significant linear regressions of Δ^{13}C as a function of depth at each island. Shaded areas represent ± 1SE of the linear fit and error bars represent ± 1SE of the mean. See also Fig. S1 and Table S1-2.

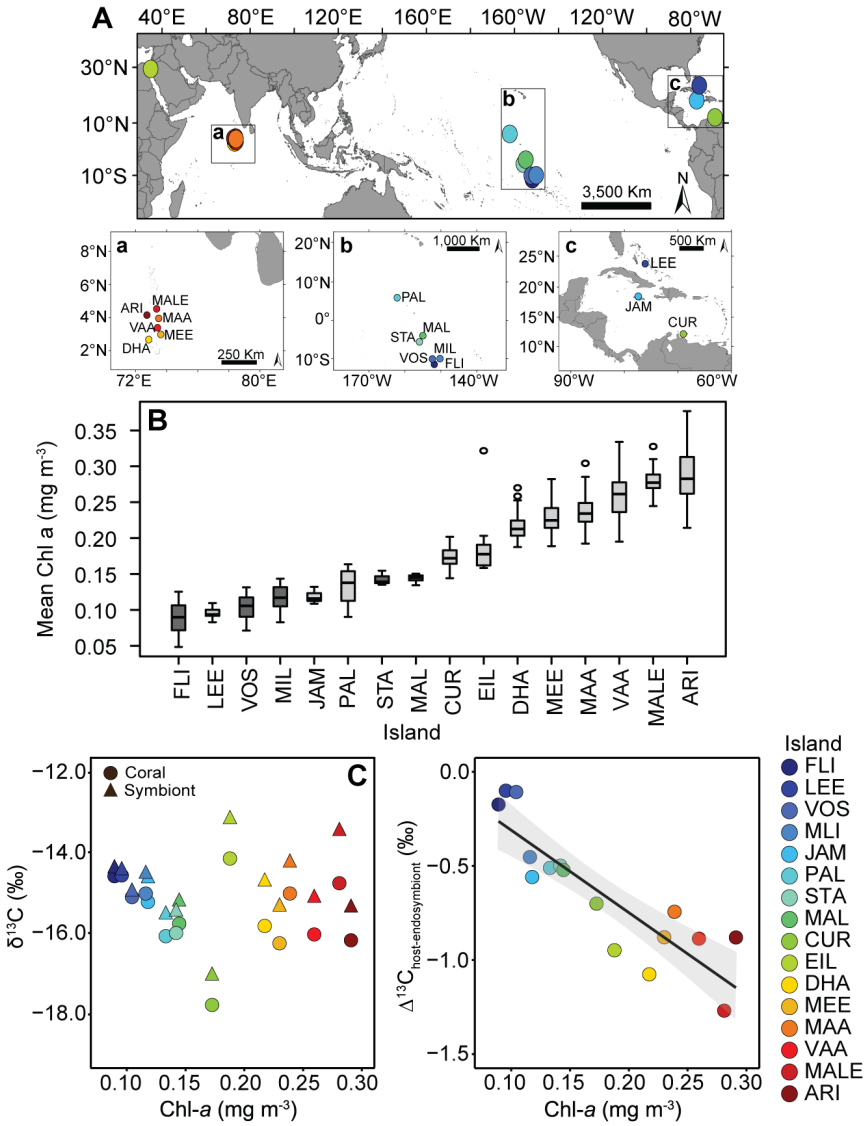

Figure 1.3. Global patterns of coral and endosymbiont $d^{13}C$ and $\Delta^{13}C$ as a function of surface chl-*a*. **A** Locations from the global data set are depicted in the maps with the first three to four letters of each location corresponding to the island name in the magnified regions for the **(a)** Maldives, **(b)** central Pacific, and **(c)** Caribbean basin. The Gulf of Eilat is shown only in the global map. Regions of lower surface chl-*a* are shown in blue and areas of higher surface chl-*a* in red. **B** Boxplot of annual mean surface chl-*a* data from 2004-2015 for all islands. Shaded boxs indicate the five SLI. **C** Mean coral and endosymbiont $d^{13}C$ as a function of surface chl-*a*. **D** Mean $\Delta^{13}C$ ($\delta^{13}C_{coral}$ - $\delta^{13}C_{endosymbiont}$) as a function of surface chl-*a*. Mean values for Jamaica (JAM), Gulf of Eilat (EIL), and all atolls in the Maldives (except MAA) are composite means of all species sampled at that location (see Table S6 for a complete list). Chl-*a* estimates are based on data from between the 7 and 13 most proximate pixels to each sampling location and represent the climatological mean from 2004 to 2015. The line represents best-fit linear regression ($p < 0.001$, $r^2 = 0.77$) and the shaded region represents ± 1SE of the linear fit. See also Fig. S2 and Tables S3-S4.

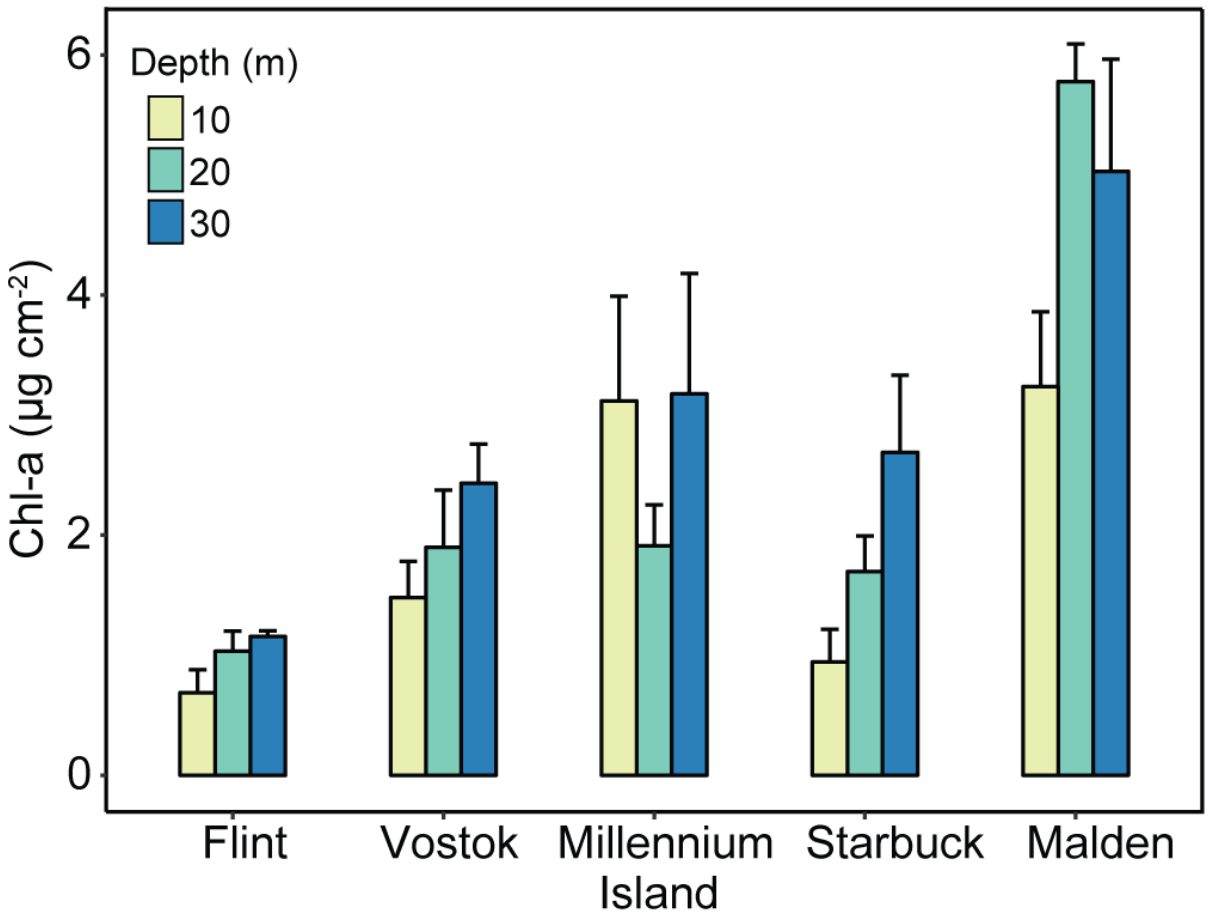

Figure 1.S1. Surface area normalized chl-*a* concentrations (µg chl-*a* cm^{-2}) of *Pocillopora meandrina* across islands and depth. On all islands n = 5 except for Flint 30 m n=3. The islands are arranged from south to north from left to right, in order of increasing surface chl-*a* Error bars ± 1 SE. Related to Figs. 1.1 and 1.2.

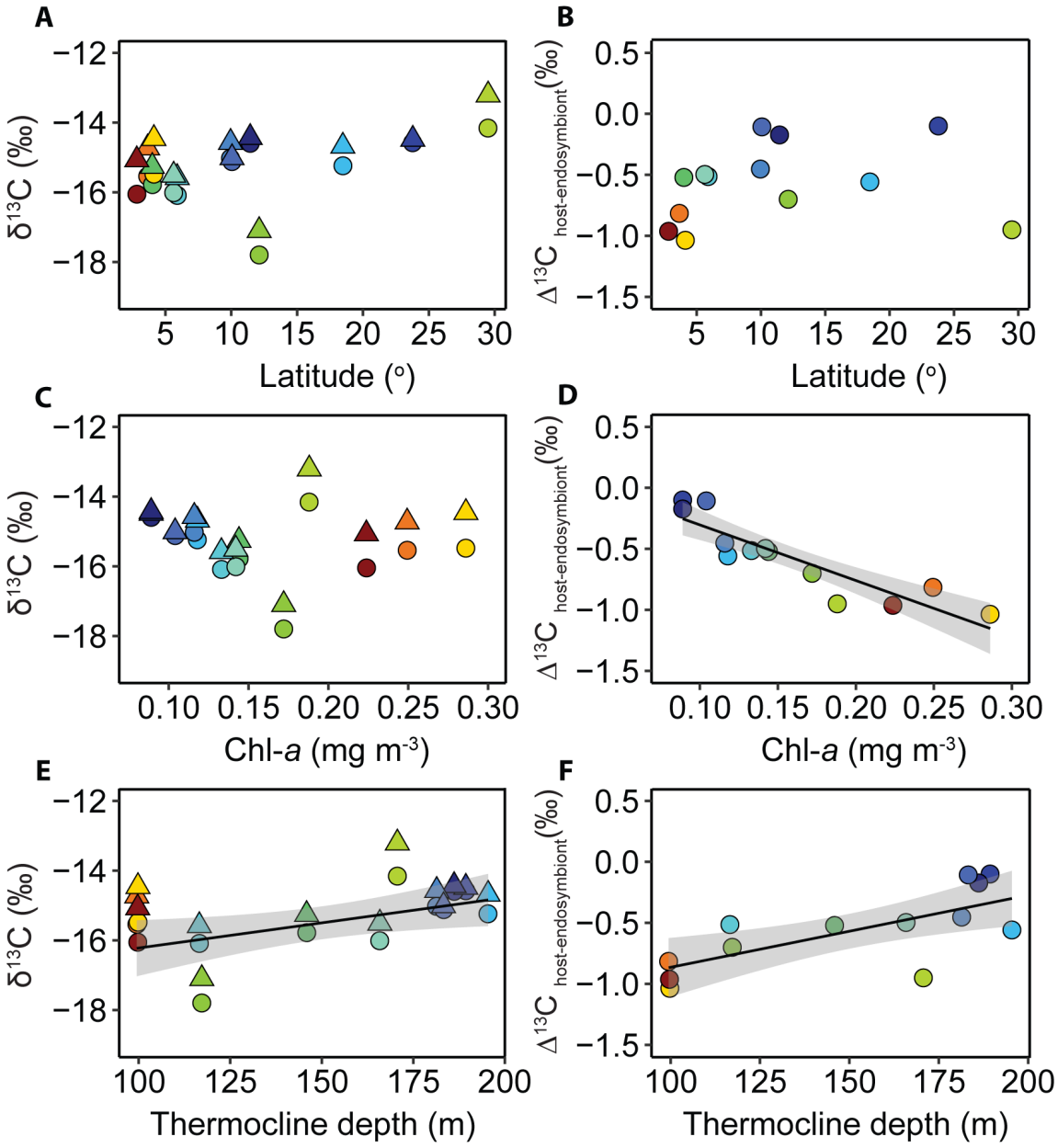

Figure 1.S2. Linear relationships between mean coral and symbionts d^{13}C and Δ^{13}C with latitude, mean chl-*a*, and estimated depth of the thermocline. Coral host values are displayed as circles and the endosymbionts as triangles. Colors correspond to the islands illustrated in Fig. 1.3. Shaded regions represent ± 1SE of linear fit and for panel **E** the sold line refers to the coral host fraction. Please see Supplemental Table 1.S5 and the supplemental methods section Quantification and Statistical Analysis - *Global relationships between coral isotopic ratios and oceanic primary productivity* for a complete explanation of all models. Related to Fig. 1.3 and Table 1.S4.

Table 1.S1. Analysis of Covariance (ANCOVA) results examining coral and endosymbiont isotope geochemistry and their difference (Δ) as a function of island and depth. Significant factors are indicated in bold and pairwise contrasts between islands at the p <0.05 level are indicated with |. Island abbreviations are the first three letters of each island. Related to Fig. 1.2.

Tissue	Variable	Factor	df	MS	F	P	Pairwise Contrasts
Coral Host	$\delta^{13}C$	**Depth**	1	22.01	109.15	**<0.001**	
		Island	4	0.72	3.57	**0.025**	FLI | MAL
		Depth*Island	4	0.28	1.34	0.29	
		Error	19	0.20			
Endosymbiont		**Depth**	1	19.05	93.83	**<0.001**	
		Island	4	0.52	2.54	0.074	
		Depth*Island	4	0.14	0.70	0.60	
		Error	19	0.20			
Host-Endosymbiont	$\Delta^{13}C$	**Depth**	1	0.11	5.98	**0.02**	
		Island	4	0.10	5.55	**< 0.01**	
		Depth*Island	4	0.06	3.472	**0.03**	FLI VOS | MIL STA MAL
		Error	19	0.02	-	-	
Coral Host	$\delta^{15}N$	**Depth**	1	4.37	11.63	**<0.01**	
		Island	4	50.88	135.46	**<0.001**	FLI VOS MIL | STA MAL
		Depth*Island	4	1.5	3.98	**0.02**	
		Error	19	0.38			
Endosymbiont	$\delta^{15}N$	**Depth**	1	5.60	10.89	**<0.01**	
		Island	4	40.70	79.22	**<0.001**	FLI VOS MIL | STA MAL
		Depth*Island	4	0.37	0.73	0.58	
		Error	19	0.51			
Host-Endosymbiont	$\Delta^{15}N$	Depth	1	0.08	0.40	0.53	
		Island	4	0.79	4.20	**0.01**	
		Depth*Island	4	0.62	3.31	**0.03**	FLI |VOS | MIL | STA ; FLI VOS | MAL
		Error	19	0.19	-	-	
Coral Host	C:N	Depth	1	0.45	3.35	0.08	
		Island	4	1.34	9.99	**<0.001**	FLI VOS MIL |STA MAL
		Depth*Island	4	0.24	1.79	0.17	
		Error	19	0.13			
Endosymbiont	C:N	Depth	1	0.21	2.11	0.16	
		Island	4	0.15	1.53	0.23	
		Depth*Island	4	0.04	0.41	0.80	
		Error	19				
Host-Endosymbiont	ΔC:N	Depth	1	0.04	0.34	0.57	
		Island	4	4.46	8.65	**<0.001**	FLI VOS | MIL STA MAL
		Depth*Island	4	0.76	1.48	0.25	
		Error	19	2.45			

Table 1.S2. Global data set of coral $\delta^{13}C$ and and nearshore chl-*a* concentrations. Mean isotopic estimates of coral host tissue and zooxanthellae data are compiled from literature and unpublished studies and are used to calculate $\Delta\delta^{13}C$ and $\Delta\delta^{15}N$. Climatological mean chl-*a* concentrations are reported for the time period 2004-2015. All reported data are from 10 m depth with the exception of Lesser et al. 2010, which had data from 9 m. Data from Maier et al. 2010 only include *M. auretenra* branch tips to be consistent with the samples collected in this study and reported elsewhere. Related to Figs 1.2 and 1.3.

Region	Island	Ocean Basin	Family	Species	Mean Host $\delta^{13}C$	Mean Symbiont $\delta^{13}C$	Mean $\Delta^{13}C$	Mean Host $\delta^{15}N$	Mean Symbiont $\delta^{15}N$	Mean $\Delta^{15}N$	12 yr Chl-*a*	Reference
Bahamans	Lee Stocking	Atlantic	Faviidae	*Montastrea cavernosa*	-14.58	-14.48	-0.10	1.72	2.15	0.435	0.095	Lesser et al. 2010
Caribbean	Curacao	Caribbean Sea	Astrocoeniidae	*Madracis auretenra*	-17.80	-17.10	-0.70	-	-	-	0.172	Maier et al. 2010
Caribbean	Jamaica	Caribbean Sea	Acroporidae	*Acropora cervicornis*	-15.34	-14.05	-1.29	1.86	1.68	0.180	0.118	Muscatine et al. 1989
-	-	-	Acroporidae	*Acropora palmata*	-15.19	-14.72	-0.47	1.48	2.13	-0.650	-	-
-	-	-	Agariciidae	*Agaricia agaricites*	-15.63	-13.91	-1.72	-	-	-	-	-
-	-	-	Meandrinidae	*Dendrogyra cylindrus*	-15.50	-14.94	-0.56	2.23	2.43	-0.200	-	-
-	-	-	Meandrinidae	*Eusmilia fastigiata*	-15.39	-15.12	-0.27	2.52	2.18	0.340	-	-
-	-	-	Astrocoeniidae	*Madracis mirabilis*	-17.74	-16.79	-0.95	3.05	3.26	-0.210	-	-
-	-	-	Faviidae	*Montastraea annularis*	-13.63	-13.87	0.24	2.41	1.83	0.580	-	-
-	-	-	Faviidae	*Montastraea cavernosa*	-13.49	-14.04	0.55	1.11	0.35	0.760	-	-
Northern Line Islands	Palmyra Atoll	-	Pocilloporidae	*Pocillopora meandrina*	-16.09	-15.58	-0.51	11.35	10.54	0.810	0.133	Williams et al. 2018
Southern Line Islands	Flint	Pacific	Pocilloporidae	*Pocillopora meandrina*	-14.60	-14.43	-0.17	15.04	14.96	0.080	0.089	This study
-	Malden	-	Pocilloporidae	-	-15.78	-15.26	-0.52	10.19	10.17	0.020	0.144	This study
-	Millennium Atoll	-	Pocilloporidae	-	-15.03	-14.57	-0.45	15.03	14.17	0.860	0.116	This study
-	Starbuck	-	Pocilloporidae	-	-16.01	-15.51	-0.50	8.57	8.65	-0.080	0.142	This study
-	Vostok	-	Pocilloporidae	-	-15.12	-15.01	-0.11	14.61	14.35	0.260	0.104	This study
Maldives	Vaavu Atoll	Indian	Pocilloporidae	*Pocillopora verrucosa*	-17.68	-16.82	-0.87	5.94	5.17	0.770	0.260	Radice Unpublished Data
-	-	-	Oculinidae	*Galaxea fascicularis*	-15.31	-14.43	-0.89	5.92	4.43	1.490	-	-
-	-	-	Agariciidae	*Pachyseris speciosa*	-15.15	-14.25	-0.91	5.30	5.41	0.070	-	-
-	Maafushi Atoll	-	Agariciidae	*Pachyseris speciosa*	-15.03	-14.29	-0.74	5.26	5.52	-0.260	0.239	Radice Unpublished Data
-	Meemu Atoll	-	Pocilloporidae	*Pocillopora verrucosa*	-18.23	-17.35	-0.88	5.57	5.35	0.220	0.230	Radice Unpublished Data
-	-	-	Oculinidae	*Galaxea fascicularis*	-15.48	-15.20	-0.27	5.36	4.08	1.280	-	-
-	-	-	Agariciidae	*Pachyseris speciosa*	-15.09	-13.60	-1.49	4.99	5.18	-0.190	-	-
-	Male Atoll	-	Agariciidae	*Pachyseris speciosa*	-14.71	-12.76	-1.95	5.22	4.94	0.280	0.281	Radice Unpublished Data
-	-	-	Oculinidae	*Galaxea fascicularis*	-14.84	-14.25	-0.59	4.89	4.32	0.570	-	-
-	Dhaalu Atoll	-	Pocilloporidae	*Pocillopora verrucosa*	-16.20	-15.11	-1.09	5.97	5.89	0.080	0.217	Radice Unpublished Data
-	-	-	Oculinidae	*Galaxea fascicularis*	-15.03	-15.20	0.17	6.07	4.44	1.630	-	-
-	-	-	Agariciidae	*Pachyseris speciosa*	-16.28	-13.98	-2.31	4.54	5.41	-0.870	-	-
-	Ari Atoll	-	Pocilloporidae	*Pocillopora verrucosa*	-17.25	-16.14	-1.12	5.66	5.21	0.450	0.291	Radice Unpublished Data
-		-	Oculinidae	*Galaxea fascicularis*	-16.60	-15.66	-0.94	5.44	4.52	0.920	-	-
-		-	Agariciidae	*Pachyseris speciosa*	-14.73	-14.43	-0.30	5.68	5.80	-0.120	-	-
Gulf of Eilat	-	Red Sea	Pocilloporidae	*Stylophora pistillata*	-16.43	-14.82	-1.61	1.42	0.20	1.221	0.188	Einbinder et al. 2009
-	-	-	Pocilloporidae	*Stylophora pistillata*	-14.21	-13.14	-1.06	-	-	-	-	Alamaru et al. 2009
-	-	-	Faviidae	*Favia favus*	-11.84	-11.67	-0.17	2.56	1.33	1.230	-	Alamaru et al. 2010

Table 1.S3. The results of linear regression analyses designed to examine the influence of taxonomic resolution and location on the global relationship between $\Delta^{13}C$ and chl-*a*. Significant models are indicated in bold and the SE of estimates of slope (m) and intercept (b) are reported in (). The coefficient of variation (CV) for all models (excluding the raw data) is calculated for the slope and intercept estimates. Please see the STAR methods section, Quantification and Statistical Analysis - *Global relationships between coral isotopic ratios and oceanic primary productivity* for a complete explanation of all models. Related to Fig. 1.3.

Tissue type	df	F	Slope (m)	Intercept (b)	p	r2
Model 1: All raw data						
$\delta^{13}C$host	32	1.32	-3.83 (3.34)	-14.79 (0.66)	0.26	0.04
$\delta^{13}C$symbiont	32	0.02	-0.47 (3.12)	-14.69 (0.61)	0.88	0
$\Delta^{13}C$	32	4.97	-3.37 (1.52)	-0.10 (0.30)	**0.03**	**0.13**
Model 2: Global model of means						
$\delta^{13}C$host	14	0.87	-3.17 (3.40)	-14.98 (0.64)	0.37	0.06
$\delta^{13}C$symbiont	14	0.09	1.04 (3.5)	-15.08 (0.66)	0.77	0.01
$\Delta^{13}C$	14	46.24	-4.34 (0.64)	0.13 (0.12)	**<0.001**	**0.77**
Model 3: No Jamaica						
$\delta^{13}C$host	13	0.72	-3.06 (3.62)	-15.00 (0.70)	0.413	0.05
$\delta^{13}C$symbiont	13	0.12	1.30 (3.72)	-15.15 (0.71)	0.73	0.01
$\Delta^{13}C$	13	47.58	-4.54 (0.66)	0.17 (0.13)	**<0.001**	**0.79**
Model 4: No Eilat						
$\delta^{13}C$host	13	1.15	-3.41 (3.18)	-15.03 (0.60)	0.30	0.08
$\delta^{13}C$symbiont	13	0.06	0.75 (3.15)	-15.14 (0.60)	0.82	0.00
$\Delta^{13}C$	13	50.51	-4.33 (0.61)	0.14 (0.12)	**<0.001**	**0.80**
Model 5: No Curacao						
$\delta^{13}C$host	13	1.7	-3.30 (2.53)	-14.8 (0.48)	0.22	0.12
$\delta^{13}C$symbiont	13	0.11	0.92 (2.75)	-14.91 (0.52)	0.74	0.01
$\Delta^{13}C$	13	43.61	-4.38 (0.66)	0.13 (0.13)	**<0.001**	**0.77**
Model 6: No Jam, Eil, Cur						
$\delta^{13}C$host	11	2.16	-3.49 (2.38)	-14.86 (0.46)	0.17	0.16
$\delta^{13}C$symbiont	11	0.12	0.86 (2.43)	-15.03 (0.47)	0.73	0.01
$\Delta^{13}C$	11	51.75	-4.52 (0.63)	0.19 (0.12)	**<0.001**	**0.81**
Model 7: Single species only per location						
$\delta^{13}C$host	11	5.75	-10.6 (4.42)	-14.16 (0.79)	**0.04**	**0.34**
$\delta^{13}C$symbiont	11	1.42	-5.44 (4.57)	-14.37 (0.82)	0.26	0.11
$\Delta^{13}C$	11	25.99	-5.12 (1.00)	0.22 (0.18)	**<0.001**	**0.70**
Model 8: *Pocillopora* spp. only						
$\delta^{13}C$host	8	5.33	-9.88 (4.28)	-14.24 (0.79)	**0.05**	**0.4**
$\delta^{13}C$symbiont	8	1.55	-5.21 (4.18)	-14.42 (0.78)	0.25	0.16
$\Delta^{13}C$	8	50.84	-4.63 (0.65)	0.18 (0.12)	**<0.001**	**0.86**
Coefficents of Variation						
$\delta^{13}C$host			65.60	2.50		
$\delta^{13}C$symbiont			372.90	2.26		
$\Delta^{13}C$			6.04	20.57		

Table 1.S4. Results of linear regression analysis examining the relationship between coral $\delta^{13}C$ and $\delta^{15}N$ with absolute latitude, chl-*a*, and estimated thermocline depth. Significant models are indicated in bold and the SE of estimates of slope (m) and intercept (b) are reported in (). Please see the STAR methods section Quantification and Statistical Analysis - *Global relationships between coral isotopic ratios and oceanic primary productivity* for a complete explanation of all models. Related to Figs 1.3 and 1.S2.

Variable		Tissue type	df	F	Slope (m)	Intercept (b)	p	r2
$\delta^{13}C$								
	Latitude	δ^{13}Chost	11	4.01	0.06 (0.03)	-16.12 (0.38)	0.07	0.27
		δ^{13}Csymbiont	11	3.2	0.05 (0.03)	-15.48 (0.38)	0.10	0.22
		$\Delta^{13}C$	11	0.37	0.01 (0.01)	-0.64 (0.15)	0.56	0.03
	Chl-*a*	δ^{13}Chost	11	0.79	-3.80 (4.28)	-14.90 (0.72)	0.39	0.07
		δ^{13}Csymbiont	11	0.03	0.73 (4.27)	-15.05 (0.72)	0.87	0.003
		$\Delta^{13}C$	11	46.41	-4.56 (0.67)	0.15 (0.11)	**<0.001**	**0.81**
	22° isotherm	**δ^{13}Chost**	11	6.14	0.01 (0.01)	-17.66 (0.90)	**0.03**	**0.36**
		δ^{13}Csymbiont	11	1.72	0.01 (0.01)	-16.21 (1.0)	0.22	0.14
		$\Delta^{13}C$	11	11.24	0.01 (0.001)	-1.46 (0.27)	**<0.01**	**0.51**
$\delta^{15}N$								
	Latitude	δ^{15}NChost	10	2.65	-0,21 (0.17)	10.98 (2.23)	0.14	0.21
		δ^{15}Nsymbiont	10	2.82	-0.28 (0.16)	10.70 (2.23)	0.12	0.22
		$\Delta^{15}N$	10	2.15	0.02 (0.01)	0.22 (0.17)	0.17	0.18
	Chl-*a*	δ^{15}NChost	10	1.98	-31.94 (22.68)	13.09 (3.83)	0.19	0.17
		δ^{15}Nsymbiont	10	2.39	-34.44 (22.23)	13.13 (3.75)	0.15	0.19
		$\Delta^{15}N$	10	0.45	1.23 (1.84)	0.23 (0.31)	0.52	0.04
	22° isotherm	δ^{15}NChost	10	0.23	0.02 (0.04)	5.06 (6.53)	0.64	0.02
		δ^{15}Nsymbiont	10	0.31	0.02 (0.04)	4.24 (6.48)	0.59	0.03
		$\Delta^{15}N$	10	0.18	-0.001 (0.003)	0.62 (0.50)	0.68	0.02
Pacific and Indian Ocean *Pocillopora*								
	Latitude	**δ^{15}NChost**	7	44.25	1.15 (0.17)	2.86 (1.23)	**<0.001**	**0.86**
		δ^{15}Nsymbiont	7	42.48	1.15 (0.18)	2.52 (1.25)	**<0.001**	**0.86**
		$\Delta^{15}N$	7	0.01	0.004 (0.04)	0.34 (0.30)	0.93	0.01
	Chl-*a*	**δ^{15}NChost**	7	33.98	-52.21 (8.96)	18.87 (1.59)	**<0.001**	**0.83**
		δ^{15}Nsymbiont	7	43.84	-53.201 (8.04)	18.66 (1.43)	**<0.001**	**0.86**
		$\Delta^{15}N$	7	0.26	0.99 (1.94)	0.21 (0.35)	0.63	0.04
	22° isotherm	**δ^{15}NChost**	7	22.79	0.09 (0.02)	-2.72 (2.80)	**0.002**	**0.77**
		δ^{15}Nsymbiont	7	30.41	0.09 (0.02)	-3.48 (2.50)	**<0.001**	**0.81**
		$\Delta^{15}N$	7	0.63	-0.003 (0.003)	0.76 (0.50)	0.45	0.08

CHAPTER 2

Amino acid $\delta^{13}C$ analysis reveals trophic plasticity in a common reef-building coral

Michael D. Fox, Emma A. Elliott Smith, Jennifer E. Smith, Seth D. Newsome

ABSTRACT

The dietary flexibility of mixotrophs makes them uniquely suited to cope with environmental perturbations, which is likely why mixotrophy has evolved repeatedly in many ecosystems. Reef-building corals are among the most widely distributed mixotrophs, yet little is known about how heterotrophic nutrition influences coral population dynamics and recovery following acute disturbances. This knowledge gap limits our ability to accurately forecast the persistence of coral populations in an era of global change. We show that amino acid carbon isotope ($\delta^{13}C$) analysis provides a powerful framework for disentangling the contribution of autotrophic and heterotrophic nutrition in a common coral that exhibits extreme trophic plasticity at the scale of meters to kilometers. This finding suggests that heterotrophy may be a critical aspect of coral resilience to environmental change, and we anticipate that this approach will facilitate comparisons among taxa that are essential for reevaluating the importance of heterotrophic nutrition for mixotrophic corals.

INTRODUCTION

Due to dietary flexibility, mixotrophs have become some of the most widespread organisms on the planet (Selosse *et al.* 2016). Mixotrophy has evolved repeatedly in vascular plants and marine organisms, underscoring the value of trophic plasticity at the individual and population levels. This dietary flexibility allows mixotrophs to play important roles in energy flow by creating novel linkages between trophic levels (Stoecker *et al.* 2017). Primary producers for example, can rely on heterotrophic nutrition to sustain metabolic demands in association with seasonal variability (Matsuda *et al.* 2012) or to enhance production in oligotrophic regions (Ellison & Gotelli 2009). Despite their integral role in ecosystem functioning, our knowledge of the trophic ecology of mixotrophs and how they are likely to respond to environmental change remains limited because their coupled trophic pathways make it challenging to disentangle the relative contributions of autotrophic vs. heterotrophic nutrition.

Reef-building corals are among the most widespread and ecologically important mixotrophs, yet the importance of coral trophic plasticity at the population and ecosystem scales is remains unknown (Ferrier-Pagès *et al.* 2011). Corals are often considered to be principally autotrophic (Muscatine & Porter 1977), however, they are also voracious carnivores (Lewis & Price 1975) and heterotrophy can account for 66% of skeletal carbon (Grottoli & Wellington 1999) and up to 46% of daily metabolic demands in healthy corals (Grottoli *et al.* 2006). Experimental work shows that heterotrophic nutrition enhances coral fecundity and promotes recovery from bleaching (Cox 2007; Baumann *et al.* 2014). Thus, coral trophic ecology is likely coupled to the resilience of coral populations following acute disturbances, but few studies have assessed this linkage (Palardy *et al.* 2005; Grottoli *et al.* 2006) due to the challenges of quantifying heterotrophy *in situ*.

Visual observations and polyp dissections (Porter 1976) are not tractable methods for studying coral heterotrophy at broad scales. To date, analysis of carbon ($\delta^{13}C$) and nitrogen ($\delta^{15}N$) isotopes has been the primary tool used to address this problem (Muscatine *et al.* 1989), however, interpreting the high degree of variability in the $\delta^{13}C$ and $\delta^{15}N$ values of coral and endosymbiont tissues is challenging (Hoogenboom *et al.* 2015). In spite of this uncertainty, estimates of coral heterotrophy based on bulk tissue isotope analysis are tightly linked to patterns of primary production across the tropics (Fox *et al.* 2018b). Therefore, coral nutrition likely varies as a function of food availibility, which underscores the need for a more precise method of quantifying coral heterotrophy across multiple species and spatial scales.

Recent methodological advancements provide a way of tracing the flow of key compounds through complex food webs (McMahon *et al.* 2016). Carbon isotope analysis of individual amino acids ($\delta^{13}C_{AA}$) is particularly insightful as these molecules are the building blocks of proteins critical for consumer metabolism. Furthermore, different primary producer taxa have distinct essential $\delta^{13}C_{AA}$ patterns. Because most consumers cannot synthesize essential amino acids *de novo* and must acquire them directly from diet, these compounds exhibit little to no carbon isotopic fractionation across trophic levels (Howland *et al.* 2003), making them powerful tracers of the ultimate source(s) of primary production that fuel food webs (Elliott Smith *et al.* 2018). This emerging technique represents an opportunity to disentangle auto- vs. heterotrophic nutrition in mixotrophs at unprecedented scales.

Here we use $\delta^{13}C_{AA}$ to address a fundamental yet poorly understood question in coral reef ecology: how variable is auto- vs. heterotrophic nutrition among corals? We collected a widely distributed coral species from Palmyra Atoll in the central Pacific because the physical drivers of food availability to corals at this site are well established and there are no confounding local

human impacts (Williams *et al.* 2018). We sampled multiple locations spanning a putative gradient of food inputs to determine: 1) the spatial scale at which coral diets are most variable, 2) whether heterotrophic carbon from different sources (lagoon vs. pelagic) is distinguishable in coral tissue, and 3) if $\delta^{13}C_{AA}$ analysis estimates coral nutrition more precisely than bulk tissue $\delta^{13}C$ and $\delta^{15}N$ data. Collectively, this study provides new insight into coral biology and highlights the power of $\delta^{13}C_{AA}$ in unraveling the nutritional complexity of mixotrophs.

METHODS

Data were collected from Palmyra Atoll National Wildlife Refuge in the Northern Line Islands (5°52' N, 162°05'W). Palmyra is an uninhabited atoll composed of small islets that modulate water flow between the lagoon and fore reef habitats, which can generate spatially variable gradients of allochthonous food resources for corals (Williams *et al.* 2018).

To assess the natural gradients in food availability around Palmyra and their influence on local coral populations, we collected paired samples of the widely distributed coral, *Pocillopora meandrina* (n=5), and the two primary heterotrophic resources for coral, zooplankton and particulate organic matter (POM), that were collected from 10 m depth on the fore reef. We used two spatial scales to compare $\delta^{13}C_{AA}$ to bulk tissue $\delta^{13}C$ and $\delta^{15}N$ analysis. First, we selected four sites at the corners of the atoll that span a known gradient in lagoon connectivity (SW>NW>SE>NE; (Rogers *et al.* 2017). At these locations, we measured $\delta^{13}C_{AA}$ values in coral host (consumer, n=4–5 per site) and endosymbiont (autotrophic source, n=3 per site) tissues along with zooplankton and POM (heterotrophic sources, n=2 per food source per site), as well as measured $\delta^{13}C$ and $\delta^{15}N$ values for the coral host and endosymbiont bulk tissue fractions (n=5 per site) (Fig. 2.S1, Table 2.S1). Second, we sampled an additional 13 sites that encircled the

atoll perimeter to assess smaller scale variation in coral trophic ecology. At these sites, however, coral host and endosymbiont fractions (n=5 per site) along with the heterotrophic resources (n=1 per food source) were only analyzed for bulk tissue $\delta^{13}C$ and $\delta^{15}N$ (Fig. 2.S1, Table 2.S1). We also sampled zooplankton and POM (n=4 for $\delta^{13}C_{AA}$, n=8 for $\delta^{13}C$ and $\delta^{15}N$) across the lagoon in randomly stratified locations.

Near-reef zooplankton (<163 μm) were collected with net tows at 3–4 m depth along the fore reef slope. All tows in reef and lagoon habitats were conducted at idle speed for 500 m and the contents were filtered onto pre-combusted GF/F filters. POM samples were concentrated from 4 L of water collected just above the benthos onto 25 mm pre-combusted GF/F filters (Whatman). All samples were frozen at -20 °C until analysis. In the lab, coral host and endosymbiont fractions were separated and loaded onto pre-combusted GF/F filters following established methods (Fox *et al.* 2018b). All samples were briefly acidified using drop-wise addition of 1N HCl to remove $CaCO_3$ and dried at 60°C for 48 hrs.

Dried filters were analyzed for $\delta^{13}C$ and $\delta^{15}N$ with a Costech 4010 Elemental Analyzer (Valencia, CA) interfaced with a Thermo Finnigan Delta Plus XP stable isotope mass spectrometer (Bremen, Germany) at Scripps Institution of Oceanography (La Jolla, CA). Isotope values are expressed as delta (δ) values ($\delta^{13}C$ or $\delta^{15}N$), where $\delta = 1000 \times [(R_{sample} / R_{standard}) - 1]$ and R_{sample} or $R_{standard}$ are the ratio of the heavy to light isotope in parts per thousand, or per mil (‰). The international reference standards are Vienna-Pee Dee Belemnite (V-PDB) for $\delta^{13}C$ and atmospheric N_2 for $\delta^{15}N$. Repeated measurements of internal reference materials calibrated against NBS-18 and IAEA-1 produced a precision (SD) of <0.1‰ for $\delta^{13}C$ and <0.2‰ for $\delta^{15}N$.

For $\delta^{13}C_{AA}$ analysis, samples were first hydrolyzed with 1.5mL of 6N HCl at 110°C for 20 hours; tubes were flushed with N_2 to prevent oxidation. Hydrolysates were passed through a

cation exchange resin column (Dowex 50WX8 100-200 mesh) to isolate amino acids (AAs) from other metabolites (Amelung & Zhang 2001). After Dowex purification, amino acids were derivatized to N-trifluoroacetic acid isopropyl esters (O'Brien *et al.* 2002; Newsome *et al.* 2011). Samples were derivatized in batches of 8–17 along with an in-house reference material containing all of the AAs for which we measured $\delta^{13}C$. Derivatized samples were injected into a 60m BPX5 gas chromatograph column for AA separation (0.32 ID, 1.0μm film thickness, SGE Analytical Science, Victoria, Australia) in a Thermo Scientific Trace 1300, then combusted into CO_2 with a GC Isolink II interfaced to a Thermo Scientific Delta V Plus isotope ratio mass spectrometer at the University of New Mexico Center for Stable Isotopes (Albuquerque, NM). Samples were run in duplicate and bracketed with our in-house AA reference material; within-run standard deviations of $\delta^{13}C$ values in this reference material ranged from 0.26‰ (isoleucine) to 0.53‰ (tyrosine). We reliably measured $\delta^{13}C$ values of thirteen AAs including seven considered nonessential: alanine (Ala), aspartic acid (Asp), glutamic acid (Glu), glycine (Gly), proline (Pro), serine (Ser), tyrosine (Tyr); and six considered essential: isoleucine (Ile), leucine (Leu), lysine (Lys), phenylalanine (Phe), threonine (Thr) and valine (Val). The reagents used during derivatization add carbon to AA side chains, and hence measured $\delta^{13}C$ values reflect a combination of the intrinsic carbon in each AA and reagent carbon (Silfer *et al.* 1991).

The reagents used during derivatization add carbon to the side chains of amino acids, and so the raw $\delta^{13}C_{AA}$ measured via GC-C-IRMS is a combination of original amino acid carbon and reagent carbon (O'Brien *et al.* 2002; Newsome *et al.* 2014). However, because amino acid standards of known $\delta^{13}C$ composition were derivatized and run with each batch of samples, we were able to correct for this carbon addition for each amino acid using the following equation (O'Brien *et al.* 2002; Newsome *et al.* 2014):

$$\delta^{13}C_{sample} = \frac{\delta^{13}C_{dsa} - \delta^{13}C_{dst} + (\delta^{13}C_{std} \times p_{std})}{p_{std}}$$

Here, $\delta^{13}C_{dsa}$ refers to the measured value of the derivatized amino acid within the sample and $\delta^{13}C_{dst}$ refers to the measured value of the same derivatized amino acid within the internal standard. $\delta^{13}C_{std}$ is the known un-derivatized value of that amino acid in the standard (measured via EA-IRMS), and p_{std} is the proportion of carbon in the measured derivative that was originally sourced from the amino acid, which varies quite substantially among amino acids.

Statistical Analyses

We compared coral and endosymbiont bulk tissue $\delta^{13}C$ and $\delta^{15}N$ values across sites using a 2-way ANOVA. We used one-way ANOVAs to examine site-level differences in the relative offset between the tissue fractions ($\Delta^{13}C$ or $\Delta^{15}N = \delta_{host}-\delta_{endosymbiont}$), a common metric used to assess coral heterotrophy (Muscatine *et al.* 1989), and to compare the putative autotrophic (site level means of endosymbionts, n=17) and heterotrophic food resources across all fore reef (POM n=3 and zooplankton, n=16) and lagoon (POM n=7 and zooplankton n=8) sites. Data for coral and endosymbiont tissues were excluded from statistical analyses if their $\delta^{13}C$ or $\delta^{15}N$ values exceeded 4 standard deviations of the global mean of the respective tissue fraction. We used MANOVA to examine variation in $\delta^{13}C_{AA}$ values as a function of autotrophic or heterotrophic resource type and to compare between the lagoon and fore reef habitats. Individual ANOVAs were used to compare differences in $\delta^{13}C$ for each AA between consumers. Pairwise contrasts between groups were conducted using Tukey's HSD.

We used linear discriminant analysis (LDA; R package MASS, (Venables & Ripley

2002) to construct a model for predicting whether individual coral hosts classified with the autotrophic (endosymbiont) or heterotrophic (zooplankton and POM) groups. We examined the classification error rate for each of our three source groups using leave-one-out cross-validation and used this training data set to predict group membership for each coral host sample. We examined classification rates of the coral consumers using $\delta^{13}C$ data for both essential ($\delta^{13}C_{ESS}$) and non-essential amino acids ($\delta^{13}C_{NESS}$), from which we obtained similar results. However, little is known about the fractionation of $\delta^{13}C_{NESS}$ in symbiotic cnidarians, so we focused primarily on $\delta^{13}C_{ESS}$. These analyses were conducted using the raw $\delta^{13}C$ values for each AA and $\delta^{13}C$ values normalized to the sample mean (Larsen *et al.* 2013) to determine the effect of normalization on the interpretation of our results. Normalization of our data did not alter the results and we therefore elected to the raw $\delta^{13}C$ data. We used a bootstrapping approach to generate confidence estimates around the heterotrophic and autotrophic classifications of corals and to model the relative contribution of heterotrophic carbon to the diet of individual corals. See the supporting information for more detail. We then used Pearson's correlation to compare this estimate of coral heterotrophy to the $\Delta^{13}C_{host\text{-}endosymbiont}$ value of each coral. Assumptions of normality and equal variances within and among groups were determined using the Shapiro-Wilk test with quantile-quantile plots and Levene's test, respectively. All analyses were conducted using R 3.5.0 (R Core Team 2013).

Modeling Heterotrophic Contributions to Coral Diets with LDA

Coral holobionts have complex trophic pathways that include endosymbiotic microalgae along with microbes and fungi that all live on or within the carnivorous host (Knowlton & Rohwer 2003). In addition, the coral host can consume highly diverse prey that span several

orders of magnitude in size, including zooplankton, picoplankton, dissolved, and particulate organic matter (Ferrier-Pagès *et al.* 2011). Thus, the extent of coral dietary niches are undetermined and we still do not know whether they consume phytoplankton or if their associated microbial communities can transfer bioactive molecules (e.g., amino acids) to the host. This natural variation in diet source(s) precluded our use of commonly applied Bayesian mixing models because the AA tracers of our autotrophic and heterotrophic sources were variable and not perfectly conserved in each coral consumer (Stock *et al.* 2018), suggesting unresolved nutritional sources. Furthermore, the strength of Bayesian mixing models is derived from applying them to well described mixing spaces (Brett 2014), which for mixotrophic corals is not yet practical.

Linear discriminant analysis (LDA) provides a powerful approach for maximizing separation among groups and classifying consumers based on the amino acid "fingerprints" of potential sources (Larsen *et al.* 2009). Most importantly, LDA offers a less rigid framework for examining diet contributions within undetermined mixing spaces caused by variable or unquantified diet sources. For example, if the corals in our study were obtaining nutrition from a third, unknown source (e.g., bacteria) we would see evidence of this in an LDA whereas a mixing model would be unable to converge on an appropriate solution. However, LDA may fail to capture subtle differences in the proportional heterotrophic versus autotrophic contributions as many corals (or other mixotrophs) that partially rely on several sources and would therefore fall somewhere between the groups, thus making their true classification ambiguous.

A primary impetus for this study was to create a broadly applicable, standardized methodology for studying the tropic ecology of mixotrophic corals *in situ* at previously untenable scales. To improve our estimate of group membership for corals as "heterotrophic" or

"autotrophic" and to estimate the proportional contribution of heterotrophy vs. autotrohy to the diet of each individual, we modified the traditional LDA with a bootstrap resampling approach. This allowed us to create 10,000 permutations of the training data set using random draws (with replacement) from the source distributions of $\delta^{13}C_{ESS}$. Each training set was used to predict group membership for individual corals, which provided iterative classifications, based on subtle variations in the source groups error distributions. First, we calculated the global classification percentage with 95% CI to describe what percentage of the *P. meandrina* population on Palmyra relies more heavily on heterotrophic nutrition. Second, we used the first linear discriminant (LD_1), which explained 98% of the variation between autotrophic and heterotrophic sources, to create a continuum of autotrophic to heterotrophic nutrition that could be applied to each individual. To do this, we determined the centroid (LD_1 mean) of both source ellipses within each LDA (n=10,000) and calculated the distance between a given coral and the autotrophic centroid (d_a). We then standardized this value to the total distance between the centroids of the autotrophic and heterotrophic sources ($d_{h\text{-}a}$) to obtain a scale of heterotrophic contribution that ranged from 0 to 1. Thus, the proportional contribution of heterotrophy can be calculated as:

$$\%\ heterotrophy\ = \frac{LD1_{coral} - d_a}{d_{h-a}}$$

We calculated this value for each coral based on the 10,000 random permutations of the source data. We used these data to generate means and 95% CI of the percent contribution of heterotrophy to each individual (Figure 2.2). Importantly, for any coral with a CI that overlapped 0 or 1 we are unable to distinguish that individual from being 100% of the respective source.

The utility of standardizing this calculation to LD_1 is that it provides a transferable metric for future studies to examine coral trophic ecology across species and locations; assuming well-sampled sources and clear separation between autotrophic and heterotrophic groups. In addition,

this approach does not preclude corals consuming an unknown source. Rather, by comparing coral nutrition this way unknown or unresolved sources will be readily apparent by corals that have values beyond 0 or 1. In our study, we observed very few corals (X/Y or X%) that exhibited 95% confidence intervals that overlapped the extent of our sources (0 or 1). This suggests that *P. meandrina* on Palmyra is not feeding on a source we failed to sample.

Modeling Heterotrophic Contributions to Coral Diets with Bayesian Mixing Models.

We acknowledge the power and practicality of commonly applied Bayesian mixing models to address very similar questions as our modified multivariate analysis. However, it is important to consider the patterns in raw $\delta^{13}C_{AA}$ values when deciding which analysis is most appropriate for a given dataset. For example, two potential sources to consumers could have very different $\delta^{13}C_{ESS}$ patterns (i.e., fingerprints), but have overlapping raw $\delta^{13}C$ values for several individual amino acids, which would ultimately limit the utility of using a mixing model to quantify source proportions. In contrast, sources could share similar $\delta^{13}C_{ESS}$ patterns but have very different raw $\delta^{13}C$ values for individual AAs, a situation in which multivariate methods (e.g., LDA) would be of limited use while mixing models would be able to quantify source proportions with high precision. Our source data (Figure 2.S2) are an example of the former scenario, where there is overlap in $\delta^{13}C$ values of three (Leu, Val, and Phe) of six essential amino acids, yet autotrophic and heterotrophic sources have very different $\delta^{13}C_{ESS}$ patterns (Figure 1A). To demonstrate conflicting analytical aspects of these two situations (i.e., overlapping vs. non-overlapping $\delta^{13}C_{AA}$ values), and assess the performance of our proposed framework we compared our modeled results to output from MixSIAR (Stock & Semmens 2016). To satisfy the assumptions of MixSIAR, we had to make several adjustments to our dataset. First, we dropped

two individual coral samples that had $\delta^{13}C_{AA}$ values for Ile and Thr beyond the mixing polygon of our two sources. Second, we included only the three essential AAs (Ile, Lys, Thr) that had significant differences in $\delta^{13}C$ between sources (Fig. 2.S2). Third, we extended the upper bound of the prior for the standard deviation (SD) calculation for our factor of "individual" from 20 (default) to 50. This provided us the capacity to resolve the error prior for our coral samples given their high level of individual variation. Lastly, we did not include site as a factor because the model was unable to resolve the error prior for that term. We ran the model at length "extreme" in order to obtain convergence. Notably, the credibility intervals for most individuals and the global means for autotrophic and heterotrophic contributions effectively ranged from 0 to 100. This indicates the model was unable to resolve source contributions for all but the most extreme consumers. We compared our modeled mean % heterotrophy to those predicted by MixSIAR using Pearson's correlation. The estimates of both approaches were highly correlated ($t=5.22$, $p<0.001$, $r=0.80$), however, the confidence of each estimate was far greater using the bootstrapped LDA approach (Fig 2.S3). Thus, we elected to develop our proxy for coral heterotrophy using LDA.

RESULTS

Zooplankton and POM had similar $\delta^{13}C_{AA}$ values and were indistinguishable between the fore reef and lagoon habitats ($\delta^{13}C_{ESS}$: Pillai trace = 0.27, $F_{(6,8)} = 0.50$, $p=0.79$; $\delta^{13}C_{NESS}$: Pillai trace = 0.58, $F_{(7,4)} = 0.79$, $p=0.63$). Therefore, we pooled all zooplankton and POM samples into a single heterotrophic resource category for subsequent analyses. We observed significant differences in $\delta^{13}C_{ESS}$ and $\delta^{13}C_{NESS}$ between our autotrophic (endosymbionts) and heterotrophic (zooplankton and POM) sources ($\delta^{13}C_{ESS}$: Pillai trace = 1.08, $F_{(12,42)} = 4.15$, $p<0.001$; $\delta^{13}C_{NESS}$:

Pillai trace = 1.26, $F_{(14,32)} = 3.93$, $p < 0.001$). Isoleucine, lysine, and threonine were the most different between the autotrophic and heterotrophic sources (Fig. 2.S2, Table 2.S3). There was greater variation among $\delta^{13}C_{NESS}$ values but glutamic acid, proline, and tyrosine showed the best separation between sources (Fig. 2.S2, Table 2.S3).

Based on the first linear discriminant (LD_1), the most important AA_{ESS} for separating the source groups were isoleucine, leucine, and lysine, which explained 98% of the overall variation. Aspartic acid, proline, and alanine explained most of the variation for AA_{NESS}. We obtained 100% successful classification within each of our source groups indicating well-differentiated autotrophic and heterotrophic carbon sources for both AA_{ESS} and AA_{NESS}. Using data for both AA_{ESS} and AA_{NESS}, 6 of 19 coral host samples classified as heterotrophic (32%) (Fig. 2.1A, Fig. 2.S3). We also achieved 100% reclassification of our source groups and 37% heterotrophic classification of coral hosts using normalized $\delta^{13}C_{ESS}$ values (Fig 2.S4). The bootstrapped reclassification indicated 34.4% (95% CI [21-53%]) of all corals obtain significantly more of their AA_{ESS} from allochthonous sources, while 65.6% (95% CI [47–79%]) relied more on autotrophic sources of AA_{ESS} (Fig. 2.1B).

Site location had no consistent influence on the diets of individual corals; colonies separated by meters were just as likely to have different diet compositions than those on opposite sides of the atoll (Fig. 2.2A, B). On average, the SW corner of the atoll near the main channel into the lagoon had the highest proportion of corals classified as heterotrophic (56.7%, 95% CI [7.4–99.9%]) and the SE corner had the lowest (13.7%, 95% CI [0–60.6%]). The large confidence intervals of heterotrophic diet proportions within each site were driven by high inter-colony variation in coral $\delta^{13}C_{ESS}$ values. Across 19 individuals, the relative contribution of

heterotrophic and autotrophic sources ranged from 0-100%, with an average of 41.34 %, 95% CI [28.93-53.93%], indicating extreme variation in trophic plasticity (Fig. 2.2A).

Coral and endosymbiont bulk tissue $\delta^{13}C$ and $\delta^{15}N$ values exhibited minimal variation on an island scale and provided no additional insight to spatial variation in food availability around Palmyra; mean (±SD) $\Delta^{13}C_{host\text{-}endosymbiont}$ was only -0.3±0.2‰ (Fig. 2.1C, Table 2.S2). Coral and endosymbiont $\delta^{15}N$ was highly variable among individuals and differed by <1‰ across sites (Fig. 2.1C, Table 2.S2). The 95% confidence ellipses around all groups overlapped (Fig. 2.1C) and the statistical separation between sources was inconsistent (Table 2.S2). POM samples from the lagoon and fore reef habitats were not distinguishable and overall showed a high degree of variation in both $\delta^{13}C$ (mean: -19.9, 95%CI: -26.6 to -13.3) and $\delta^{15}N$ (mean = 5.2, 95%CI: 1.9 to 8.4). Finally, the classic proxy for coral heterotrophy ($\Delta^{13}C_{host\text{-}endosymbiont}$) was significantly correlated with our estimates of coral nutrition using $\delta^{13}C_{ESS}$. Corals that consumed greater amounts of heterotrophic carbon tended to have lower $\Delta^{13}C$ values ($r = -0.54$, $p = 0.03$, Fig. 2.2C).

DISCUSSION

The physiological benefits of heterotrophic nutrition to mixotrophic corals are diverse and may be critical for survival following disturbance events, methodological limitations impede our ability to quantify nutritional variability in corals. Here we demonstrate that $\delta^{13}C_{AA}$ analysis offers a powerful technique for differentiating heterotrophic vs. autotrophic nutrition in a widely distributed coral. Our study shows that coral trophic ecology can be highly variable among conspecifics, and our results provide a much-needed framework for rigorously investigating coral trophic plasticity across multiple species and spatiotemporal scales (Ferrier-Pagès *et al.* 2011).

Recent work reveals that heterotrophic nutrition is more fundamental to coral ecology than previously considered (Ferrier-Pagès et al. 2011). Recent work using bulk tissue $\delta^{13}C$ and $\delta^{15}N$ data has shown that coral trophic ecology varies spatially and is strongly influenced by food availability (Fox *et al.* 2018b; Williams *et al.* 2018). This approach, however, has been hindered by small (~1‰) differences in $\delta^{13}C$ values between the coral host and endosymbionts ($\Delta^{13}C_{host\text{-}endosymbiont}$), coupled with high degree of isotopic variability within and among coral species (Hoogenboom *et al.* 2015). Thus, there is a need to identify precise but broadly applicable techniques for assessing variation in coral nutrition. The results of our study demonstrate that $\delta^{13}C_{AA}$ analysis can evaluate subtle differences in coral trophic ecology in a location where bulk tissue $\delta^{13}C$ and $\delta^{15}N$ data failed to find pattern.

We achieved 100% separation and reclassification of the autotrophic (endosymbionts) and common heterotrophic resources for corals (zooplankton and POM) based on LDA of both essential and non-essential $\delta^{13}C_{AA}$. Notably, patterns of $\delta^{13}C_{ESS}$ values of 19 colonies of *P. meandrina* separated cleanly along an informative continuum of autotrophic and heterotrophic nutrition, allowing for quantitative estimates of the proportion of heterotrophic carbon used by the corals (Fig. 2.1A, 2.2A). In contrast, the bulk tissue $\delta^{13}C$ and $\delta^{15}N$ data of our coral and source datasets were indistinguishable despite general agreement between $\Delta^{13}C_{host\text{-}symbiont}$ and $\delta^{13}C_{AA}$ -based estimates of coral heterotrophy (Fig. 2.2C). While some corals appear to be capable of synthesizing essential AAs (Fitzgerald & Szmant 1997), and coral hosts can translocate AAs from ingested prey to their endosymbionts (Piniak *et al.* 2003), $\delta^{13}C_{ESS}$ fingerprints of endosymbionts in *P. meandrina* did not vary as a function of host nutrition.

The separation we achieved between autotrophic and heterotrophic source groups underscores the power of $\delta^{13}C_{AA}$ analysis for studying the trophic ecology of mixotrophs, but it

remains to be seen how consistent this separation is across larger spatial scales. Additional studies should place particular emphasis on rigorously sampling local autotrophic and heterotrophic resources to assess the global generality of the $\delta^{13}C_{ESS}$ fingerprints for *Symbiodinium* and reef-associated planktonic communities. $\delta^{13}C_{ESS}$ fingerprints also did not differ between POM and zooplankton communities from the lagoon and fore reef habitats so we were unable to assess the relative contribution of each habitat to coral nutrition. This suggests the planktonic communities in the lagoon and fore reef may be taxonomically similar and is consistent with the observation that pelagic and lagoon zooplankton on Palmyra only differ in bulk tissue $\delta^{34}S$ and not in $\delta^{13}C$ or $\delta^{15}N$ (McCauley *et al.* 2014). Atoll lagoons likely provide important heterotrophic resources for corals and their influence can be spatially variable (Williams *et al.* 2018). Our study suggests that $\delta^{13}C_{AA}$ is a powerful tool for disentangling auto- vs. heterotrophic nutrition in corals but that it may not be as useful as other tracers (e.g., $\delta^{34}S$) in distinguishing multiple sources of heterotrophic nutrition.

The extreme variation in heterotrophic nutrition we observed among individual colonies of *P. meandraina* suggests a high degree of trophic plasticity in this species. The extent of individual variation in our data overwhelms well-established island-scale variation in particulate resource availability on Palmyra (Williams *et al.* 2018). Not all coral species are capable of altering their nutritional strategies in response to stress or patterns of food availability, which can impair their survival and recovery from thermally-induced bleaching when symbiont derived resources are scarce (Grottoli *et al.* 2006). Notably, Teece *et al.* (2011) also showed that variation in heterotrophic nutrition among individual colonies is greater than across space. Such high variation among individual colonies helps explain the global relationship between coral heterotrophy ($\Delta^{13}C$) and surface chl-*a* (Fox *et al.* 2018b) because there is a higher probability of

more heterotrophic individuals on reefs with greater food availability. Individual level variation in nutritional strategy has largely been ignored in studies of coral population dynamics and community structure and it is likely a critical driver in these processes. If many coral species share this level of trophic plasticity, spatial patterns of food availability (e.g., chl-*a*) likely play a more important role in coral persistence following acute disturbances than previously considered.

Our samples were collected during the onset of a thermal stress event and associated coral bleaching on Palmyra atoll (Fox *et al.* 2018a). While no sampled corals were visibly bleached, it is possible that the magnitude of trophic plasticity we observed was driven by differential responses to thermal stress among colonies. Thus, we cannot conclude that *P. meandraina* colonies always exhibit such extreme trophic plasticity. Importantly, our ability to capture this variation highlights the potential power of $\delta^{13}C_{AA}$ analysis. Physiological deficits from bleaching can remain following visual recovery of a colony by months (Baumann *et al.* 2014; Grottoli *et al.* 2014; Schoepf *et al.* 2015). Our data suggest that nutritional and metabolic deficits associated with thermal stress may necessitate increased heterotrophy prior to the onset of bleaching. Collectively, this implies that heterotrophic nutrition likely plays an important role in sustaining coral metabolic demands before and after bleaching occurs. As such, $\delta^{13}C_{AA}$ may provide a powerful tool for broadly monitoring coral stress levels.

$\delta^{13}C_{AA}$ analysis of the coral host as well as dominant autotrophic (endosymbiont) and heterotrophic (zooplankton and POM) resources revealed that coral nutrition can be most variable at the level of individual colonies within an island. Our results conclusively demonstrate that $\delta^{13}C_{AA}$ analysis improves our ability to resolve the relative contribution of auto- vs. heterotrophic sources to the diet of mixotrophic corals. Interestingly, using just bulk tissue $\delta^{13}C$ and $\delta^{15}N$ we were unable to identify differences in nutrition among individuals or at an island-

scale, despite a much larger dataset. The $\delta^{13}C_{AA}$ methods we have applied here offer a standardized approach for quantifying the heterotrophic contributions to coral diets, which will facilitate investigations of species-specific trophic plasticity. This information will advance our understanding of spatial and taxonomic variation in coral survival following disturbances and reveal critical differences in coral trophic ecology across environmental gradients such as depth, oceanic primary production, pH, and water quality. Given the importance of heterotrophic nutrition to coral survival and recovery from bleaching, knowledge about the extent of trophic plasticity within and among species will greatly enhance our capacity to forecast the persistence of coral populations in an era of rapid environmental change.

ACKNOWLEDGEMENTS

We are grateful to the U.S. Fish and Wildlife Service (USFWS) and The Nature Conservancy for logistical support. We thank the Scripps Family Foundation and several other private donors for financial support. We thank Brian Stock, Brice Semmens, and Stuart Sandin for extensive discussions that improved this manuscript. We also thank Jessica Glanz, and Spencer Breining-Aday for assistance in the lab. MDF was supported by a Nancy Foster Scholarship from the NOAA Office of National Marine Sanctuaries. Graphics used in the figures are courtesy of Jane Thomas (sun) and Christine Thurber (copepod) at the Integration and Application Network, Univ. of Maryland (ian.umces.edu/imagelibrary/).

Chapter 2, in full, has been submitted to *Ecology Letters*. Fox, Michael D.; Elliott Smith, E.A.; Smith, Jennifer E.; Newsome, Seth D. The dissertation author was the primary investigator and author of this material.

References

Amelung, W. & Zhang, X. (2001). Determination of amino acid enantiomers in soils. *Soil Biology and Biochemistry*, 33, 553-562.

Baumann, J., Grottoli, A.G., Hughes, A.D. & Matsui, Y. (2014). Photoautotrophic and heterotrophic carbon in bleached and non-bleached coral lipid acquisition and storage. *J. Exp. Mar. Biol. Ecol.*, 461, 469-478.

Brett, M.T. (2014). Resource polygon geometry predicts Bayesian stable isotope mixing model bias. *Mar. Ecol. Prog. Ser.*, 514, 1-12.

Cox, E.F. (2007). Continuation of sexual reproduction in *Montipora capitata* following bleaching. *Coral Reefs*, 26, 721-724.

Elliott Smith, E.A., Harrod, C., Von Humboldt, A. & Newsome, S.D. (2018). Methodological insights from amino acid $\partial^{13}C$ analysis: characterizing energy flow in an interidal ecosystem. *Ecosphere*, In revision.

Ellison, A.M. & Gotelli, N.J. (2009). Energetics and the evolution of carnivorous plants—Darwin's 'most wonderful plants in the world'. *J. Exp. Bot.*, 60, 19-42.

Ferrier-Pagès, C., Hoogenboom, M. & Houlbrèque, F. (2011). The role of plankton in coral trophodynamics. In: *Coral Reefs: an ecosystem in transition* (eds. Dubinsky, Z & Stambler, N). Springer Netherlands, pp. 215-229.

Fitzgerald, L.M. & Szmant, A.M. (1997). Biosynthesis of 'essential'amino acids by scleractinian corals. *Biochem. J.*, 322, 213-221.

Fox, M.D., Carter, A.C., Edwards, C.B., Takeshita, Y., Johnson, M.D., Petrovic, V., Amir, C.G., Sandin, S.A. & Smith, J., E. (2018a). Limited coral mortality following acute thermal stress and widespread bleaching on Palmyra Atoll, central Pacific. *Coral Reefs*, in review

Fox, M.D., Williams, G.J., Johnson, M.D., Kelly, E.L.A., Radice, V.A., Zgliczynski, B.J., Rohwer, F.L., Sandin, S.A. & Smith, J., E. (2018b). Gradients in primary production predict trophic strategies of mixotrophic corals across spatial scales. *Curr. Biol.*, in press (accepted).

Grottoli, A.G., Rodrigues, L.J. & Palardy, J.E. (2006). Heterotrophic plasticity and resilience in bleached corals. *Nature*, 440, 1186-1189.

Grottoli, A.G., Warner, M.E., Levas, S.J., Aschaffenburg, M.D., Schoepf, V., McGinley, M., Baumann, J. & Matsui, Y. (2014). The cumulative impact of annual coral bleaching can turn some coral species winners into losers. *Global Change Biol.*, 20, 3823-3833.

Grottoli, A.G. & Wellington, G.M. (1999). Effect of light and zooplankton on skeletal $\delta^{13}C$ values in the eastern tropical Pacific corals *Pavona clavus* and *Pavona gigantea*. *Coral Reefs*, 18, 29-41.

Hoogenboom, M., Rottier, C., Sikorski, S. & Ferrier-Pagès, C. (2015). Among-species variation in the energy budgets of reef-building corals: scaling from coral polyps to communities. *J. Exp. Biol.*, 218, 3866-3877.

Howland, M.R., Corr, L.T., Young, S.M.M., Jones, V., Jim, S., Van Der Merwe, N.J., Mitchell, A.D. & Evershed, R.P. (2003). Expression of the dietary isotope signal in the compound‐specific δ13C values of pig bone lipids and amino acids. *International Journal of Osteoarchaeology*, 13, 54-65.

Knowlton, N. & Rohwer, F. (2003). Multispecies microbial mutualisms on coral reefs: the host as a habitat. *the american naturalist*, 162, S51-S62.

Larsen, T., Taylor, D.L., Leigh, M.B. & O'Brien, D.M. (2009). Stable isotope fingerprinting: a novel method for identifying plant, fungal, or bacterial origins of amino acids. *Ecology*, 90, 3526-3535.

Larsen, T., Ventura, M., Andersen, N., O'Brien, D.M., Piatkowski, U. & McCarthy, M.D. (2013). Tracing carbon sources through aquatic and terrestrial food webs using amino acid stable isotope fingerprinting. *PLoS One*, 8, e73441.

Lewis, J.B. & Price, W.S. (1975). Feeding mechanisms and feeding strategies of Atlantic reef corals. *J. Zool.*, 176, 527-544.

Matsuda, Y., Shimizu, S., Mori, M., Ito, S.I. & Selosse, M.A. (2012). Seasonal and environmental changes of mycorrhizal associations and heterotrophy levels in mixotrophic *Pyrola japonica* (Ericaceae) growing under different light environments. *Am. J. Bot.*, 99, 1177-1188.

McCauley, D.J., DeSalles, P.A., Young, H.S., Papastamatiou, Y.P., Caselle, J.E., Deakos, M.H., Gardner, J.P.A., Garton, D.W., Collen, J.D. & Micheli, F. (2014). Reliance of mobile species on sensitive habitats: a case study of manta rays (Manta alfredi) and lagoons. *Mar. Biol.*, 161, 1987-1998.

McMahon, K.W., Thorrold, S.R., Houghton, L.A. & Berumen, M.L. (2016). Tracing carbon flow through coral reef food webs using a compound-specific stable isotope approach. *Oecologia*, 180, 809-821.

Muscatine, L. & Porter, J.W. (1977). Reef corals: mutualistic symbioses adapted to nutrient-poor environments. *Bioscience*, 27, 454-460.

Muscatine, L., Porter, J.W. & Kaplan, I.R. (1989). Resource partitioning by reef corals as determined from stable isotope composition. I $\delta^{13}C$ of zooxanthellae and animal tissue vs depth. *Mar. Biol.*, 100, 185-193.

Newsome, S.D., Fogel, M.L., Kelly, L. & del Rio, C.M. (2011). Contributions of direct incorporation from diet and microbial amino acids to protein synthesis in Nile tilapia. *Funct. Ecol.*, 25, 1051-1062.

Newsome, S.D., Wolf, N., Peters, J. & Fogel, M.L. (2014). Amino acid δ13C analysis shows flexibility in the routing of dietary protein and lipids to the tissue of an omnivore. The Society for Integrative and Comparative Biology.

O'Brien, D.M., Fogel, M.L. & Boggs, C.L. (2002). Renewable and nonrenewable resources: amino acid turnover and allocation to reproduction in Lepidoptera. *Proc. Natl. Acad. Sci. USA.*, 99, 4413-4418.

Palardy, J.E., Grottoli, A.G. & Matthews, K.A. (2005). Effects of upwelling, depth, morphology and polyp size on feeding in three species of Panamanian corals. *Mar. Ecol. Prog. Ser.*, 300, 79-89.

Piniak, G.A., Lipschultz, F. & McClelland, J. (2003). Assimilation and partitioning of prey nitrogen within two anthozoans and their endosymbiotic zooxanthellae. *Mar. Ecol. Prog. Ser.*, 262, 125-136.

Porter, J.W. (1976). Autotrophy, heterotrophy, and resource partitioning in Caribbean reef-building corals. *Am. Nat.*, 110, 731-742.

R Core Team (2013). R: A language and environment for statistical computing. R Foundation for Statistical Computing Vienna, Austria http://www.R-project.org/.

Rogers, J.S., Monismith, S.G., Fringer, O.B., Koweek, D.A. & Dunbar, R.B. (2017). A coupled wave-hydrodynamic model of an atoll with high friction: Mechanisms for flow, connectivity, and ecological implications. *Ocean Modelling*, 110, 66-82.

Schoepf, V., Grottoli, A.G., Levas, S.J., Aschaffenburg, M.D., Baumann, J.H., Matsui, Y. & Warner, M.E. (2015). Annual coral bleaching and the long-term recovery capacity of coral. *Proc. R. Soc. B.*, 282.

Selosse, M.-A., Charpin, M. & Not, F. (2016). Mixotrophy everywhere on land and in water: the grand écart hypothesis. *Ecol. Lett.*, doi: 10.1111/ele.12714.

Silfer, J.A., Engel, M.H., Macko, S.A. & Jumeau, E.J. (1991). Stable carbon isotope analysis of amino acid enantiomers by conventional isotope ratio mass spectrometry and combined gas chromatography/isotope ratio mass spectrometry. *Anal. Chem.*, 63, 370-374.

Stock, B.C., Jackson, A.L., Ward, E.J., Parnell, A.C., Phillips, D.L. & Semmens, B.X. (2018). Analyzing mixing systems using a new generation of Bayesian tracer mixing models. *PeerJ*, 6, e5096.

Stock, B.C. & Semmens, B.X. (2016). MixSIAR GUI User Manual Version 3.1. Https://github.com/brianstock/MixSIAR/.

Stoecker, D.K., Hansen, P.J., Caron, D., A. & Mitra, A. (2017). Mixotrophy in the Marine Plankton. *Ann. Rev. Mar. Sci.*, 9, 311-335.

Teece, M.A., Estes, B., Gelsleichter, E. & Lirman, D. (2011). Heterotrophic and autotrophic assimilation of fatty acids by two scleractinian corals, Montastraea faveolata and Porites astreoides. *Limnol. Oceanogr.*, 56, 1285-1296.

Venables, W.N. & Ripley, B.D. (2002). *Modern Applied Statistics with S.* Fourth edn. Springer, New York.

Williams, G.J., Sandin, S.A., Zgliczynski, B., Fox, M.D., Furby, K., Gove, J.M., Rogers, J.S., Hartmann, A.C., Caldwell, Z.R., Price, N.N. & Smith, J., E. (2018). Biophysical drivers of coral trophic depth zonation. *Mar. Biol.*, 165, 60.

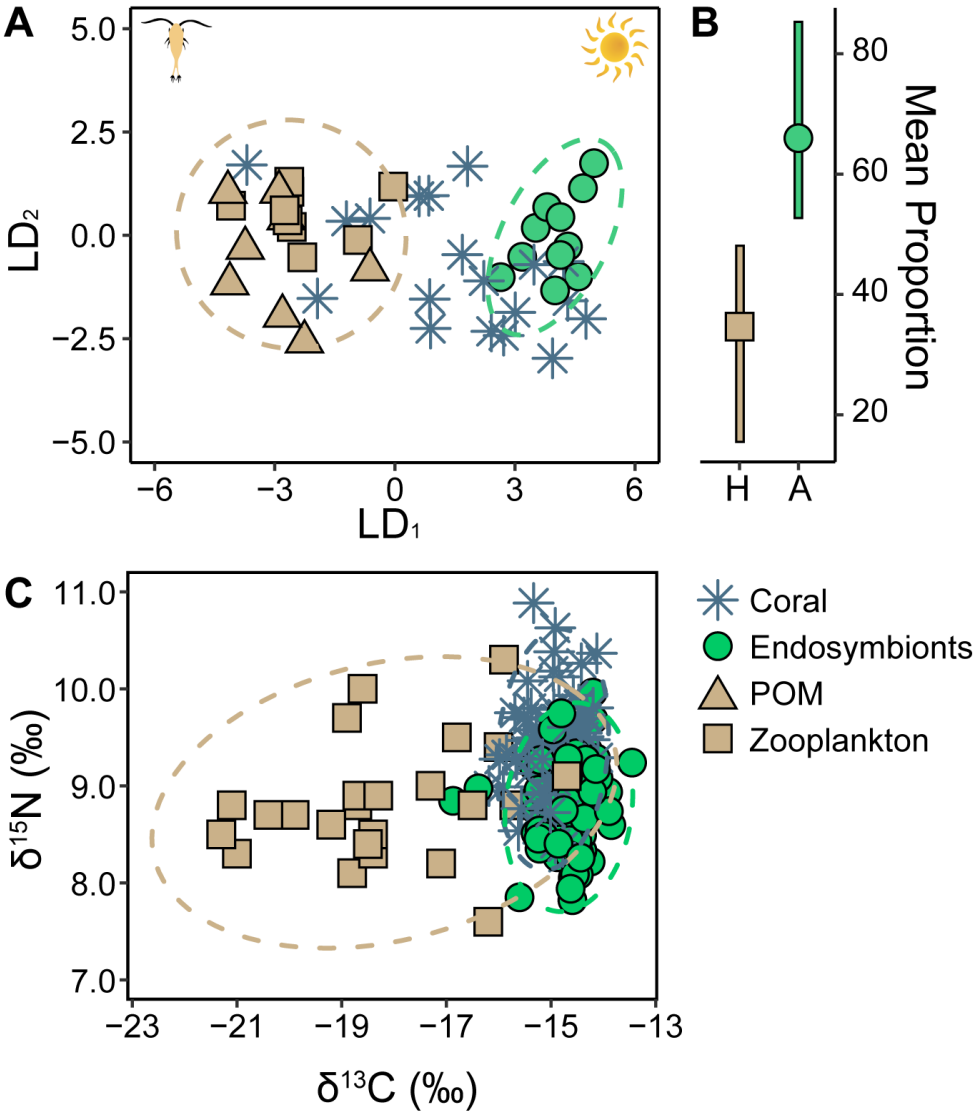

Figure 2.1. A comparison between $\delta^{13}C$ analysis of six essential amino acids (AA_{ESS}) and bulk tissue $\delta^{13}C$ and $\delta^{15}N$ analysis of a mixotrophic coral and the common autotrophic (endosymbiont tissue) and heterotrophic (zooplankton and POM) resources on Palmyra Atoll. **A** Linear discriminant analysis of six AA_{ESS} for coral tissue (n=19), endosymbionts (n=11), zooplankton (n=9), and POM (n=8). Dashed lines represent 95% confidence ellipses around each source group. **B** The mean proportion and 95% confidence intervals of colonies that were classified as belonging to the autotrophic (A) vs. heterotrophic (H) groups based on 10,000 random permutations of the source data. **C)** Biplot of bulk tissue $\delta^{13}C$ and $\delta^{15}N$ values for all coral and endosymbiont samples collected around Palmyra (n=87) and zooplankton samples from the lagoon and fore reef (n=24); data for POM are not shown for visual clarity due to variation among samples. For reference, the group means (95% confidence intervals) are -19.9‰ (-26.6 to -13.26) for $\delta^{13}C$ and 5.2‰ (1.94 to 8.4) for $\delta^{15}N$.

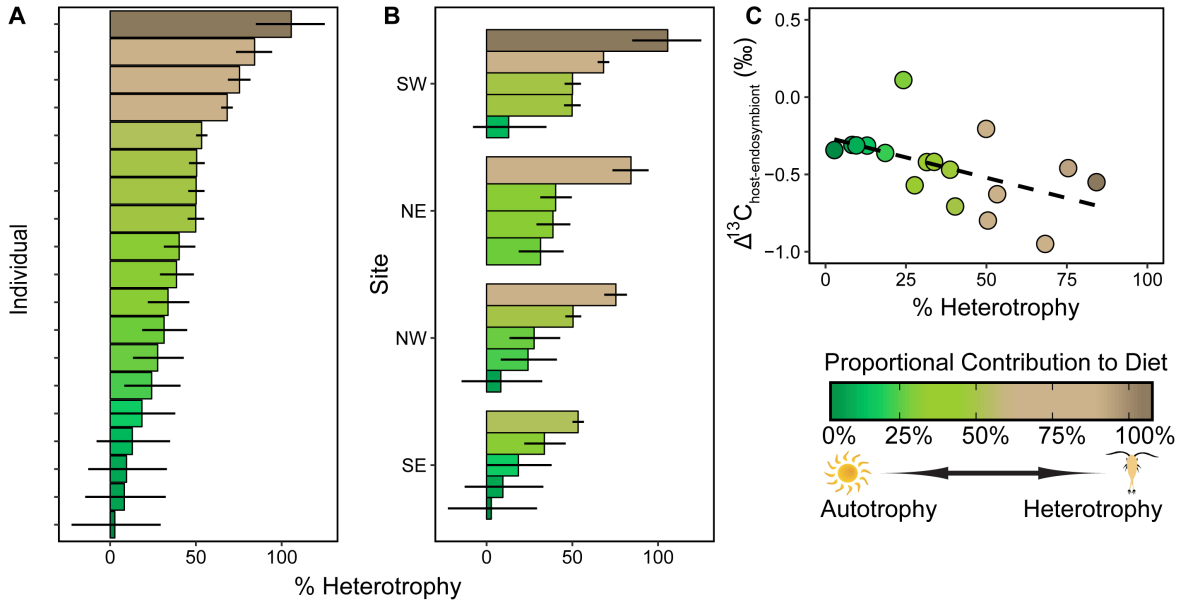

Figure 2.2. Individual variation in coral nutrition across 19 colonies from four locations around Palmyra Atoll. **A** The estimated mean percent contribution of heterotrophy to coral nutrition. Error bars denote 95% CI and any bar that overlaps 0 (100% autotrophy) or 1 (100% heterotrophy) is statistically indistinguishable from the respective source. **B** Individual coral colonies from A arranged by site. Error bars denote 95% CI. **C** $\Delta^{13}C_{host\text{-}endosymbiont}$ as a function of the average percent contribution of heterotrophic resources to coral nutrition. See the supporting information for details on calculating relative proportions of autotrophy and heterotrophy to coral nutrition using $\delta^{13}C_{AA}$.

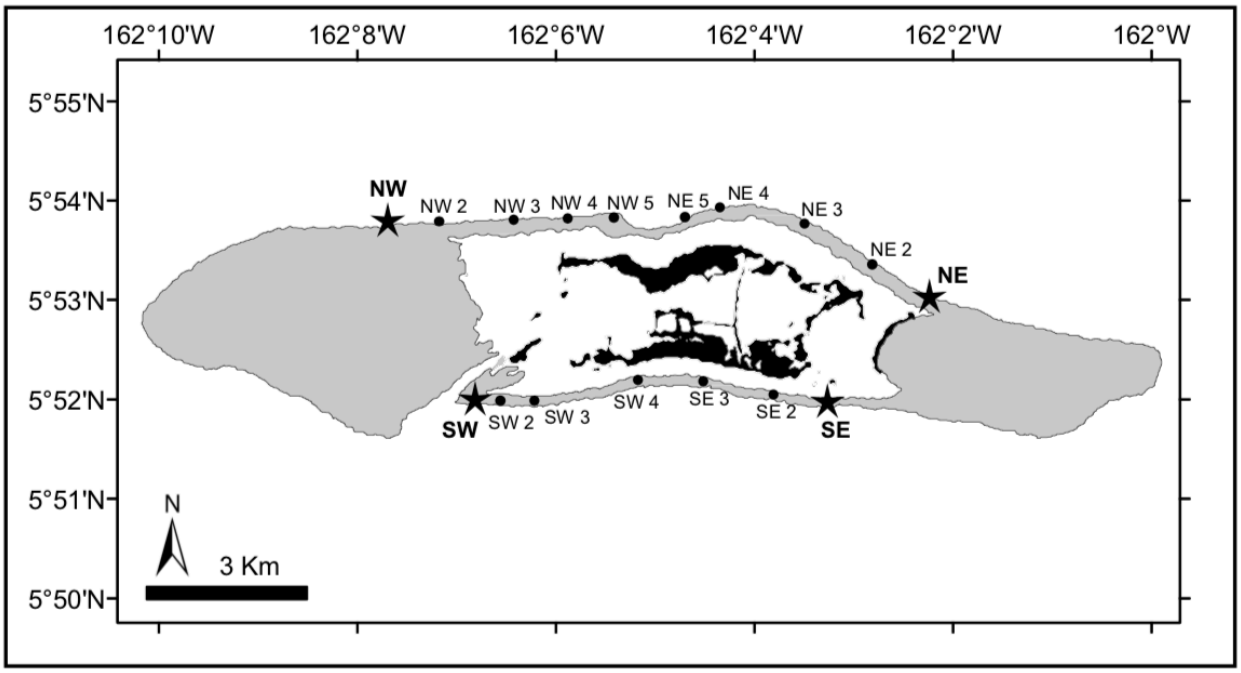

Figure 2.S1. Map of Palmyra Atoll National Wildlife Refuge displaying sampling locations. All emergent land is black and shallow reef habitat is shown in gray. All fore reef sampling locations were situated on the reef slope at 10 m depth. Stars indicate the four corner sites (SW, NW, NE, SE) that were targeted for $\delta^{13}C_{AA}$ sampling. All locations where additional samples were collected for bulk tissue $\delta^{13}C$ and $\delta^{15}N$ analysis are indicated with black circles. Each of these locations is name for the corner of the atoll it is closest to and they are numbered sequentially starting at 2.

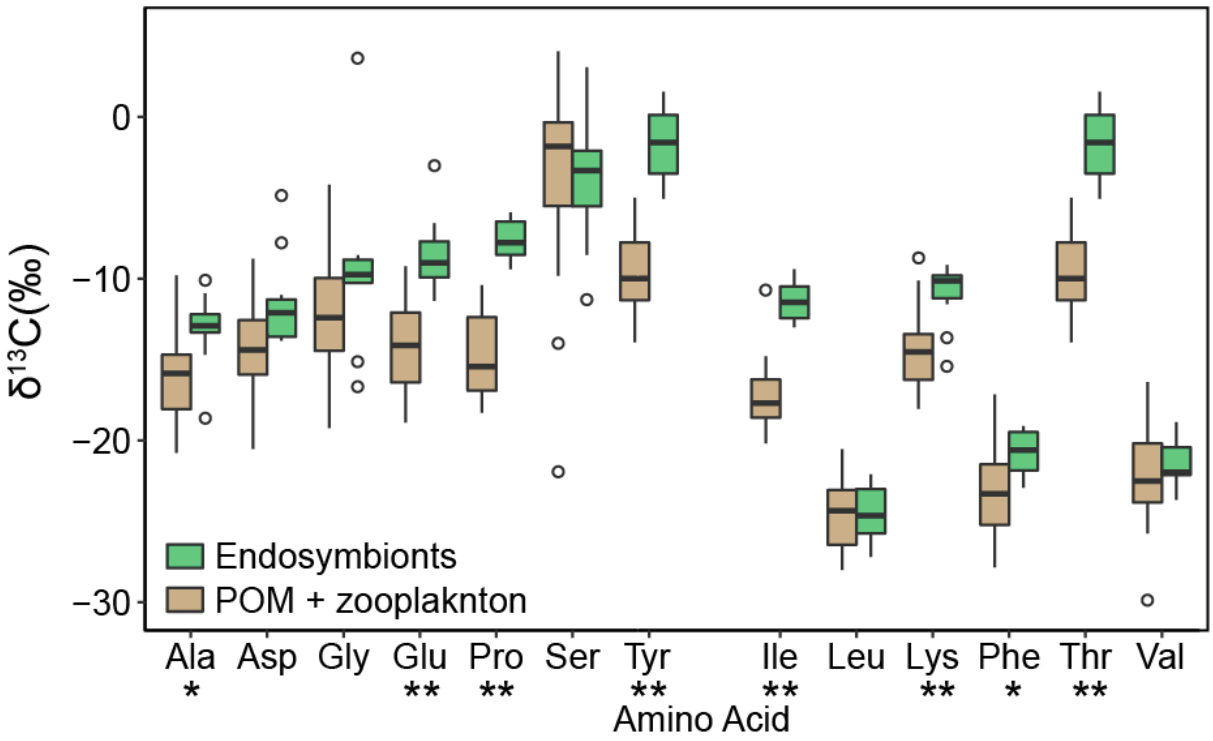

Figure 2.S2. Boxplot of $\delta^{13}C$ values of seven non-essential (left) and six essential (right) amino acids. The boxes encompass the first and third quartiles of the data and the whiskers are calculated as 1.58*IQR (range between first and third quartiles). Outlier points beyond this range are plotted individually as dots. The median of the data distribution for each group is indicated with a horizontal line. Significant differences between the mean values of the two resource groups at the $p < 0.05$ level are indicated with (*) and differences $p < 0.01$ with (**).

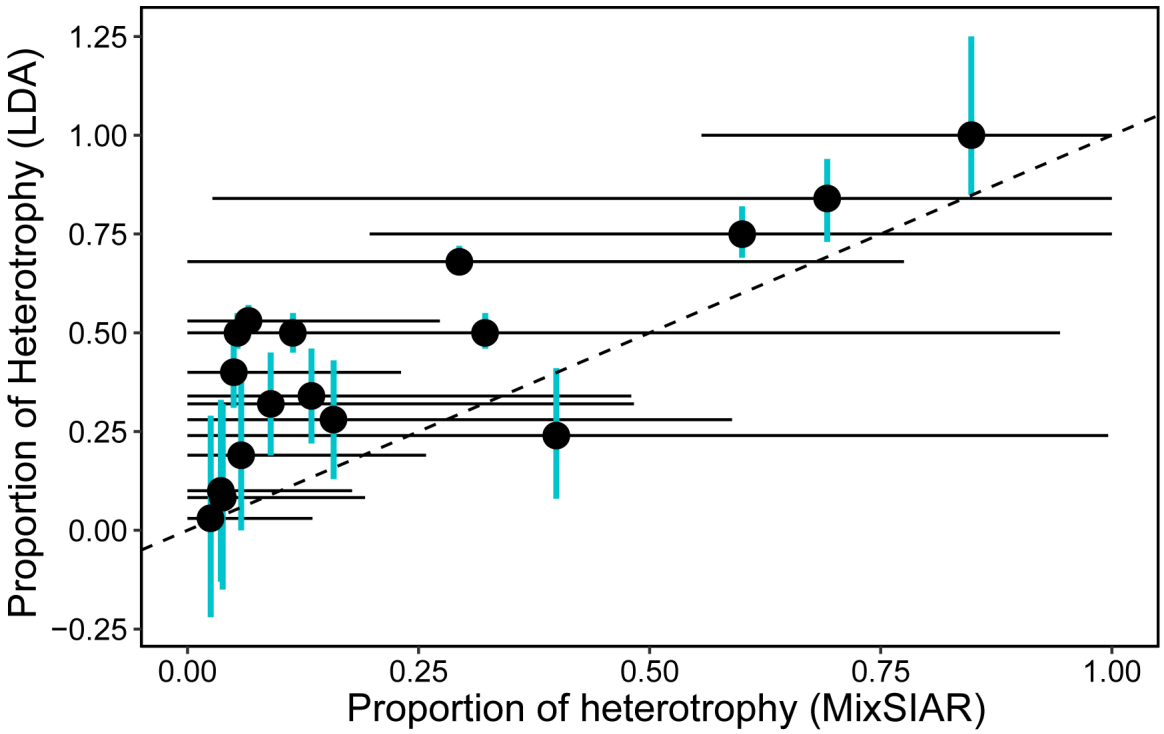

Figure 2.S3. A comparison of the modeled percent contribution of heterotrophy to *P. meandrina* diets using MixSIAR and the bootstrapped LDA approach. Black error bars denote 95% credibility intervals from MixSIAR and blue bars represent the 95% CI of our modeled estimates from the bootstrapped LDA. The dashed line is a 1:1 line. Notice that the two methods are more in agreement on the most extreme instances of heterotrophic contribution yet MixSIAR remains unable to resolve the diet contributions with confidence. Blue error bars that overlap 0 or 1 on the y-axis are statistically indistinguishable from being 100% of the respective source. Estimated values from MixSIAR (x-axis) are constrained between 0 and 1.

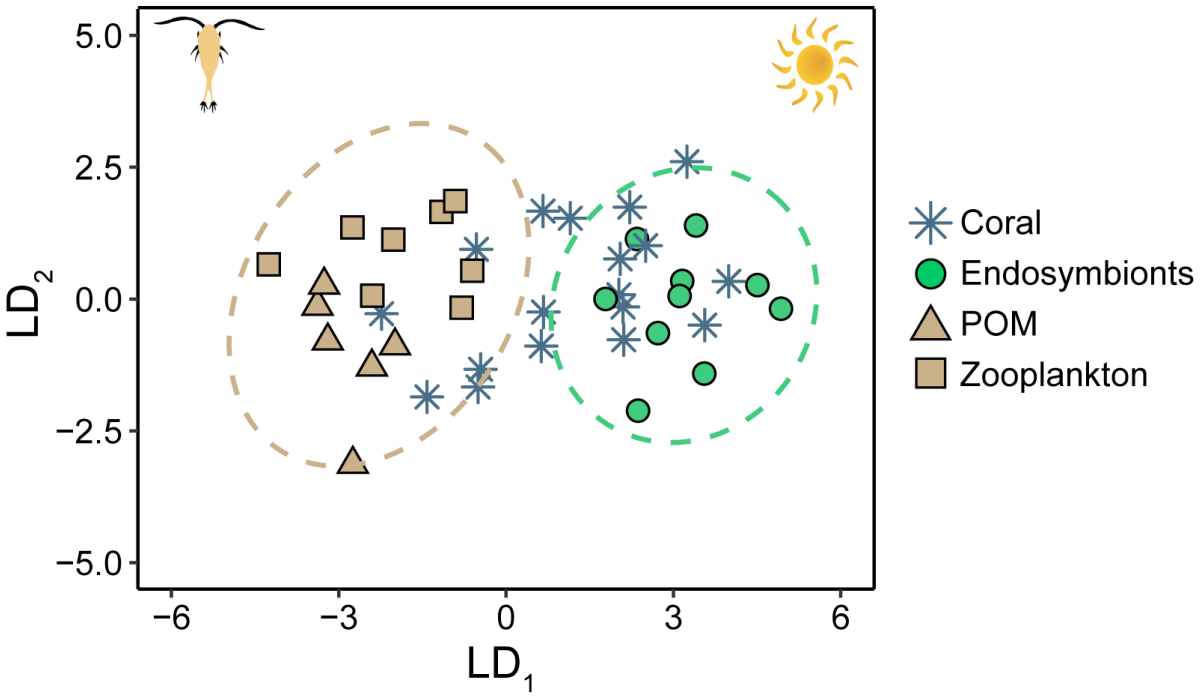

Figure 2.S4. Linear discriminant analysis of the seven analyzed non-essential amino acids for coral tissue (n=19), endosymbionts (n=10), zooplankton (n=8) and POM (n=6). Dashed lines represent 95% confidence ellipses around each resource group.

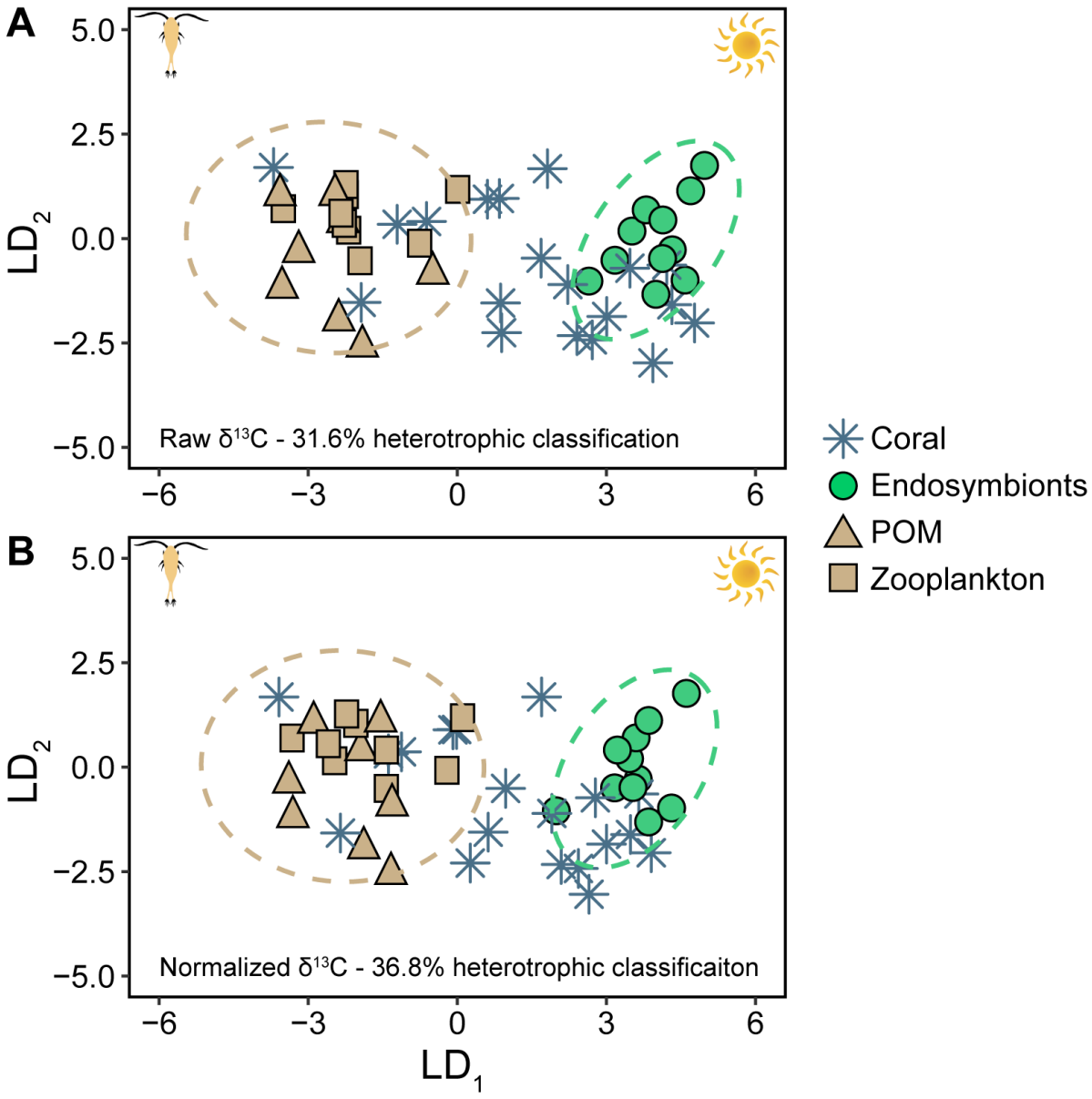

Figure 2.S5. Linear discriminant analysis of six essential amino acids for coral tissue (n=19), endosymbionts (n=10), zooplankton (n=8) and POM (n=6). Dashed lines represent 95% confidence ellipses around each resource group. **A** Raw $\delta^{13}C$ values for amino acids. **B** $\delta^{13}C$ values normalized to the sample mean per Larsen et al. 2013. In both cases reclassification for the heterotrophic and autotrophic sources was 100%.

Table 2.S1. All sites around Palmyra and the sample size for each isotopic metric analyzed. For the coral and endosymbionts $\delta^{13}C_{AA}$ values the number of endosymbiont samples measured are indicated in ().

	Coral and Endosymbionts			Zooplankton			POM		
Site	$\delta^{13}C$	$\delta^{15}N$	$\delta^{13}C_{AA}$	$\delta^{13}C$	$\delta^{15}N$	$\delta^{13}C_{AA}$	$\delta^{13}C$	$\delta^{15}N$	$\delta^{13}C_{AA}$
NW	5	5	5 (3)	1	1	1	1	1	1
SW	4	4	4 (3)	1	1	1	1	1	1
NE	6	6	5 (3)	1	1	1	1	1	0
SE	6	6	5 (3)	1	1	2	1	1	1
NW 2	5	5	-	1	1	-	1	1	-
NW 3	5	5	-	1	1	-	1	1	-
NW 4	6	6	-	1	1	-	1	1	-
NW 5	5	5	-	1	1	-	0	0	-
NE 2	5	5	-	1	1	-	1	1	-
NE 3	5	5	-	1	1	-	1	1	-
NE 4	5	5	-	1	1	-	0	0	-
NE 5	5	5	-	1	1	-	1	1	-
SE 2	5	5	-	1	1	-	1	1	-
SE 3	5	5	-	1	1	-	1	1	-
SW 2	5	5	-	1	1	-	1	1	-
SW 3	5	5	-	0	0	-	0	0	-
SW 4	5	5	-	1	1	-	1	1	-
Lagoon			-	8	8	4	7	7	5
Total	**87**	**87**	**19 (11)**	**24**	**24**	**9**	**21**	**21**	**8**

Table 2.S2. Analysis of Variance (ANOVA) results examining coral and endosymbiont stable isotope values as well as their relative difference (Δ). Isotope values were compared within corals (host and endosymbiont tissues) as a function of site and tissue type. Differences between the two tissues were compared across sites. Additionally, we compared site-level means of the endosymbiont fraction (autotrophic nutrition) to heterotrophic sources (zooplankton and POM) from the fore reef and lagoon habitats. Pairwise contrasts are based on Tukey's HSD and significant differences at the $p<0.05$ level are indicated with | and all significant factors are indicated in bold.

Variable	Factor	df	MS	F	P	Pairwise Contrasts
$\delta^{13}C$	**Site**	16	0.50	2.37	**< 0.01**	FR 13, 239 | FR 40, Strawn
	Tissue	1	4.41	21.09	**< 0.001**	Host | endosymbiont
	Site*Tissue	16	0.06	0.27	0.99	
	error	138	0.31	-	-	
$\delta^{15}N$	**Site**	16	1.02	7.13	**<0.001**	
	Tissue	1	15.17	105.99	**<0.001**	Host | endosymbiont
	Site*Tissue	16	0.13	0.93	0.54	
	error	138	0.143	-	-	
$\Delta^{13}C$	**Site**	16	0.12	2.71	**<0.01**	FR 13, 7 | FR 39; FR 3 | FR 14
	error	69				
$\Delta^{15}N$	**Site**	16	0.71	1.58	0.1	
	error	69	0.45			
$\delta^{13}C$ Sources	**Source**	4	114.87	52.6	**<0.001**	Endosymbiont |Reef-Plkt, Lagoo-POM | Lagoon-Plkt, Lagoon-POM |Reef- POM
	error	50				
$\delta^{15}N$ Sources	**Source**	4	31.28	90.79	**<0.001**	Endosymbiont, Reef-Plkt, Lagoon-Plkt| Lagoon-POM | Reef-POM
	error	46				

Table 2.S3. Table S3. Individual ANOVAs comparing differences in $\delta^{13}C_{AA}$ across the three source groups. Pairwise contrasts are based on Tukey's HSD and significant differences at the $p<0.05$ level are indicated with |. Amino acids that differed significantly between sources are indicated in bold.

Group	AA	df	MS	F	P	Pairwise Contrasts
Essential	**Ile**	2	112.10	28.17	**<0.001**	Endosymbionts | Zooplankton, POM
		error 25	6.95			
	Leu	2	0.14	0.03	0.97	
		error 25	4.30			
	Lys	2	43.3	7.19	**0.003**	Endosymbionts | Zooplankton, POM
		error 25	6.02			
	Phe	2	22.58	3.84	**0.04**	Endosymbionts | POM
		error 25	5.88			
	Thr	2	225.08	43.21	**<0.001**	Endosymbionts | Zooplankton, POM
		error 25	5.21			
	Val	2	5.43	0.78	0.47	
		error 25	6.95			
Non-Essential	**Ala**	2	143.40	3.77	**0.04**	Endosymbionts | POM
		error 21	38.05			
	Asp	2	33.72	2.66	0.094	
		error 21	12.70			
	Gly	2	53.22	2.47	0.11	
		error 21	21.58			
	Glu	2	100.79	13.73	**<0.001**	Endosymbionts | Zooplankton, POM
		error 21	7.34			
	Pro	2	133.26	24.18	**<0.001**	Endosymbionts | Zooplankton, POM
		error 21	5.51			
	Ser	2	105.50	3.26	0.06	
		error 21	32.35			
	Tyr	2	199.35	33.61	**<0.001**	Endosymbionts | Zooplankton, POM
		error 21	5.93			

CHAPTER 3

Nutrient enrichment differentially affects calcification in two Hawaiian coral species

Michael D. Fox, Craig E. Nelson, Zachery A. Quinlan, Kristina Remple, Hollie Putnam, Jennifer E. Smith, Thomas A. Oliver

ABSTRACT

The effects of nutrient pollution on coral reef ecosystems are multifaceted and context dependent. Numerous experiments have sought to identify the physiological effects of nutrient enrichment on reef-building corals but the results have been highly variable and sensitive to changes in the relative abundance of nitrogen to phosphorous or the source of nitrogen (i.e., nitrate vs. ammonium). Here we used a 5-week nutrient enrichment experiment to assess the effects of elevated nitrogen and phosphorous concentrations on the growth and photophysiology of two Hawaiian coral species. We acclimated corals to 5 nutrient levels that spanned a range of ecologically relevant concentrations measured on nearshore reefs across the Pacific and maintained constant nitrogen to phosphorous ratios to avoid the confounding effects of phosphate limitation. Our study revealed similar enhancements of coral photophysiolgocal performance across all nutrient levels in both species. However, the ultimate consequence of increased photosynthetic production varied by species. *Pocillopra acuta* exhibited enhanced skeletal growth at low nutrient concentrations (~1 μmol NO_3^-) and growth rates comparable to the control treatment at greater nutrient concentrations. In contrast, *Porites compressa* experienced reduced skeletal growth (30-35%) at concentrations above 3 μmol NO_3^-. These results imply that the effect of nutrient enrichment on calcification in reef-building corals is likely non-linear and species-specific. Our findings provide evidence to support reduced translocation of photosynthates to the coral host when endosymbiont populations are released from nutrition limitation but that the consequences of this can vary among species. Collectively, our study highlights the importance for considering species-specific responses when estimating the effects of nutrition pollution on coral communities and emergent ecosystem properties such as net ecosystem calcification.

INTRODUCTION

The transport of land-based nutrient sources to coastal waters is considered one of the greatest threats to marine ecosystems worldwide (Smith & Schindler 2009). The negative consequences of nutrient loading is particularly acute on coral reef ecosystems (Halpern *et al.* 2008), which have evolved under naturally oligotrophic conditions with the aid of efficient recycling of limiting nutrients (Muscatine & Porter 1977; Cardini *et al.* 2015). The addition of inorganic nutrients to coral reefs commonly occurs in the presence of additional stressors (e.g., sedimentation and over-fishing) that collectively can drive coral-dominated systems towards algal-dominated states (Fabricius *et al.* 2005; Hughes *et al.* 2007; Smith *et al.* 2010). As such, isolating the direct physiological effects of nutrient enrichment on the key foundation species in these ecosystems (e.g., reef-building corals and crustose coralline algae) is challenging.

Nutrient enrichment experiments on coral physiology have often yielded contrasting or inconclusive results (Shantz & Burkepile 2014), in large part due to variations in the recycling of carbon and nitrogen in the coral-algal symbiosis. Many nutrient enrichment experiments have relied on few treatment levels (Stimson & Kinzie 1991; Snidvongs & Kinzie 1994) that fail to capture the range of nutrient conditions commonly observed on coral reefs (Quinlan *et al.*). Thus, our understanding of the relative effects of increasing nutrient concentrations is incomplete. Nutrient enrichment also interacts differentially with global change stressors (i.e., warming and ocean acidification) depending on the taxa, nutrient type, and the ratio of nitrogen to phosphorous (D'Angelo & Wiedenmann 2014; Ezzat *et al.* 2016; Zaneveld *et al.* 2016; Johnson & Carpenter 2018). Given these complex interactions and the pervasive nature of global change, a more resolved understanding of the consequences of nutrient enrichment on the coral-algal symbiosis is required to improve current forecasts of the persistence of coral reef ecosystems.

Recent evidence suggests that coral reef islands across the Pacific exist in more naturally productive waters than previously considered (Gove *et al.* 2016). Elevated nutrient concentrations on coral reefs due to physical processes such as internal waves (Leichter *et al.* 2003) or via natural vectors such as seabirds (McCauley *et al.* 2012; Lorrain *et al.* 2017; Graham *et al.* 2018) likely play important roles in ecosystem functioning and may not negatively affect coral populations. Notably, the inorganic nutrient concentrations in the central Line Islands are among the highest known for uninhabited, tropical reef locations (> 4 μmol NO_3^-) (Kelly *et al.* 2014; Fox *et al.* 2018) yet these islands support some of the highest live coral cover found in the Pacific islands (Smith *et al.* 2016). Furthermore, corals on Jarvis Island were competitively dominant against turf algae despite elevated nutrient concentrations, which is in direct contrast to nearby Kiritimati Island where turf algae regularly outcompeted corals (Barott *et al.* 2012b). The opposing patterns from these islands imply that naturally elevated nutrients, in isolation, may negatively impact coral physiology and that corals may be affected be more strongly by interactions between nutrients and concurrent human impacts (e.g., over fishing or sedimentation). However, species-specific differences in the coral-algal symbiosis (e.g., natural symbionts densities or clade associations) (Baker *et al.* 2013) may ultimately dictate the response of individual coral taxa to nutrient enrichment.

An important challenge in accurately quantifying the effects of nutrient enrichment on symbiotic corals is capturing the possibility of non-linear effects. Few experiments have applied adequate treatment levels to assess the potential for positive, neutral, or negative responses to nutrient availability (but see Marubini & Davies 1996). For example, Gil (2013) showed that at low levels of nutrient enrichment growth of massive *Porites* sp. corals doubled while at higher nutrient levels growth rates subsided until returning to ambient levels at the highest

concentration. Additionally, there may be non-linear consequences of increased endosymbiont density, which has been proposed as a physiological driver of decreased growth and increased thermal sensitivity in corals under to enriched nutrient conditions (Wooldridge 2016). Collectively, these responses at the organismal level likely underpin community level responses to widespread eutrophication, such as dramatic reductions in coral species diversity (Duprey *et al.* 2016) but they are insufficiently resolved to make accurate predications about the direct impact of nutrient pollution on coral communities. Thus, more fine scale nutrient enrichment experiments are necessary to tease apart the independent responses of the coral hosts and algal endosymbionts and establish the effects on coral growth across a continuum of ecologically relevant nutrient concentrations.

Here we exposed two coral species to 5 levels of elevated inorganic nitrogen (NO_3^- + NO_2^-) and phosphate (PO_4^{3-}) continuously for five weeks. We used an outdoor mesocosm facility in Kāneʻohe Bay, Oahu, Hawaii to assess the effects of inorganic nutrient enrichment on the calcification and photophysiology of one widely distributed coral species, *Pocillopora acuta,* and another endemic to the Hawaiian Islands, *Porites compressa*. Specifically, we sought to determine 1) if the responses to nutrient addition differed between species, 2) if non-linear responses to nutrient enrichment were present in either species, and 3) if endosymbiont densities were related to changes in growth under elevated nutrient concentrations.

METHODS

Experimental set up and sample collection

For this experiment we used an outdoor mesocosm facility at the Hawaiʻi Institute of Marine Biology for five weeks (37 days) between 19 October and 24 November 2015. Seawater

was filtered through a sand filter followed by a 20 µm polyethylene pre-filter prior to entering our aquaria. We used 15 (n=3 per treatment) 8 L aquaria arranged within a single 1300 L flow through incubation tank to ensure stable temperature. Temperature in the incubation tank was monitored at 15 min intervals using a HOBO Pendant logger (Onset Computer Corp., Bourne, MA). The mean temperature throughout the experiment was 26 ± 0.42 s.d. °C (Fig. 3.S1) and twice weekly measurements of individual aquaria indicated consistently homogenous temperatures with a mean standard deviation of 0.14°C. Ambient irradiance was monitored using a LiCor 192SA (5 second sampling interval averaged every 5 min) affixed to the center of the incubation tank. Aquaria were shaded to 60% of natural irradiance and the daily range was 374 ± 111.78 s.d. µE m^{-2} s^{-1} (Fig. 3.S1). Weekly light measurements within each aquaria using a Apogee Quantum Sensor MQ-2000 revealed a homogenous light environment among aquaria with a standard deviation of 56 µE m^{-2} s^{-1}. All aquaria and the bases of each nubbin were cleaned weekly to avoid fouling and the position of aquaria was shuffled to account for natural variability in light and temperature.

Five nutrient chemostat treatments were established through continuous perastalisis of a concentrated nutrient mixture (2 mmol L^{-1} sodium nitrate and 0.67 mmol L^{-1} monosodium phosphate, 20L) for 5 weeks. See Quinlan *et al.* (2018) for a detailed description of the nutrient dosing system. Our nutrient levels were designed to span a range of inorganic nutrient conditions measured across the US Pacific Islands (Quinlan *et al.* 2018). Nitrate + nitrite and phosphate concentrations in each treatment were maintained at: Ambient (*N0*) = 0.14 ± 0.05 s.e. µmol L^{-1} NO^{3-} + $NO^{2-}$and 0.06 ± 0.01 s.e. µmol PO_4^{3-}, *N1* = 1.08 ± 0.18 s.e. µmol L^{-1} NO^{3-} + NO^{2-} and 0.56 ± 0.03 s.e. µmol PO_4^{3-}, *N2* = 2.73 ± 0.32 s.e. µmol L^{-1} NO^{3-} + NO^{2-} and 1.14 ± 0.10 s.e. µmol PO_4^{3-}, *N3* = 4.24 ± 0.34 s.e. µmol L^{-1} NO^{3-} + NO^{2-} and 1.54 ± 0.12 s.e. µmol PO_4^{3-}, and *N4*

= 6.84 ± 0.43 s.e. µmol L^{-1} NO^{3-} + NO^{2-} and 2.24 ± 0.15 s.e. µmol PO_4^{3-} [9] (Fig. 3.1). The nitrogen to phosphorous ratio (N:P = 2.4-3.5) was constant across treatments (Quinlan *et al.* 2018) and well below stressful levels (>40) known to destabilize the coral-algal symbiosis (Wiedenmann *et al.* 2012). Nutrient samples were collected from each aquarium on a weekly basis (50 mL filtered through 0.7 µm GF/F) to ensure treatment concentrations were constant. Samples were frozen at -20°C until analysis and processed on a Seal Analytical AA3 HR Nutrient Analyzer at the University of Hawaii's SOEST Lab for Analytical Chemistry for NO_3^- + NO_2^- and PO_4^{3-} (Quinlan *et al.* 2018).

Independent colonies of *Pocillopora acuta* and *Porites compressa* (n=7) were collected between 4 and 7 m depth on patch reefs near the entrance to Kaneohe Bay, HI in September 2015. Each colony was fragmented into similarly size nubbins (n=20) that were mounded to pvc tiles with epoxy putty and allowed to acclimate for one month under ambient conditions. Following acclimation, 4 replicate nubbins per colony were randomly placed into one of five nutrient enrichment treatments (N0-N4, n=28 per species).

Physiological parameters

All coral nubbins were measured for photochemical efficiency, net calcification, total protein content, *Symbiodinium* densities, and photopigment concentrations. Coral tissue was removed from the skeleton with an airbrush and 0.7 µm filtered seawater. The resulting slurry was homogenized and 1 mL aliquots were subsampled, samples for cell counts were fixed in 4% paraformaldehyde and the rest were frozen at -20 °C until analysis.

Photochemical efficiency was measured as maximum quantum yield (F_v/F_m) of dark-adapted PSII reaction centers using pulse amplitude modulation (PAM) fluorometry and a

Diving-PAM (Waltc, GmbH, Effeltrich, Germany). This allowed for repeated, non-intrusive measurements of coral photophysiological performance throughout the experiment. Measurements were taken weekly, 2 hours after sunset to ensure relaxation of photo-protective processes and PSII reaction centers. Each nubbin was marked at the beginning of the experiment and all PAM measurements were recorded from the same location on each colony through time. For both species the instrument was calibrated to produce F_o measurements of 300-500 units to avoid actinic effects and gain was minimized to avoid amplifying noise (Fitt *et al.* 2001). We used a saturation intensity of 8, saturation pulse width of 0.8s, Gain and Damping of 1. Measuring light intensity was adjusted to 9 for *Pocillopora* and 4 for *Porites.* The 5mm fiber-optic probe was positioned 5 mm above the coral surface for all measurements.

Coral skeletal growth was measured as net calcification determined by change in buoyant weight (Davies 1989) and converted to dry weight using a density of aragonite of 2.93 cm^{-3}. Total protein content (soluble and in soluble) was measured using the Pierce BCA Protein Assay Kit (Pierce Biotechnology, Waltham, MA). Proteins were solubilized through the addition of 1M NaOH, heating to 90°C for one hour, and neutralizing the pH to ~ 7.5 with 1 N HCl (Wall *et al.* 2018). We measured protein content was measured in triplicate at $\lambda = 562$nm against a bovine serum albumin standard curve and normalized to coral surface area (mg protein cm^{-2}). Growth and all other physiological parameters were standardized to colony surface area determined via wax dipping (Stimson & Kinzie 1991) and total protein content (Edmunds & Gates 2002). *Symbiodinium* densities were determined using flowcytometry (Lee *et al.* 2012). We ensured accurate cell density estimates by verifying a 1:1 relationship between flow cytometer counts and manual counts of a 10-step dilution for both species determined from 6 replicate counts on a haemocytometer. To quantify the total concentration of chl-*a* and chl-*c*, the endosymbionts were

separated from the coral host tissue (13,000 rpm x 3min) and resuspended in 100% acetone for extraction in the dark at -20°C for 36 hrs. Absorbance was measured at 630 and 663 nm in duplicate and concentrations were determined following (Jeffrey & Humphrey 1975). Concentrations of chl-*a* and chl-*c* were combined and reported as total chl standardized to surface area (μg cm^{-2}) and to symbiodinium cell density (pg $cell^{-1}$).

Statistical analysis

Linear mixed effects model with the random factors of tank nested within treatment and a crossed random factor of colony were conducted using the package lme4 (Bates *et al.* 2015). Significant differences between factors were determined using Type-II sum of squares with Satterthwaite approximate of degrees of freedom in the *lmerTest* package (Kuznetsova *et al.* 2017). For measurements of maximum quantum yield we included a random effect of individual to account for repeated measures through time. We had no interest in directly comparing the two species so independent tests were run to examine species-specific responses to the treatment levels. Fourteen nubbins died throughout the experiment (*Pocillopora* n=6 and *Porites* n=8) and they were randomly distributed through all treatment levels so they were removed from subsequent analyses. Measurements of chl concentrations were log transformed to satisfy the assumptions of normality and homoscedasticity, which were confirmed for all variables using visual assessment of the residuals and Levene's test, respectively. Finally, to examine the influence of *Symbiodinium* density on coral growth we used Pearson's correlations to compare total percent growth and biomass normalized *Symbiodinium* density.

RESULTS

The effect of nutrient enrichment on coral calcification differed between species. Skeletal growth was reduced relative to the control treatment (N0) in *Porites* by 30% in treatments N2-N4 (Fig 3.2A, Table 3.1). This pattern was consistent when calcification was normalized to total protein content (coral biomass) (Fig. 3.2A, C). In contrast, calcification in *Pocillopora* was enhanced by 50% in the low nutrient enrichment (N1) and returned to the levels of the control at higher nutrient concentrations (Fig. 3.2D, Table 3.1). Calcification normalized to total protein content was slightly more variable but differed between treatments N1 and N3-N4 (Fig. 3.2F, Table 3.1). Total protein content, however, did not change across all treatments for either species (Fig. 3.2 B, E, Table 3.1).

The photophysiolgoical response of both coral species to nutrient enrichment was similar. *Symbiodinium* concentrations were highly variable among individuals and colonies in *Porites* and did not differ significantly across treatments despite an overall increasing trend (Fig. 3.3A, B, Table 3.1). *Symbiodinium* densities in *Pocillopora* increased linearly as a function of nutrient enrichment when normalized to surface area and differed between low (N0) and enriched treatments (N3, N4) when normalized to total protein content (Fig. 3.4A, B, Table 3.1). Total chlorophyll concentration in *Porites* was elevated relative to the control in all treatments but did not differ per *Symbiodinium* cell (Fig. 3.3C, D, Table 3.1). Cell-specific chlorophyll content was greatest at moderate nutrient concentrations (N2) and declined marginally with increased nutrient enrichment (Fig. 3.3D, N2 > N4, $p = 0.07$). Chlorophyll content in *Pocillopora* increased in a stepwise fashion with elevated concentrations relative to the control at moderate nutrient enrichment and the highest concentrations at N4 (Fig 3.4C, Table 3.1). Cell-specific chlorophyll was variable across treatments but generally increased with nutrient enrichment ($p=0.08$, Fig. 3.4D, Table 3.1).

Maximum quantum yield mirrored patterns of endosymbiont density and chlorophyll concentration in both species. *Porites* F_v/F_m increased through time in all treatments but increased most rapidly in enriched treatments relative to the control (Treatment*Time, SS = 0.02, $F_{(16,504)} = 4.32$, $p < 0.01$). F_v/F_m increased relative to the control in the highest nutrient treatment (N4) by week 2 and was elevated in all treatments by week 3 (Fig. 5). *Pocillopora* F_v/F_m varied as a function of nutrient concentration through time. Similar to *Porites*, F_v/F_m increased relative to N0 by week 3 but by the end of the experiment the lowest nutrient enrichment (N1) enhanced F_v/F_m relative to the control but not as much as the higher nutrient treatments (Treatment*Time, SS = 0.04, $F_{(16,504)} = 4.20$, $p < 0.01$; Fig. 3.5).

The effects of nutrient enrichment on coral growth differed by species but were not dependent on the relative abundance of *Symbiodinium* cells. The decline in coral calcification observed in *Porites* was not correlated with endosymbiont density ($t = 0.39$, $df = 116$, $p = 0.70$, $r = 0.04$) indicating that compromised coral growth under nutrient enrichment is driven by more complex interactions in the coral-algal symbiosis than endosymbiont density alone. Similarly, symbionts density was not correlated with growth patterns in *Pocillopora* ($t = 1.0783$, $df = 116$, $p = 0.2832$, $r=0.10$).

DISCUSSION

The physiological effects of nutrient enrichment on symbiotic, reef-building corals are multifaceted and species-specific. The results of our study highlight that teasing apart the influence of nutrient availability on the physiology of the coral host and the algal endosymbionts is challenging but essential for future studies of coastal coral reef ecosystems. We show that low levels of nutrient enrichment can stimulate coral calcification in *Pocilopora acuta* yet decrease it

in *Porites compressa*. Notably, in both species the response to nutrient enrichment was non-linear. At the three highest nutrient concentrations, calcification in *P. acuta* was comparable to natural levels, while in *P. compressa* calcification was reduced 30-35%. In both cases, however, coral calcification rates were constant across a 2.5-fold increase in nitrogen and phosphorous concentrations. This suggests that the physiological effects of nutrient enrichment on coral growth are dynamic across a range of nutrient concentrations. Furthermore, the endosymbiont communities of both species responded similarly to increased nutrient availability (i.e., increased density and overall photosynthetic pigment concentration) despite the contrasting patterns of growth. The results from our study indicate that elevated concentrations of dissolved inorganic nitrogen and phosphate can have varying consequences for individual coral taxa and that this must be considered in future studies aiming to predict the effects of nutrient pollution on coral reef ecosystems.

Nutrient enrichment disproportionately affected the endosymbiont communities in both species of coral. Despite elevated endosymbiont populations and photosynthetic efficiency (F_v/F_m) at higher nutrient levels, neither coral species increased skeletal growth or total protein content. This indicates that excess carbon from photosynthesis was not being used to promote calcification (Muscatine *et al.* 1989) or incorporated into biomass by the coral host. Rather the excess carbon was likely being used to support increased growth rates of the endosymbiont populations (Ezzat *et al.* 2015) or released as dissolved organic carbon (Tremblay *et al.* 2012). It is also unlikely that either species used this excess carbon to build lipid stores as lipid content tends to decrease with nutrient enrichment in other coral species or is more closely associated with heterotrophic nutrition (Koop *et al.* 2001; Grottoli & Rodrigues 2011; Fox *et al.* 2018). *Pocillopora acuta* exhibited increased skeletal growth at the lowest level of nutrient enrichment

(N1= 1.08 ± 0.18 s.e. μmol L^{-1} NO^{3-} + NO^{2-} and 0.56 ± 0.03 s.e. μmol PO_4^{3-}), however, this concentration of nutrients was insufficient to increase overall symbionts density and therefore may not have led to the DIC competition that can inhibit calcification in the presence of increased endosymbiont densities (Stambler *et al.* 1991; Marubini & Davies 1996). Interestingly, the consequence of elevated endosymbiont densities differed between species. *P. acuta* was able to maintain normal levels of calcification whereas *P. compressa* experienced reduced growth despite symbionts concentrations that were not statistically distinguishable from the control treatment.

The pattern of increased endosymbionts density, maximum quantum yield, and elevated concentrations of photosynthetic pigments observed under nutrient enriched conditions is consistent with most previous experiments (Shantz & Burkepile 2014). In *Pocillopora acuta,* we observed a strong, linear increase in symbionts density, which lead to a doubling of endosymbionts per cm^2 of coral skeleton and greater maximum quantum yield in the highest nutrient treatment. Growth of endosymbiont populations by this magnitude was previously observed in Kaneohe Bay in a related species (*P. damicornis*) under ammonium enrichment (Stimson & Kinzie 1991), however, our results contrast the conclusion of a meta-analysis suggesting that nitrate enrichment does not appreciably increase *Symbiodinium* densities (Shantz & Burkepile 2014). Notably, ammonium (NH_4^+) enrichment can enhance the growth coral endosymbionts without compromising skeletal growth in several coral species (Shantz & Burkepile 2014), which may be due to the lower metabolic cost of ammonium uptake relative to nitrate that allows for more carbon to be available for the coral host (Dagenais-Bellefeuille & Morse 2013). This energetic trade off may partially explain the pattern of reduced growth we observed in *P. compressa* but it does not explain how *P. acuta* was able to maintain growth with

such high endosymbiont populations. Notably, the maximum quantum yield and endosymbiont densities in *P. acuta* showed no evidence of saturation across our nutrient treatments, which suggest that this species has a particularly high tolerance for nutrient enrichment. Indeed, Stambler et al. (1991) found that growth in *P. damicornis* in Kaneohe Bay increased at nitrate concentrations almost twice our highest treatment level (15 μmol). Thus, its possible that the nutrient concentration at which growth becomes compromised can be quite variable among coral species. Overall, our findings are consistent with the hypothesis that endosymbiont populations are naturally nutrient limited and will translocate less photosynthetically fixed carbon to the coral host when nutrient concentrations are increased in order to promote the growth or their own population (Muscatine *et al.* 1989; McGuire & Szmant 1997; Ezzat *et al.* 2015). However, the resulting impacts on the coral host can be positive, neutral, or negative depending on species and the respective concentrations of nitrogen and phosphorous.

We found no evidence that elevated endosymbiont density was closely associated with the reduced growth rates we observed in *P. compressa*. This result argues that elevated endosymbiont densities alone do not inherently compromise coral growth (Wooldridge 2016) but rather the resulting enhancement of primary production and respiration drives competition for DIC, which in turn may reduce coral calcification (Marubini & Thake 1999; Langdon & Atkinson 2005). Thus, identifying changes in the metabolic rates of different coral species is an important next step in understanding divergent responses to nutrient enrichment. Changes in skeletal growth of coral colonies exposed to nutrient enrichment have strong implications for benthic community structure on coral reefs (Smith *et al.* 2001; Smith *et al.* 2010; Barott *et al.* 2012a; Barott *et al.* 2012b) but can also influence larger ecosystem processes such as net accretion of $CaCO_3$ (Silbiger *et al.* 2018). Our results indicate that the overall effect of nutrient

enrichment on emergent ecosystem processes, such as net ecosystem calcification, may be influenced by species diversity or relative abundance and is likely spatially variable. While laboratory experiments can aid in identifying some of the key mechanisms behind altered calcification rates, extending similar studies to natural gradients of nutrient enrichment will enhance our ability to accurately quantify consequences of nutrient enrichment on coral reef at the level of communities and ecosystems. Across a natural upwelling gradient in the Southern Line Islands, *Pocillopora meandrina* increased endosymbiont density and chl-*a* concentrations (Fox *et al.* 2018), which is consistent with the patterns observed in our expeirment but the consequences for coral growth across these islands are unknown. Similar nutrient gradients impact natural patterns of bioerosion (DeCarlo *et al.* 2015) as well as the overall metabolic rates of key benthic primary producers (Maggie Johnson unpublished data) both of which influence carbonate budgets on reefs. Natural nutrient gradients also promote primary production and food availability for corals (Fox *et al.* 2018), which can alleviate the negative effects of nutrient enrichment on coral growth (Ezzat *et al.* 2016). Thus, there are likely a suite of natural factors that will further modulate the effects of nutrients *in situ* beyond what we can quantify in the lab.

The non-linear effect of nutrient enrichment on coral growth revealed by our study provides important insight into identifying management thresholds for nutrient runoff on nearshore reefs. For example, we show that at low levels of nutrient enrichment (< 2.7 μmol NO_3^-) growth in some coral species may be enhanced while in others there is no quantifiable effect. However, at concentrations beyond this value the positive benefits observed in some species are eroded and other species exhibit strongly reduced growth (Gil 2013). By establishing nutrient thresholds for reduction in growth across additional coral taxa we will be able to more accurately quantify the overall consequences of nutrient pollution for nearshore coral reef

ecosystems. This approach will also provide important insight to the generality of the physiological mechanisms that drive reduced growth in symbiotic corals under elevated nutrient concentrations. To date, we lack the information to determine if the variation observed in numerous experiments is an artifact of the nutrient concentrations used, the type of nutrients added, or differences in the resource sharing dynamics of coral-algal symbioses (Shantz & Burkepile 2014). Finally, this information will promote our understanding of how large-scale patterns of nutrient enrichment can compromise coral reef ecosystem functioning and lead to increased bleaching sensitivity (Vega Thurber *et al.* 2014; Zaneveld *et al.* 2016).

In conclusion, the results of our study highlight the importance of examining the effects of nutrient enrichment on coral physiology across multiple concentrations. By acclimating two coral species to five distinct nutrient treatments over five weeks, we identified similar photophysiological responses between species but contrasting patterns of skeletal growth. Notably, *Pocillopora acuta* is more tolerant of elevated nitrogen and phosphorous concentrations than *Porites compressa*. These results illustrate the importance of considering multiple metrics of coral physiology when trying to understand how species will respond to changing environmental conditions. From a photophysiological perspective, both species used in this experiment had elevated rates of primary production and enhanced photosynthetic efficiency. However, this surplus production did not enhance growth of coral host tissue and only promoted skeletal growth for *P. acuta* under the lowest nutrient enrichment concentration (~ 1 μmol). As such, our results confirm previous observations that *Symbiodinium* populations contribute less carbon to the coral host when they are released from nutrient limitation but add the complexity that some species appear less adept at maintain growth under such circumstances than others. Refining our understanding of species-specific differences in calcification under nutrient stress is an important

next step for improving estimates of nutrient pollution impacts to nearshore reefs as well as for quantifying large ecosystems processes, such as net ecosystem calcification over larger spatial scales.

Acknowledgements

We thank Ruth Gates and the Hawaii Institute of Marine Biology for generously providing laboratory and mesocosm space for this experiment. We also thank Claire Lager and Jessica Sevilla for assistance with sampling. This work was financially supported by the National Fish and Wildlife Foundation (Grant #44447 to CEN and TAO) and the US National Science Foundation (Grants OCE-1538393 to CEN and OCE-PRF 1323822 to HMP). This paper is funded in part by a grant/cooperative agreement from the National Oceanic and Atmospheric Administration, Project R/WR-3, which is sponsored by the University of Hawai‘i Sea Grant College Program, SOEST, under Institutional Grant No. NA14OAR4170071 from NOAA office of Sea Grant, Department of Commerce. The views expressed herein are those of the authors and do not necessarily reflect the views of NOAA or any of its sub-agencies. This is publication number 10330 of the School of Ocean and Earth Science and Technology. MDF was supported by a Nancy Foster Scholarship from the NOAA department of National Marine Sanctuaries.

Chapter 3, in part, is currently being prepared for submission for publication of the material. Fox, Michael D.; Nelson, Craig E.; Quinlan, Zachery A.; Remple, Kristina; Putnam, Hollie M.; Smith, Jennifer E.; Oliver, Thomas A. The dissertation author was the primary investigator and author of this material.

References

Baker, D.M., Andras, J.P., Jordan-Garza, A.G. & Fogel, M.L. (2013). Nitrate competition in a coral symbiosis varies with temperature among Symbiodinium clades. *ISME J*, 7, 1248-1251.

Barott, K.L., Rodriguez-Mueller, B., Youle, M., Marhaver, K.L., Vermeij, M.J., Smith, J.E. & Rohwer, F.L. (2012a). Microbial to reef scale interactions between the reef-building coral Montastraea annularis and benthic algae. *Proc Biol Sci*, 279, 1655-1664.

Barott, K.L., Williams, G.J., Vermeij, M.J.A., Harris, J., Smith, J.E., Rohwer, F.L. & Sandin, S.A. (2012b). Natural history of coral−algae competition across a gradient of human activity in the Line Islands. *Mar. Ecol. Prog. Ser.*, 460, 1-12.

Bates, D., Mächler, M., Bolker, B.M. & Walker, S. (2015). Fitting linear mixed-effects models using lme4. *J. Stat. Software*, 67, 1-48.

Cardini, U., Bednarz, V.N., Naumann, M.S., van Hoytema, N., Rix, L., Foster, R.A., Al-Rshaidat, M.M.D. & Wild, C. (2015). Functional significance of dinitrogen fixation in sustaining coral productivity under oligotrophic conditions. *Proceedings of the Royal Society B: Biological Sciences*, 282.

D'Angelo, C. & Wiedenmann, J. (2014). Impacts of nutrient enrichment on coral reefs: new perspectives and implications for coastal management and reef survival. *Current Opinion in Environmental Sustainability*, 7, 82-93.

Dagenais-Bellefeuille, S. & Morse, D. (2013). Putting the N in dinoflagellates. *Frontiers in microbiology*, 4, 369.

Davies, P.S. (1989). Short-term growth measurements of corals using an accurate buoyant weighing technique. *Mar. Biol.*, 101, 389-395.

DeCarlo, T.M., Cohen, A.L., Barkley, H.C., Cobban, Q., Young, C., Shamberger, K.E., Brainard, R.E. & Golbuu, Y. (2015). Coral macrobioerosion is accelerated by ocean acidification and nutrients. *Geology*, 43, 7-10.

Duprey, N.N., Yasuhara, M. & Baker, D.M. (2016). Reefs of tomorrow: Eutrophication reduces coral biodiversity in an urbanized seascape. *Global Change Biol.*, 22, 3550-3565.

Edmunds, P.J. & Gates, R.D. (2002). Normalizing physiological data for scleractinian corals *Coral Reefs*, 21, 193-197.

Ezzat, L., Maguer, J.-F., Grover, R. & Ferrier-Pagès, C. (2015). New insights into carbon acquisition and exchanges within the coral–dinoflagellate symbiosis under NH_4^+ and NO_3^- supply. *Proc. R. Soc. B*, 282, 20150610.

Ezzat, L., Towle, E., Irisson, J.O., Langdon, C. & Ferrier-Pagès, C. (2016). The relationship between heterotrophic feeding and inorganic nutrient availability in the scleractinian

coral *T. reniformis* under a short-term temperature increase. *Limnol. Oceanogr.*, 61, 89-102.

Fabricius, K., De'ath, G., McCook, L., Turak, E. & Williams, D.M. (2005). Changes in algal, coral and fish assemblages along water quality gradients on the inshore Great Barrier Reef. *Mar Pollut Bull*, 51, 384-398.

Fitt, W.K., Brown, B.E., Warner, M.E. & Dunne, R.P. (2001). Coral bleaching: interpretation of thermal tolerance limits and thermal thresholds in tropical corals. *Coral Reefs*, 20, 51-65.

Fox, M.D., Williams, G.J., Johnson, M.D., Kelly, E.L.A., Radice, V.A., Zgliczynski, B.J., Rohwer, F.L., Sandin, S.A. & Smith, J., E. (2018). Gradients in primary production predict trophic strategies of mixotrophic corals across spatial scales. *Curr. Biol.*, in press (accepted).

Gil, M.A. (2013). Unity through nonlinearity: a unimodal coral–nutrient interaction. *Ecology*, 94, 1871-1877.

Gove, J.M., McManus, M.A., Neuheimer, A.B., Polovina, J.J., Drazen, J.C., Smith, C.R., Merrifield, M.A., Friedlander, A.M., Ehses, J.S., Young, C.W., Dillon, A.K. & Williams, G.J. (2016). Near-island biological hotspots in barren ocean basins. *Nat Commun*, 7, 10581.

Graham, N.A.J., Wilson, S.K., Carr, P., Hoey, A.S., Jennings, S. & MacNeil, M.A. (2018). Seabirds enhance coral reef productivity and functioning in the absence of invasive rats. *Nature*, 559, 250.

Grottoli, A.G. & Rodrigues, L.J. (2011). Bleached *Porites compressa* and *Montipora capitata* corals catabolize δ^{13}C-enriched lipids. *Coral Reefs*, 30, 687-692.

Halpern, B.S., Walbridge, S., Selkoe, K.A., Kappel, C.V., Micheli, F., Agrosa, C., Bruno, J.F., Casey, K.S., Ebert, C., Fox, H.E., Fujita, R., Heinemann, D., Lenihan, H.S., Madin, E.M.P., Perry, M.T., Selig, E.R., Spalding, M., Steneck, R. & Watson, R. (2008). A global map of human impact on marine ecosystems. *Science*, 319, 948.

Hughes, T.P., Rodrigues, M.J., Bellwood, D.R., Ceccarelli, D., Hoegh-Guldberg, O., McCook, L., Moltschaniwskyj, N., Pratchett, M.S., Steneck, R.S. & Willis, B. (2007). Phase Shifts, Herbivory, and the Resilience of Coral Reefs to Climate Change. *Curr. Biol.*, 17, 360-365.

Jeffrey, S.W.t. & Humphrey, G.F. (1975). New spectrophotometric equations for determining chlorophylls a, b, c1 and c2 in higher plants, algae and natural phytoplankton. *Bioche. Physiol. Pflanz*, 167, 191-194.

Johnson, M.D. & Carpenter, R.C. (2018). Nitrogen enrichment offsets direct negative effects of ocean acidification on a reef-building crustose coralline alga. *Biology Letters*, 14.

Kelly, L.W., Williams, G.J., Barott, K.L., Carlson, C.A., Dinsdale, E.A., Edwards, R.A., Haas, A.F., Haynes, M., Lim, Y.W., McDole, T., Nelson, C.E., Sala, E., Sandin, S., Smith, J., E., Vermeij, M.J., Youle, M. & Rohwer, F. (2014). Local genomic adaptation of coral reef-associated microbiomes to gradients of natural variability and anthropogenic stressors. *Proceedings of the National Academy of Sciences of the United States of America*, 111, 10227-10232.

Koop, K., Booth, D., Broadbent, A., Brodie, J., Bucher, D., Capone, D., Coll, J., Dennison, W., Erdmann, M. & Harrison, P. (2001). ENCORE: the effect of nutrient enrichment on coral reefs. Synthesis of results and conclusions. *Mar. Pollut. Bull.*, 42, 91-120.

Kuznetsova, A., Brockhoff, P.B. & Christensen, R.H.B. (2017). lmerTest Package: Tests in Linear Mixed Effects Models *Journal of Statistical Software* 82, 1-26.

Langdon, C. & Atkinson, M.J. (2005). Effect of elevated pCO2 on photosynthesis and calcification of corals and interactions with seasonal change in temperature/irradiance and nutrient enrichment. *J. Geophys. Res. Oceans*, 110.

Lee, C.S., Yeo, Y.S. & Sin, T.M. (2012). Bleaching response of Symbiodinium (zooxanthellae): determination by flow cytometry. *Cytometry A*, 81, 888-895.

Leichter, J.J., Stewart, H.L. & Miller, S.L. (2003). Episodic nutrient transport to Florida coral reefs. *Limnol. Oceanogr.*, 48, 1394-1407.

Lorrain, A., Houlbrèque, F., Benzoni, F., Barjon, L., Tremblay-Boyer, L., Menkes, C., Gillikin, D.P., Payri, C., Jourdan, H., Boussarie, G., Verheyden, A. & Vidal, E. (2017). Seabirds supply nitrogen to reef-building corals on remote Pacific islets. *Sci. Rep.*, 7, 3721.

Marubini, F. & Davies, P.S. (1996). Nitrate increases zooxanthellae population density and reduces skeletogenesis in corals. *Mar. Biol.*, 127, 319-328.

Marubini, F. & Thake, B. (1999). Bicarbonate addition promotes coral growth *Limnol. Oceanogr.*, 44, 716-720.

McCauley, D.J., Desalles, P.A., Young, H.S., Dunbar, R.B., Dirzo, R., Mills, M.M. & Micheli, F. (2012). From wing to wing: the persistence of long ecological interaction chains in less-disturbed ecosystems. *Sci Rep*, 2, 409.

McGuire, M.P. & Szmant, A.M. (1997). Time course of physiological responses to NH_4 enrichment by a coral-zooxanthellae symbiosis. *Proceedings of the International Coral Reef Symposium*, 8, 909-914.

Muscatine, L., Falkowski, P.G., Dubinsky, Z., Cook, P.A. & McCloskey, L.R. (1989). The effect of external nutrient resources on the population dynamics of zooxanthellae in a reef coral *Proc. R. Soc. B*, 236, 311-324.

Muscatine, L. & Porter, J.W. (1977). Reef corals: mutualistic symbioses adapted to nutrient-poor environments. *Bioscience*, 27, 454-460.

Quinlan, Z.A., Remple, K., Fox, M.D., Silbiger, N.J., Oliver, T.A., Putnam, H.M., Linda, W.K., Carlson, C.A., Donahue, M.J. & Nelson, C.E. (2018). Fluorescent organic exudates of corals and algae in tropical reefs are compositionally distinct and increase with nutrient enrichment. *Limnology and Oceanography Letters*, LOL210074.

Shantz, A.A. & Burkepile, D.E. (2014). Context-dependent effects of nutrient loading on the coral-algal mutualism *Ecology*, 95, 1995-2005.

Silbiger, N.J., Nelson, C.E., Remple, K., Sevilla, J.K., Quinlan, Z.A., Putnam, H.M., Fox, M.D. & Donahue, M.J. (2018). Nutrient pollution disrupts key ecosystem functions on coral reefs. *Proc. R. Soc. B*, 285, 20172718.

Smith, J., Smith, C. & Hunter, C. (2001). An experimental analysis of the effects of herbivory and nutrient enrichment on benthic community dynamics on a Hawaiian reef. *Coral Reefs*, 19, 332-342.

Smith, J.E., Brainard, R., Carter, A., Grillo, S., Edwards, C., Harris, J., Lewis, L., Obura, D., Rohwer, F. & Sala, E. (2016). Re-evaluating the health of coral reef communities: baselines and evidence for human impacts across the central Pacific. *Proc. R. Soc. B*, 283, 20151985.

Smith, J.E., Hunter, C.L. & Smith, C.M. (2010). The effects of top-down versus bottom-up control on benthic coral reef community structure. *Oecologia*, 163, 497-507.

Smith, V.H. & Schindler, D.W. (2009). Eutrophication science: where do we go from here? *Trends Ecol Evol*, 24, 201-207.

Snidvongs, A. & Kinzie, R.A. (1994). Effects of nitrogen and phosphorus enrichment on in vivo symbiotic zooxanthellae of Pocillopora damicornis *Mar. Biol.*, 118, 705-711.

Stambler, N., Popper, N., Dubinsky, Z. & Stimson, J. (1991). Effects of nutrient enrichment and water motion on the coral *Pocillopora damicornis*. *Pac. Sci.*, 45, 299-307.

Stimson, J. & Kinzie, R.A. (1991). The temporal pattern and rate of release of zooxanthellae from the reef coral *Pocillopora damicornis* (Linnaeus) under nitrogen-enrichment and control conditions *J. Exp. Mar. Biol. Ecol.*, 153, 63-74.

Tremblay, P., Grover, R., Maguer, J.F., Legendre, L. & Ferrier-Pagès, C. (2012). Autotrophic carbon budget in coral tissue: a new ^{13}C-based model of photosynthate translocation. *The Journal of Experimental Biology*, 215, 1384-1393.

Vega Thurber, R.L., Burkepile, D.E., Fuchs, C., Shantz, A.A., McMinds, R. & Zaneveld, J.R. (2014). Chronic nutrient enrichment increases prevalence and severity of coral disease and bleaching. *Global Change Biol.*, 20, 544-554.

Wall, C.B., Ricci, C.A., Foulds, G.E., Mydlarz, L.D., Gates, R.D. & Putnam, H.M. (2018). The effects of environmental history and thermal stress on coral physiology and immunity. *Mar. Biol.*, 165, 56.

Wiedenmann, J., D'Angelo, C., Smith, E.G., Hunt, A.N., Legiret, F.-E., Postle, A.D. & Achterberg, E.P. (2012). Nutrient enrichment can increase the susceptibility of reef corals to bleaching. *Nat. Clim. Chang.*, 3, 160-164.

Wooldridge, S.A. (2016). Excess seawater nutrients, enlarged algal symbiont densities and bleaching sensitive reef locations: 1. Identifying thresholds of concern for the Great Barrier Reef, Australia. *Mar. Pollut. Bull.*

Zaneveld, J.R., Burkepile, D.E., Shantz, A.A., Pritchard, C.E., McMinds, R., Payet, J.P., Welsh, R., Correa, A.M.S., Lemoine, N.P., Rosales, S., Fuchs, C., Maynard, J.A. & Thurber, R.V. (2016). Overfishing and nutrient pollution interact with temperature to disrupt coral reefs down to microbial scales. *Nat Commun*, 7, 11833.

Table 3.1. Statistical summary for the fixed effects of linear mixed effects models. Results are presented for each species individually and significant response variables are indicated in bold. Significant differences in pairwise contrasts of treatment levels are indicated with |.

Species	Variable	Factor	SS	df	F	P	Pairwise Contrasts
Porites	**Calcification - Surface area**	Nutrient Level	4.08	4	6.24	**<0.01**	N0 | N2, N3, N4
		Error	18.46	112			
	Calcification - Protein	Nutrient Level	1.88	4	3.63	**0.03**	N0 | N2, N3, N4
		Error	13.39	15			
	Total Protein - Surface area	Nutrient Level	0.07	4	0.19	0.94	
		Error	10.01	15			
	Endosymbiont density - Surface area	Nutrient Level	1.81×10^5	4	0.81	0.54	
		Error	5.6×10^6	15			
	Endosymbiont density - Protein	Nutrient Level	1.28×10^5	4	0.77	0.56	
		Error	4.19×10^6	15			
	Total Chl - Surface area	Nutrient Level	9.97×10^3	4	8.85	**<0.001**	N0 | N1, N2, N3, N4
		Error	3.14×10^4	102			
	Total Chl per Endosymbiont	Nutrient Level	1.30	4	2.68	0.07	
		Error	12.68	15			
Pocillopora	**Calcification - Surface area**	Nutrient Level	0.93	4	7.77	**<0.01**	N1 | N0, N2, N3, N4
		Error	3.47	112			
	Calcification - Protein	Nutrient Level	0.38	4	5.06	**0.01**	N1 |N3 N4
		Error	1.97	100			
	Total Protein - Surface area	Nutrient Level	0.15	4	1.32	0.27	
		Error	3.23	111			
	Endosymbiont density - Surface area	Nutrient Level	1.47×10^{12}	4	13.90	**<0.001**	N0|N2, N3, N4; N1, N2 |N4
		Error	2.99×10^{12}	111			
	Endosymbiont density - Protein	Nutrient Level	3.33	4	7.02	**<0.01**	N0 | N3, N4
		Error	12.14	14			
	Total Chl - Surface area	Nutrient Level	358.93	4	7.30	**<0.001**	N0 | N2, N3, N4; N1 N2 | N4
		Error	5244.59	15			
	Total Chl per Endosymbiont	Nutrient Level	1.67	4	2.50	0.08	
		Error	17.23	15			

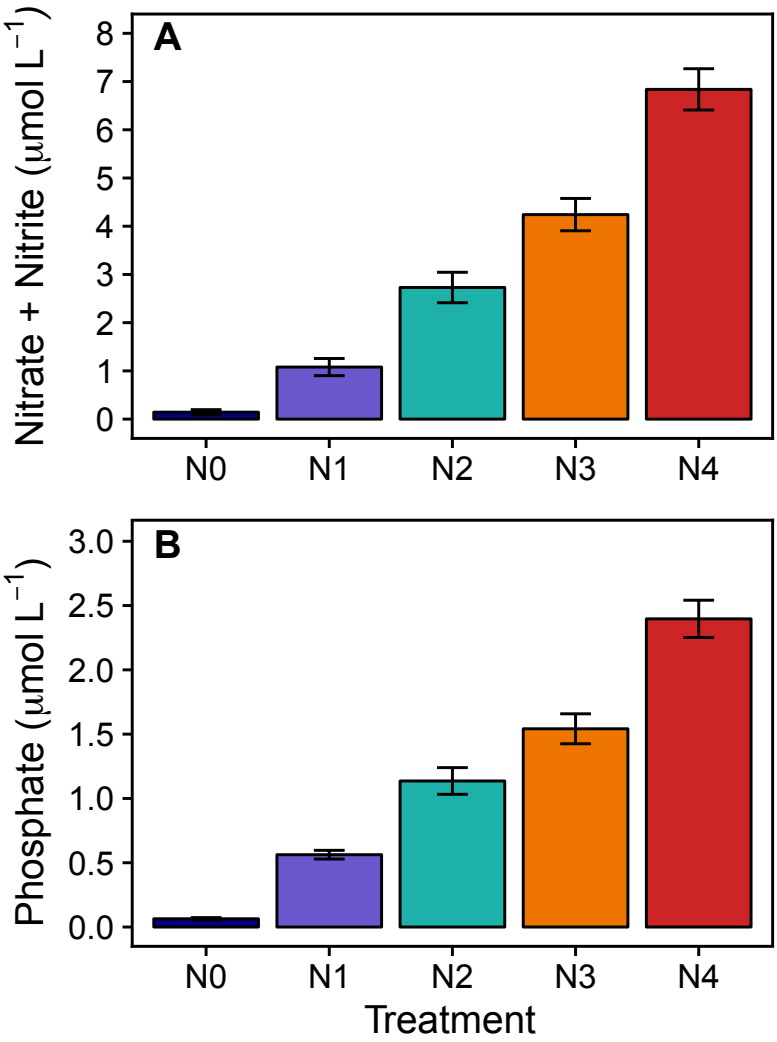

Figure 3.1. Mean inorganic nutrient concentrations for each treatment level. **A** Nitrate + nitrite and **B** Phosphate. Values represent the mean of all samples collected from each treatment level throughout the experiment (n=12). Error bars represent standard error of the mean.

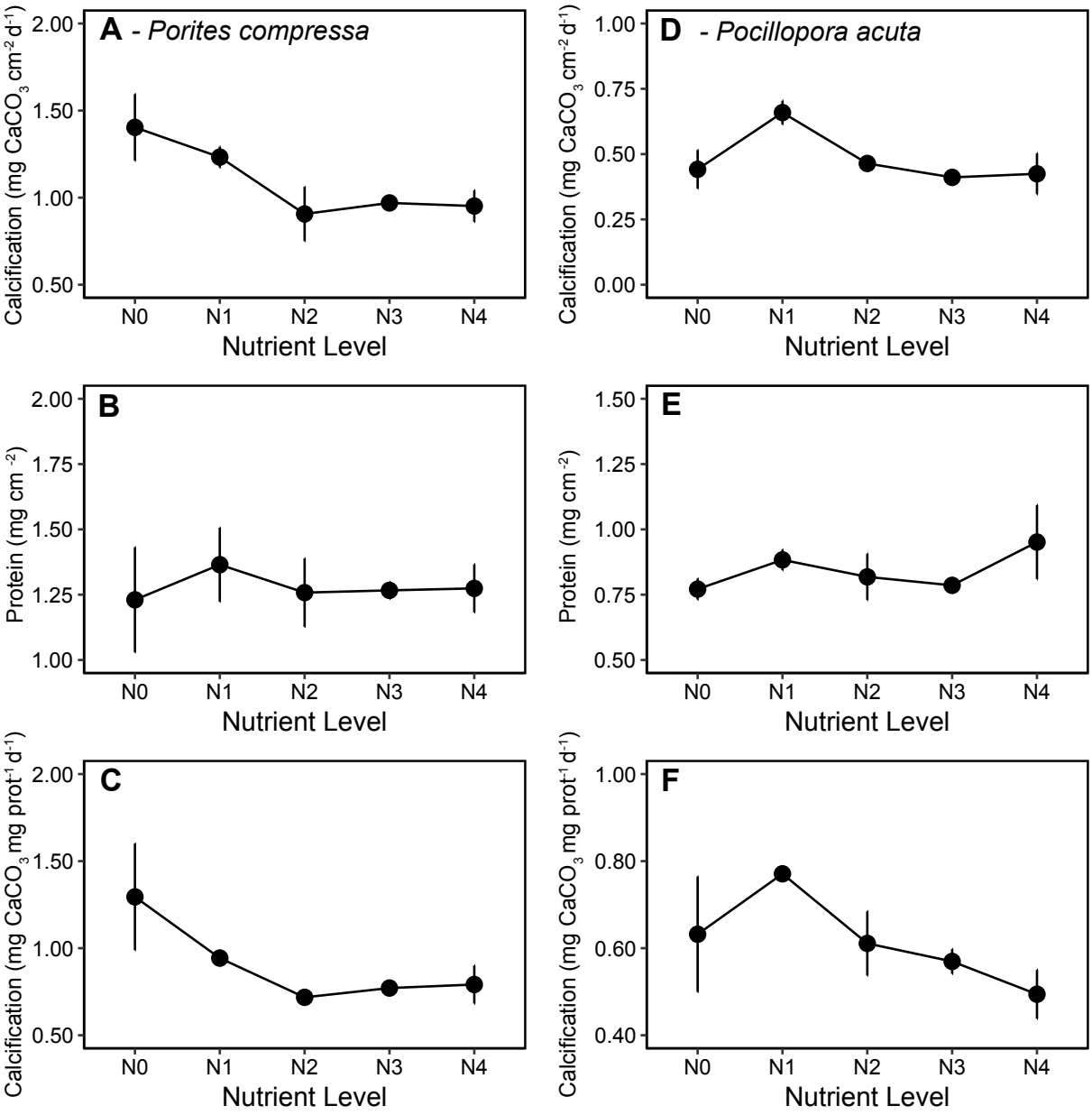

Figure 3.2. Growth and total protein content in *Porites compressa* and *Pocillopora acuta*. **A** and **D** skeletal growth normalized surface area, **B** and **E** total protein content normalized to surface area, **C** and **F** skeletal growth normalized to total protein content. Nutrient treatment levels are depicted on the x-axis and values represent the mean of all colonies in a given treatment (n=7). Error bars represent standard error of the mean.

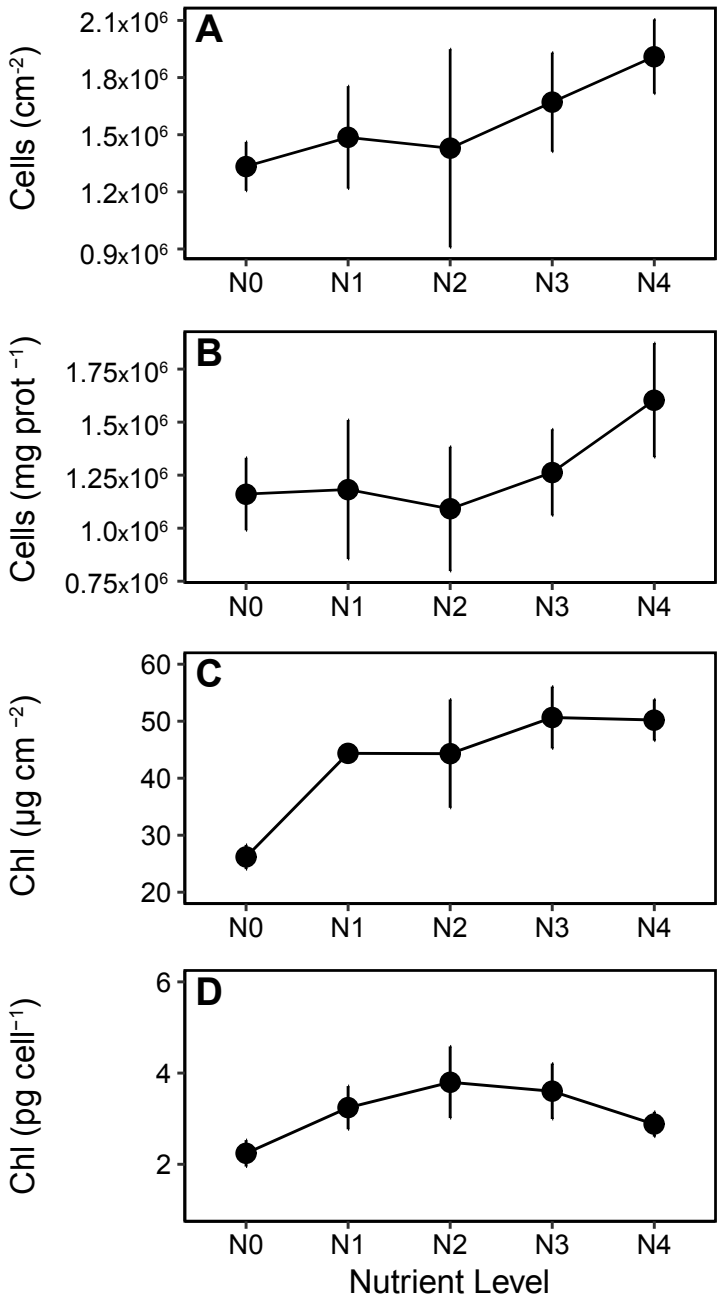

Figure 3.3. Photophysiological response of *Porites compressa* to nutrient enrichment. **A** *Symbiodinium* density normalized to surface area. **B** *Symbiodinium* density normalized to total protein content. **C** Total chlorophyll (chl-*a* + chl-*c*) concentration normalized to surface area. **D** Cell-specific chlorophyll concentrations. Nutrient treatment levels are depicted on the x-axis and values represent the mean of all colonies in a given treatment (n=7). Error bars represent standard error of the mean.

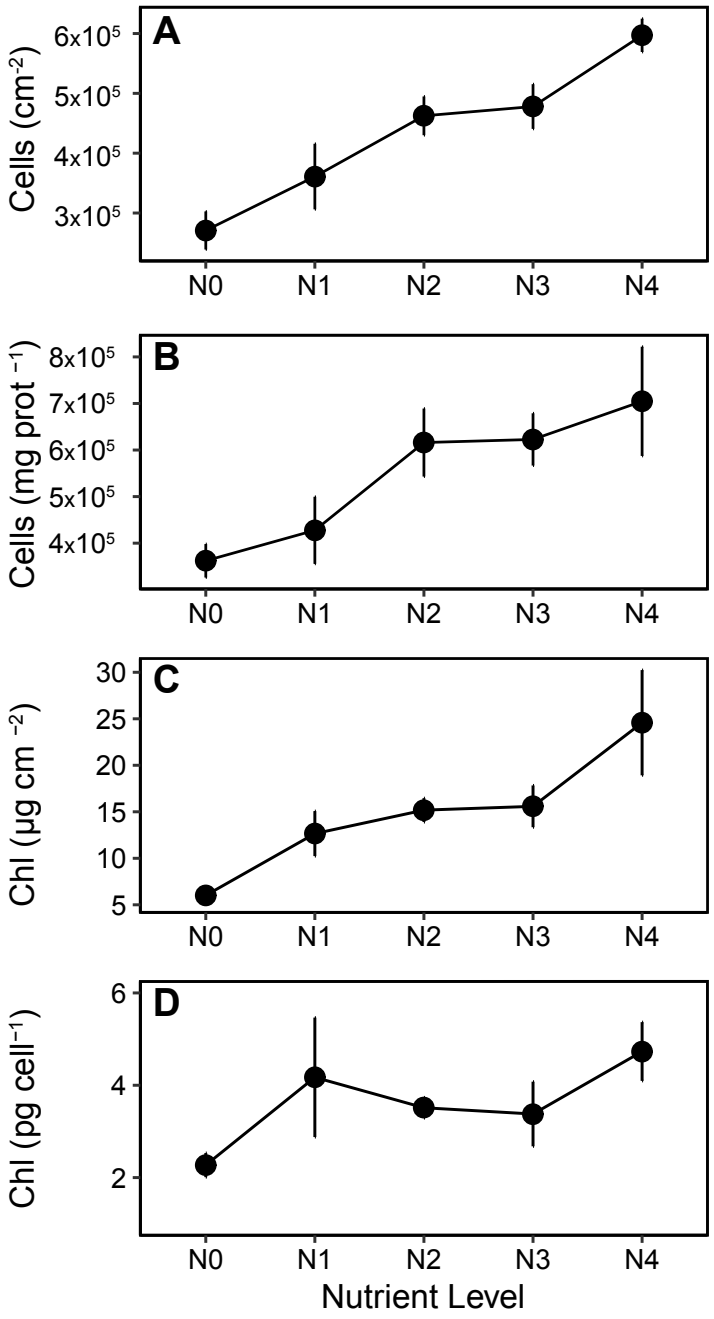

Figure 3.4. Photophysiological response of *Pocillopora acuta* to nutrient enrichment. **A** *Symbiodinium* density normalized to surface area. **B** *Symbiodinium* density normalized to total protein content. **C** Total chlorophyll (chl-*a* + chl-*c*) concentration normalized to surface area. **D** Cell-specific chlorophyll concentrations. Nutrient treatment levels are depicted on the x-axis and values represent the mean of all colonies in a given treatment (n=7). Error bars represent standard error of the mean.

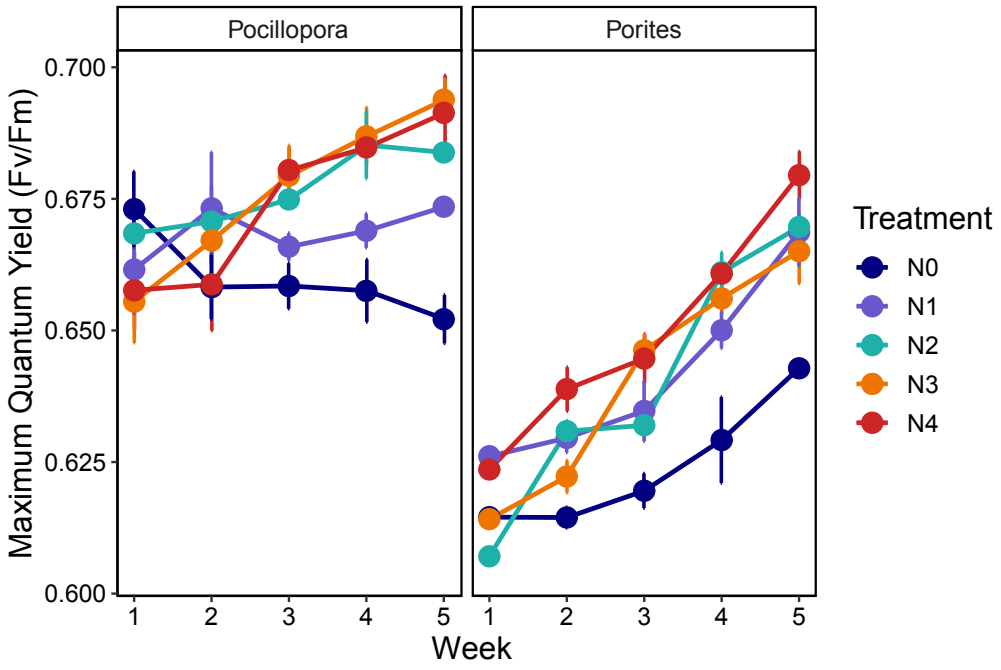

Figure 3.5. Maximum quantum yield in both coral species over the course of the experiment. Time in weeks is depicted on the x-axis and each nutrient treatment is indicated by color. Nutrient treatment levels are depicted on the x-axis and values represent the mean of all colonies in a given treatment (n=7). Error bars represent standard error of the mean.

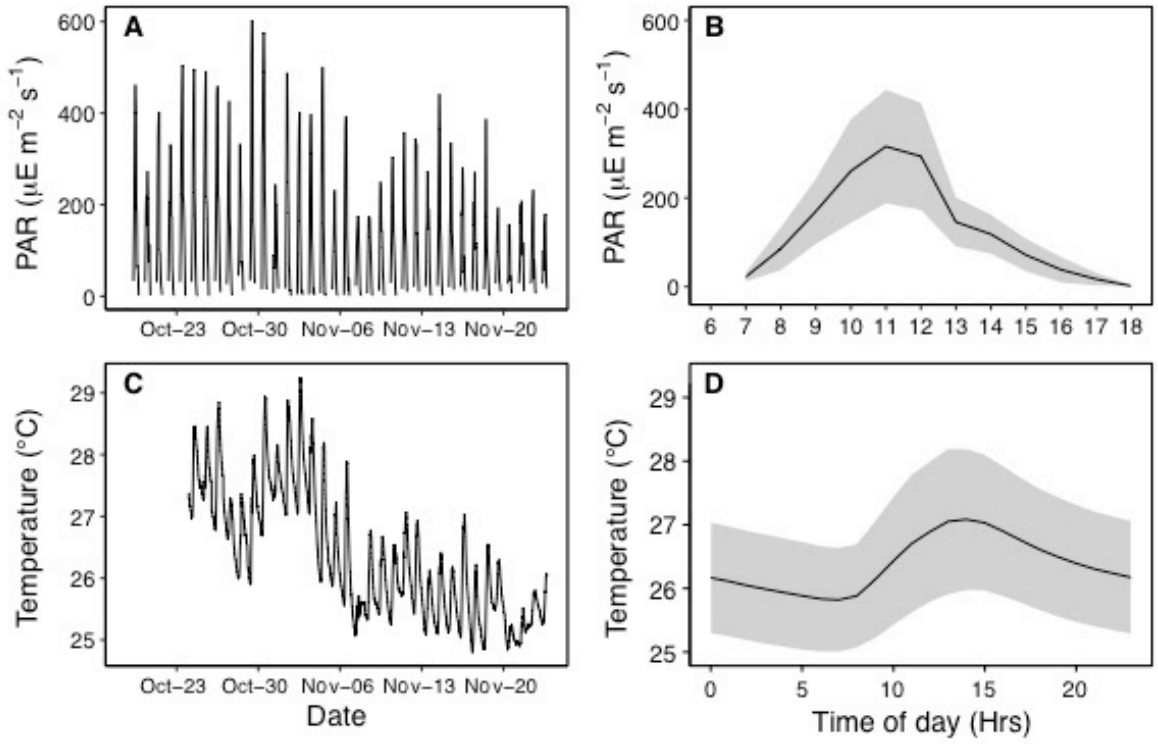

Figure 3.S1. Environmental conditions throughout the experiment. **A** Ambient light levels measured at the center of the large incubation tank. **B** The mean daily irradiance cycle based on hourly means between 0600 and 1800. The shaded region indicates standard deviation across all full days in the experiment. **C** Daily temperature in the incubation tank. **D** Natural mean daily temperature fluctuations across 24 hours. The shaded region represents the standard deviation across all full days in the experiment.

CONCLUSION

Mixotrophy is one of the most ubiquitous trophic strategies across all ecosystems (Selosse *et al.* 2016) and has evolved multiple times in terrestrial plant communities and marine invertebrates due to natural variations in resource availability (Venn *et al.* 2008; Ellison & Gotelli 2009). Due to their ability to obtain nutrition from both autotrophic and heterotrophic sources, mixotrophs are a critical component of dynamic marine environments because they create important linkages among trophic levels (Stoecker *et al.* 2017). On tropical coral reefs, limiting resources in the form of inorganic nutrients and planktonic biomass are highly variable, which has hindered our understanding of how mixotrophic corals respond to fluctuations in these resources. Studying the role of resource availability in the trophic ecology of corals is an essential aspect of understanding coral reef ecosystems better as whole. The central focus of this dissertation was to reevaluate the linkages between patterns of oceanic primary production and coral trophic ecology and to develop a framework for studying this relationship more accurately at multiple scales.

In Chapter 1, I used a natural gradient in primary production across the Southern Line Islands (SLI) to determine if reef-building corals can alter their trophic strategy to exploit increases in particulate resource availability. This natural gradient in food availability proved to be a valuable tool for elucidating that mixotrophic coral might have more complex trophic ecologies that we thought. Across the SLI, a common coral species became increasingly heterotrophic with increasing nearshore primary production. Notably, the increase in food availability in the surface waters at more productive islands also broke down a classically assumed pattern of coral trophic ecology – an increase in heterotrophic nutrition to compensate for decreasing light availability at depth. In the SLI, this depth defined trophic zonation was

present on oligotrophic islands but corals showed no variation in heterotrophic nutrition with depth at more productive islands. This result argues that broad generalizations of coral trophic ecology are likely inaccurate, especially in regions of varying primary production. This chapter also revealed that the pattern of increased heterotrophy in more productive regions holds globally for multiple coral species. Thus, regional and global patterns of primary production are more intimately linked with coral reef ecosystem functioning that previously considered. One important aspect of this chapter is the validation of remotely sensed estimates of surface ocean chl-*a* concentrations as a relevant proxy for food availability to primary consumers in shallow habitats across the tropics. The strong predictive relationship established in this chapter will facilitate future studies of the influence of primary production on the trophic ecology of corals and other mixotrophic organisms.

The influence of food availability on coral nutrition revealed in Chapter 1 suggests that the trophic ecology of mixotrophic corals is complex and likely flexible. Because corals appear capable of altering their use of heterotrophic nutrition on larger scales, why would they not respond to patters of food availability around an island or within a single tract of reef? Indeed, spatial variation in coral heterotrophy has been observed at the scale of kilometers in several species (Teece *et al.* 2011; Williams *et al.* 2018). However, the present application of bulk tissue stable isotope analysis to evaluate coral nutrition can be highly variable and is not consistent across taxa (Hoogenboom *et al.* 2015), which has restricted our ability to study these patterns effectively. As such, I developed a new approach for quantifying coral nutrition with much greater precision in Chapter 2. The application of amino acid $\delta^{13}C$ analysis revealed that individual corals of the same species could have fundamentally different trophic strategies even when they are immediately adjacent to one another. Furthermore, the extreme trophic plasticity

revealed by this new method overwhelms the response of corals to spatial patterns in food availability, and identifies a level of nutritional flexibility among conspecific coral colonies that should arouse great interest. The analytical framework offered by amino acid $\delta^{13}C$ analysis will hopefully aid cross-species comparison in coral trophic ecology and promote larger-scale assessments of heterotrophic nutrition within coral assemblages. Such information would markedly improve our understanding of how coral reefs are likely to differ in their response to future global change due to their background patterns of heterotrophic resource availability.

A key next step for improving our ability to predict how coral communities in different regions are likely to change in the future is to identifying the relative influence of different environmental drivers on the autotrophic and heterotrophic nutrition of corals. For example, Chapter 1 revealed that surface chl-*a* concentrations can predict areas where corals are likely to be more heterotrophic, which may enhance their capacity to survive and recovery from bleaching. In contrast, nearshore reefs in polluted areas can also have high surface chl-*a* concentrations and artificially enriched nutrient concentrations, which can erode corals resistance to thermal stress (Wooldridge 2009, 2016). Thus, in two locations the relationship between surface chl-*a* and coral resilience to bleaching could be decoupled by elevated concentrations of inorganic nutrients. Controlled laboratory experiments offer a way to disentangle the relative effects of food availability (heterotrophic nutrition) and nutrient availability, which primarily affects a coral's algal endosymbionts (autotrophic nutrition).

In Chapter 3, I conducted a nutrient enrichment experiment on two coral species and removed sources of heterotrophic nutrition by filtering all water before it entered the experimental aquaria. This chapter represents the first step towards decoupling the positive and negative effects of variations in limiting resource availability and the respective impact on

autotrophic and heterotrophic nutrition in corals. This study revealed that coral endosymbionts respond similarly to increases in nutrient concentrations but that as nutrient concentrations increase their contribution of autotrophic nutrition to the coral host may change. Notably, this loss of autotrophic nutrition appears to lead to metabolic deficits and reduced skeletal growth in some coral species but not others. These results further highlight the need to resolve differences in trophic ecology among coral species and to identify unifying taxonomic or morphological patterns that help explain some of the variation. But perhaps most importantly, the results of this chapter also reveal that some coral species may increase heterotrophic nutrition in response to changes in the quantity or quality of autotrophic nutrition they receive from their endosymbionts. If this is true, global patterns of coral trophic ecology are influenced by much more than primary production therefore studying the trophic ecology of corals may be an effective way to better understand the effects of environmental variation on coral physiology.

The results of this dissertation provide a new perspective on the trophic ecology of reef-building corals. Importantly, there is a strong need to consider the role of heterotrophic nutrition in coral population dynamics and persistence under global change and this dissertation provides a useful framework for addressing that knowledge gap in future studies. Overall, I found that many species of reef-building corals rely more on heterotrophic nutrition that previously thought and that large-scale variation in coral nutrition can be well explained by patterns of oceanic primary production but variation at small scales is dominated by differences among individuals. These findings contribute to our broader understanding of the biophysical connections between large-scale oceanographic processes and the functioning of coral reef ecosystems. The results of this dissertation will facilitate future research designed to evaluate the role of nearshore primary production in the survival and persistence of coral populations in a warming ocean.

References

Ellison, A.M. & Gotelli, N.J. (2009). Energetics and the evolution of carnivorous plants—Darwin's 'most wonderful plants in the world'. *J. Exp. Bot.*, 60, 19-42.

Hoogenboom, M., Rottier, C., Sikorski, S. & Ferrier-Pagès, C. (2015). Among-species variation in the energy budgets of reef-building corals: scaling from coral polyps to communities. *J. Exp. Biol.*, 218, 3866-3877.

Selosse, M.-A., Charpin, M. & Not, F. (2016). Mixotrophy everywhere on land and in water: the grand écart hypothesis. *Ecol. Lett.*, doi: 10.1111/ele.12714.

Stoecker, D.K., Hansen, P.J., Caron, D., A. & Mitra, A. (2017). Mixotrophy in the Marine Plankton. *Ann. Rev. Mar. Sci.*, 9, 311-335.

Teece, M.A., Estes, B., Gelsleichter, E. & Lirman, D. (2011). Heterotrophic and autotrophic assimilation of fatty acids by two scleractinian corals, Montastraea faveolata and Porites astreoides. *Limnol. Oceanogr.*, 56, 1285-1296.

Venn, A.A., Loram, J.E. & Douglas, A.E. (2008). Photosynthetic symbioses in animals. *J. Exp. Bot.*, 59, 1069-1080.

Williams, G.J., Sandin, S.A., Zgliczynski, B., Fox, M.D., Furby, K., Gove, J.M., Rogers, J.S., Hartmann, A.C., Caldwell, Z.R., Price, N.N. & Smith, J., E. (2018). Biophysical drivers of coral trophic depth zonation. *Mar. Biol.*, 165, 60.

Wooldridge, S.A. (2009). Water quality and coral bleaching thresholds: Formalising the linkage for the inshore reefs of the Great Barrier Reef, Australia. *Mar. Pollut. Bull.*, 58, 745-751.

Wooldridge, S.A. (2016). Excess seawater nutrients, enlarged algal symbiont densities and bleaching sensitive reef locations: 1. Identifying thresholds of concern for the Great Barrier Reef, Australia. *Mar. Pollut. Bull.*